MICROBIAL ADAPTATION TO CULTIVATION STRESS USING STORAGE COMPOUNDS

by

Adrienne Dale Arnold

A thesis submitted in partial fulfillment
of the requirements for the degree

of

Master of Science

in

Microbiology and Immunology

MONTANA STATE UNIVERSITY
Bozeman, Montana

July 2022

ACKNOWLEDGEMENTS

Funding for this project was provided by the Molecular Biosciences Program at Montana State University, NSF Award #1736255, and DOE Award # DE-EE0008247 / 000. Thanks to fellow lab members Dr. Laura Camilleri and Charles Holcomb for their guidance and assistance on all things lab and life related. Thanks as well to my advisor, Dr. Ross Carlson, for the years of instruction and encouragement, to former and current Biochemical Engineering Lab members Ashley Beck, Lee McGill, and Martina Du, and to my committee members Dr. Ellen Lauchnor, Dr. Robin Gerlach, and Dr. Matthew Fields.

TABLE OF CONTENTS

TABLE OF CONTENTS CONTINUED

TABLE OF CONTENTS CONTINUED

LIST OF TABLES

Table Page

LIST OF FIGURES

Figure Page

LIST OF FIGURES CONTINUED

LIST OF FIGURES CONTINUED

ABSTRACT

Methanotrophs and green algae are microorganisms that grow on single carbon substrates. Methanotrophs are bacteria that use methane as their carbon source, and green algae are eukaryotic phototrophs that grow on CO_2. They are of interest both as primary producers in the environment and as biological catalysts for the conversion of greenhouse gases into value-added compounds. Understanding how methanotrophs and green algae adapt to cultivation stresses is key to understanding carbon cycling in the environment and in industrial settings.

This work uses stoichiometric metabolic modeling to investigate the role of carbon storage compounds in the metabolism of C1-utilizing organisms. Storage compounds are accumulated as intracellular reserves of polysaccharides or lipids, which can be catabolized under stress conditions to provide carbon and energy to the cell. Catabolism of carbon storage compounds often results in the excretion of multi-carbon organic compounds that can be utilized as carbon substrates by other members of the microbial community. *In silico* metabolic models were developed for methanotroph and algal systems and used to examine the breakdown of storage compounds in response to common cultivation stresses. For the aerobic methanotrophs, predictions focused on the use of polyhydroxybutyrate and glycogen in adaptation to O_2 limitation. For the green algae, starch and triacylglycerol reserves are analyzed as sources for compatible solutes, which are produced by cells in response to high salinity conditions. Metabolic modeling of storage compound utilization by methanotrophs and algae helps elucidate the role of these organisms as primary producers and presents an opportunity for industrial production of multi-carbon compounds from single carbon substrates.

CHAPTER ONE

THE CARBON STORAGE COMPOUNDS OF AEROBIC METHANOTROPHS AND GREEN ALGAE

Introduction

This work focuses on two types of microorganisms: aerobic methanotrophs and photoautotrophic green algae. Aerobic methanotrophs are a subset of methylotrophic bacteria that are able to use methane as their sole carbon and energy source (C. Anthony, 1982). Green algae are photosynthetic eukaryotes that use the energy from sunlight to drive CO_2 fixation (Borowitzka et al., 2016). Methane is the most reduced form of carbon, and CO_2 is the most oxidized form, but growth on these compounds poses a similar problem for both organisms: the conversion of a single-carbon substrate into the multi-carbon macromolecules that make up the cell (Wood et al., 2004).

Both methanotrophs and green algae have been intensively researched as potential biocatalysts because of their ability to transform methane and CO_2 into useful products at ambient temperature and pressure. Methanotrophs have been used as a source of single-cell protein. They have also been investigated for their ability to produce a variety of chemical feedstocks, including methanol, ectoine, and biocompatible polymers (Strong et al., 2015). Green algae are often researched for biofuel production (Vitova et al., 2014), but they have also been cultivated as a source of single-cell protein and compounds like carotenoids, which can be used as nutritional supplements (Gong & Bassi, 2016). Methane and CO_2 are readily available

substrates, and since both are potent greenhouse gases, the products made using these microorganisms could help mitigate the effects of climate change.

Methanotrophs and green algae often serve as primary producers in the environment (Shelley et al., 2014). They provide metabolites to other microorganisms, either by biomass turnover via cell lysis (Hunt et al., 2016; Ramanan et al., 2016), direct metabolite transfer between closely associated community members (Abby et al., 2014), indirect metabolite leaking of compounds from the cell (Hagemann, 2016), or by excretion of waste products (A. E. Beck et al., 2017). To understand carbon cycling in the environment, we must understand the metabolism and ecology of these primary producers.

CO_2 fixation and methane assimilation are both metabolically expensive processes. Methanotrophs and algae, however, both accumulate carbon storage compounds that act as a repository of carbon and energy. In methanotrophs, algae, and many other microorganisms, degradation of these compounds helps cells survive during times of stress or starvation. While it may seem inefficient for methanotrophs and algae to excrete multi-carbon compounds as byproducts when they are growing on single carbon compounds, byproduct excretion is commonly observed, especially when the microorganisms are catabolizing storage compounds. Investigations into carbon storage compounds are important not just for the insight they provide into the metabolism of the cell, but also because the byproducts can provide reduced carbon to nearby microorganisms, establishing food webs.

This thesis investigates the accumulation and consumption of carbon storage compounds by methanotrophs and algae, with an emphasis placed on the role lipid and polysaccharide stores play in stress acclimation for these organisms. The role of storage compound degradation by

autotrophs and methanotrophs is also examined as a source of reduced carbon compounds for heterotrophic microbial communities associated with the primary producers.

Accumulation of Carbon Storage Compounds

Nutrient availability in the environment often fluctuates between abundance and scarcity. Aerobic methanotrophs experience seasonal changes in the availability of methane (Shelley et al., 2014) and even more frequent changes in O_2 levels (Roslev & King, 1995). Diurnal shifts in light limit the amount of time that algae can power carbon fixation by photosynthesis (Raven & Beardall, 2016). Like many other microorganisms, aerobic methanotrophs and green algae both accumulate carbon storage compounds under conditions of excess carbon or energy relative to the availability of other nutrients like nitrogen or phosphorus. These intracellular storage compounds can then be degraded for energy and carbon when resources like light, methane, or O_2 are scarce (Wilkinson, 1959).

Carbon storage compounds are broadly divided into two classes: polysaccharides and lipids. The polysaccharide storage compounds include glycogen and starch, which are synthesized in an ATP-dependent pathway that links glucose monomers via glycosidic bonds. Glycogen and starch have essentially the same chemical composition but differ in their branching patterns (Brust et al., 2020). Glycogen is highly branched, making it easier to be degraded and accessed for quick energy, as degradative enzymes have many terminal sugar molecules with which to bind and act on. Starch, meanwhile, typically has a more linear organization with fewer branch points (M. A. Sutherland, 2000). The branching results in different chemical properties; glycogen is typically water-soluble, while starch packs tightly and is insoluble in water (Brust et al., 2020).

Lipids are hydrophobic compounds that are typically present in the cell as either phospholipids or triacylglycerols. Phospholipids and other polar lipids make up membranes in the cell, as their polar nature gives them a hydrophobic tail and hydrophilic head that readily form the lipid bilayers that separate the cell interior from the environment (Tymoczko et al., 2015). Nonpolar lipids are used by cells as intracellular storage compounds (M. A. Sutherland, 2000). In algae, storage lipids typically take the form of triacylglycerols, which are fatty acids of various lengths bound together by a glycerol backbone (Vitova et al., 2014). In alphaproteobacterial methanotrophs, polyhydroxybutyrate (PHB) and other polyhydroxyalkanoates are used as lipid storage compounds (Pieja, Rostkowski, et al., 2011; Ren et al., 2009).

Carbon Storage Compounds of Aerobic Methanotrophs

This work focuses on two types of aerobic methanotrophs: the gammaproteobacterial methanotrophs, which use the ribulose monophosphate (RuMP) pathway for methane assimilation, and the alphaproteobacterial methanotrophs, which use the serine pathway for methane assimilation (Hanson & Hanson, 1996). The gammaproteobacterial methanotrophs funnel methane from the RuMP pathway into glycolytic pathways, allowing for easy production of glycogen (S. Yu But et al., 2020). The serine pathway methanotrophs, however, use the ethylmalonyl-CoA (EMC) pathway to replenish intermediates in the serine pathway and continue methane assimilation. The EMC pathway shares several metabolic intermediates with polyhydroxybutyrate (PHB) synthesis (Peyraud et al., 2009). The alphaproteobacterial methanotrophs are able to accumulate PHB, while the gammaproteobacterial methanotrophs use glycogen as a storage compound (Pieja, Rostkowski, et al., 2011).

Figure 1.1. Methane assimilation pathway of alphaproteobacterial methanotrophs showing the formation of polyhydroxybutyrate (PHB) from intermediates of the serine pathway.

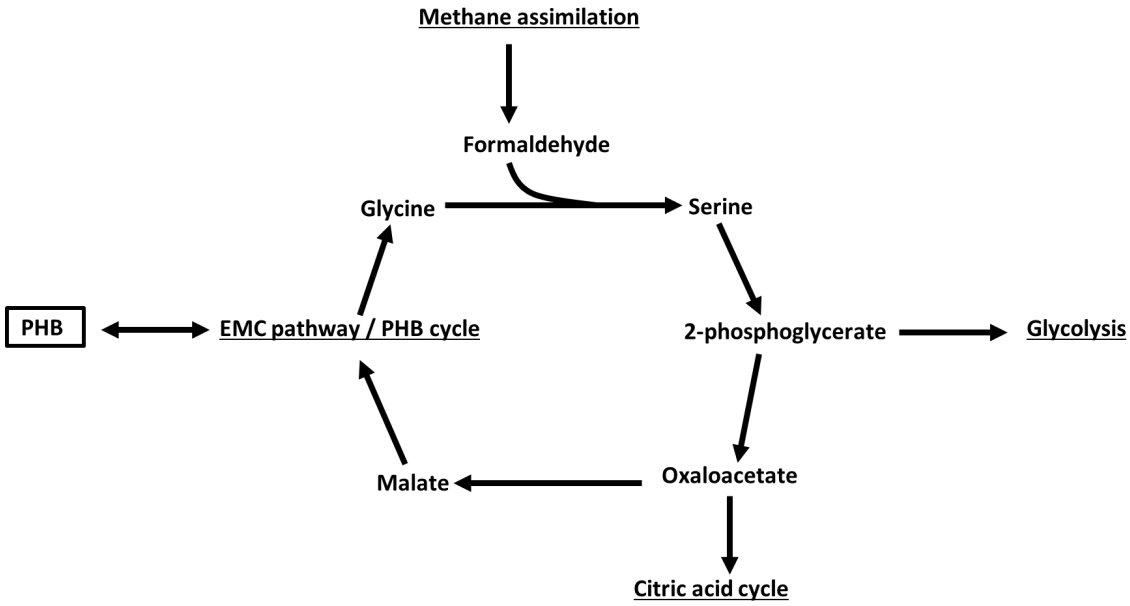

Figure 1.2. Methane assimilation pathway of gammaproteobacterial methanotrophs, showing the formation of glycogen from intermediates of glycolysis.

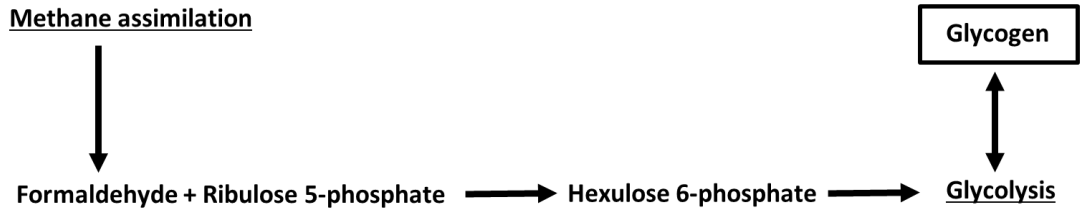

Carbon Storage Compounds of Green Algae

Green algae are known to accumulate both starch and lipids. Starch is a combination of the polysaccharides amylose and amylopectin and forms hydrophobic granules. The nonpolar storage lipids in algae are typically triacylglycerols, with chain length determined by the species. Chain lengths of 16 to 20 are most common (Vitova et al., 2014). Starch is accumulated in the

chloroplast. Lipids are typically found in the cytoplasm (Moriyama et al., 2018). Starch is a common carbon storage compound in algae, and it appears to be favored over lipids for providing energy to the cell. Lipids, however, make good electron sinks because of their high degree of reduction and can be favored under growth conditions with a high amount of energy, like high light conditions (Cecchin et al., 2019). As lipids are more electron dense, they allow for more energy storage while occupying a smaller volume than starch (Vitova et al., 2014).

Figure 1.3. Abbreviated carbon fixation in green algae, including starch and triacylglycerol synthesis.

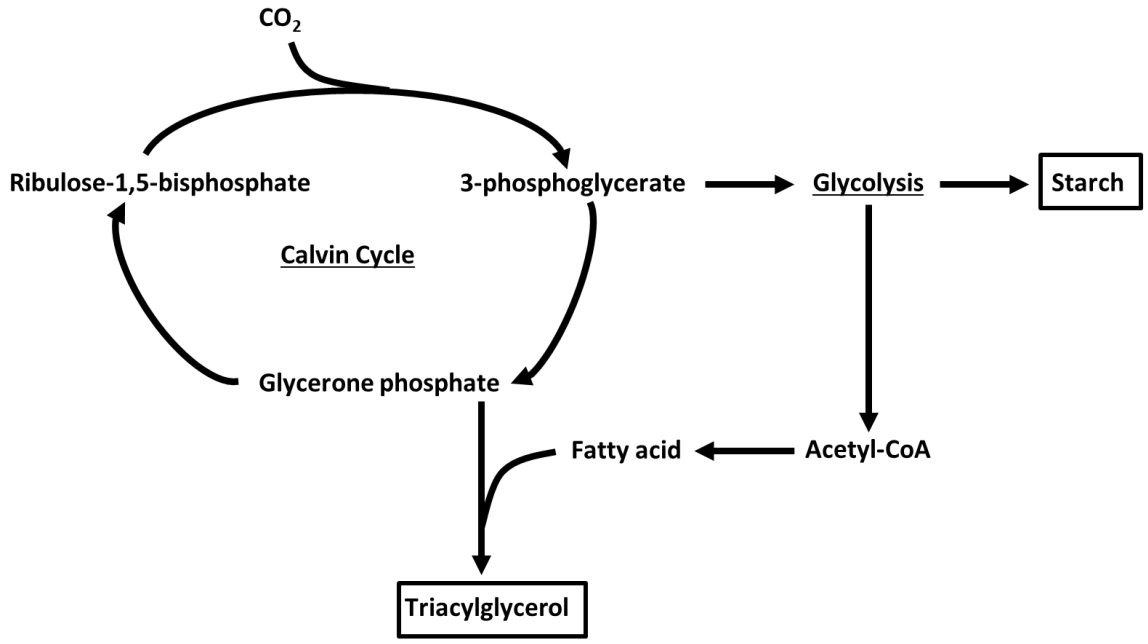

Lipid and Polysaccharide Accumulation Triggers

Nitrogen limitation triggers lipid accumulation in methanotrophs and algae (Pieja, Sundstrom, et al., 2011; Yap et al., 2016). This is the most common lipid production strategy used in industry and in research. Because cells require nitrogen for amino acids and other

macromolecules, they cannot grow without nitrogen. Two-stage cultivation methods are often used to trigger lipid accumulation, where the first stage focuses on a high biomass production and the second stage limits nitrogen in order to trigger lipid overproduction (Pieja, Sundstrom, et al., 2011; Vitova et al., 2014). Nitrogen limitation can also trigger polysaccharide accumulation in both algae and methanotrophs, although algae subjected to nitrogen limitation often preferentially accumulate lipids over starch (Khmelenina et al., 1999; Vitova et al., 2014). Phosphorous limitation can have similar effects as nitrogen limitation in algae (Guschina & Harwood, 2006). In green algae, salt stress has been shown to trigger lipid and starch accumulation (Goyal, 2007; Morales-Sánchez et al., 2017). High light conditions have been shown to favor production of lipids over starch in microalgae, likely because lipids are more electron dense and act as a better electron sink (Cecchin et al., 2019). Micronutrient limitation can trigger lipid and starch accumulation, as well. Algal cultivation under Mg^{2+} or Ca^{2+} limitation has been shown to trigger both *de novo* synthesis of lipids (rather than conversion of starch to lipids) and starch accumulation (Hanifzadeh et al., 2018).

Benefits of Degradation

Energy Production

During the day, green algae use energy from sunlight to power carbon fixation via the Calvin cycle. At night, when no light energy is available, they use carbon storage compounds to produce cellular energy. While starch is the main energy reserve utilized by algae, triacylglycerols can also be broken down for energy, provided O_2 is available as an electron sink (Vitova et al., 2014).

In alphaproteobacterial methanotrophs, PHB degradation is used mainly to provide energy for the cell under either O_2 or methane limited conditions (Pieja, Sundstrom, et al., 2011). PHB degradation has also been hypothesized to provide energy for nitrogen fixation and for methane oxidation, even during carbon replete growth (Pieja, Sundstrom, et al., 2011; Zhang et al., 2019).

Low O_2 Conditions

O_2 is needed by the aerobic methanotrophs both for methane assimilation via methane monooxygenases and as a terminal electron acceptor. Some gammaproteobacterial methanotrophs can directly ferment methane to reduced carbon byproducts, effectively partitioning O_2 between biosynthetic processes and the electron transport chain (Kalyuzhnaya et al., 2013). Other methanotrophs rely on fermentation of carbon storage compounds to survive low O_2 conditions (Thomson et al., 1976; Margarita Vecherskaya et al., 2009). PHB fermentation could also supply reducing power for methane assimilation during recovery from O_2 or methane limitation, which would shorten the lag phase and provide a competitive growth advantage (Pieja, Sundstrom, et al., 2011).

Green algae produce O_2 as a byproduct of oxygenic photosynthesis in the presence of light. In the dark, however, cultures can become anoxic due to a high demand for O_2. Starch can be fermented in the dark under low O_2 conditions to provide maintenance energy and potentially to help prepare the cell for greater metabolic activity once light becomes available (Raven & Beardall, 2016). Triacylglycerol stores, however, are broken down via the O_2-requiring β oxidation pathway, limiting their utility during dark O_2 limitation.

Production of Compatible Solutes

Compatible solutes are small, water soluble organic compounds that are produced by cells in order to maintain appropriate intracellular osmotic pressure relative to the environment (Hagemann, 2016; Oren, 2001). They are often produced under conditions of high environmental osmotic pressure in places like the ocean or soda lakes. In green algae, starch can be degraded to the compatible solute glycerol even during light conditions, when Calvin cycle carbon could also be used to form glycerol. The amount of glycerol produced from starch vs. the Calvin cycle increases in a *Dunaliella* species with increasing salt stress, showing that starch reserves are beneficial for survival under high salt conditions (Goyal, 2007). Glycerol could also be produced from starch at night. Sucrose is another common compatible solute and is produced by both methanotrophs and green algae. Sucrose accumulation has been shown in a salt-tolerant gammaproteobacterial methanotroph and is tightly linked to glycogen accumulation (S. Yu But et al., 2020; Khmelenina et al., 1999). In green algae, sucrose has been hypothesized to be protective from heat stress in addition to osmotic pressure (Hagemann, 2016).

Metabolic Modeling

Stoichiometric metabolic modeling is used in this work to investigate carbon and energy flow through microbial biochemical networks. Building an *in silico* metabolic model often uses the genome of an organism, which defines the list of potential biochemical reactions that can be catalyzed by the organism. Computational predictions can then be made for microorganisms growth on different substrates or under different stress conditions. Models must be carefully curated, mass and charge balanced, and have an accurate representation of the biomass

composition of the organism to produce accurate results (A. Beck et al., 2018; Thiele & Palsson, 2010).

Chapter Two of this work uses Elementary Flux Mode Analysis (EFMA) to analyze core metabolic models of aerobic methanotrophs. EFMA calculates all possible, minimal, biochemical pathways for substrate flux through a metabolic system (elementary flux modes, referred to here as EFMs or modes) (Trinh et al., 2009). This method is thus considered an unbiased approach as the initial solutions are not limited by assumptions about constraints and optimization criteria (A. E. Beck et al., 2017; Hunt et al., 2014). Each mode represents a potential phenotype that could be realized by the organism of interest, and, because a large number of possible modes are often predicted, different analytical methods are used to determine which potential phenotypes are physiologically relevant for a given environment. One common method is to rank the possible EFMs based on criteria or constraints that are proposed to be competitive for survival of an organism. For example, a low resource cost criterion will select for phenotypes that allow an organism to use a limiting substrate more efficiently. However, metabolic pathways that produce a large amount of energy or biomass precursors, both of which could be useful for an organism, often require a large input of resources from the environment (R. P. Carlson, 2009). Competing multiple criteria against each other in this way defines a tradeoff curve of optimal phenotypes that would be likely to be expressed by the organism. EFMA is computationally demanding and as a result is best suited to analyzing modest models of central carbon metabolism.

Chapter Three of this work uses Flux Balance Analysis (FBA) to analyze a model of *Chlorella sorokiniana* SLA-04, a eukaryotic microalga. FBA is a linear optimization technique

that incorporates optimization criteria directly, using an objective function to predict a single optimal phenotype for a given scenario. Common optimality principles include maximization of biomass yield, maximization of energy production, or minimization of limiting resources like O_2 or nitrogen. FBA is commonly used to analyze larger metabolic models that are computationally difficult to investigate using other methods (Orth et al., 2010).

Overview of Chapters

Chapter Two investigates the role of PHB and glycogen degradation in methanotroph metabolism under O_2 stress. Chapter Two also provides step-by-step instructions for building core metabolic models of organisms with biochemistries that are not easily captured by automated model building systems. Chapter Three compares the role of starch and lipids in algal survival in the dark and under conditions of high osmotic stress. Chapter Four presents a KBase workflow for analysis of microbial community interactions in a high alkalinity system. These chapters have all been prepared as manuscript drafts. Chapter Five provides a summary of results and proposes future research directions for each project.

CHAPTER TWO

THE ROLE OF CARBON STORAGE COMPOUNDS IN METHANOTROPH METABOLISM UNDER HYPOXIC/ANOXIC GROWTH CONDITIONS: A MODELING APPROACH

Contribution of Authors and Co-Authors

Author: Adrienne D. Arnold

Contributions: Conceived and directed the research, performed analysis, conducted literature review, wrote the manuscript

Co-Author: Dr. Ross P. Carlson

Contributions: Conceived and directed the research

Manuscript Information

Adrienne D. Arnold and Ross P. Carlson

[TBD]

Status of Manuscript:
__X__ Prepared for submission to a peer-reviewed journal
____ Officially submitted to a peer-reviewed journal
____ Accepted by a peer-reviewed journal
____ Published in a peer-reviewed journal

Abstract

Aerobic methanotrophs grow at oxic-anoxic interfaces and use competitive strategies to survive low O_2 conditions. Partial denitrification and degradation of accumulated carbon storage compounds are two common methods for producing cellular energy under O_2-limited conditions. These two strategies are both ecologically important; partial denitrification produces nitrous oxide, a potent greenhouse gas, and catabolism of carbon storage compounds produces organic byproducts that can support associated heterotrophic organisms and thus influences methane cycling. Two metabolic models were constructed, one for gammaproteobacterial (type I) and one for alphaproteobacterial (type II) methanotrophs. These models quantify the physiological limits of the two methanotroph metabolisms at low O_2 availability.

Motivation

Methanotrophs are prokaryotes that can utilize methane as their sole carbon and energy source. These organisms convert methane to methanol and to multi-carbon compounds, a process which is of both ecological and industrial importance. Methanotrophs can act as primary producers in the environment by supplying multi-carbon compounds that support associated microbiomes (Shelley et al., 2014). In industry, biological conversion of methane to chemical feedstocks like methanol, formate, formaldehyde, and acetate can take place at ambient temperature and pressure, allowing for a safer and less energy-intensive process that uses a widely available and comparatively cheap carbon substrate (Strong et al., 2015).

The original categorization of methanotrophs by Whittenbury et al. in 1970 divided methanotrophs into two main groups based on membrane morphology: the alphaproteobacterial

(type II) methanotrophs, and the gammaproteobacterial (type I) methanotrophs (C. Anthony, 1982; Lawrence & Quayle, 1970; Whittenbury et al., 1970). This classification system has held, and these two groups remain the best-studied aerobic methanotrophs. In addition to membrane structure, several key metabolic functions delineate the two. Alphaproteobacterial methanotrophs use the serine pathway for methane assimilation and can accumulate the storage compound polyhydroxybutyrate (PHB). Gammaproteobacterial methanotrophs use the ribulose monophosphate (RuMP) pathway for methane assimilation and accumulate glycogen as a storage compound.

Type I and type II methanotrophs both use methane monooxygenases as the first step in both assimilatory and dissimilatory methane metabolism. These enzymes require both electrons and O_2 to convert methane to methanol, which is then converted to formaldehyde. For assimilatory metabolism, formaldehyde is incorporated into biomass; for dissimilatory metabolism, it is oxidized to CO_2 (Ross & Rosenzweig, 2017). Despite their obligate requirement for O_2, however, natural populations of methanotrophs are often found growing at oxic-anoxic interfaces (reviewed in Guerrero-Cruz et al., 2021). This raises the question of how obligately aerobic methanotrophs both survive and remain competitive under low O_2 conditions.

Many methanotrophs have genes encoding the partial (aerobic) denitrification pathway, where NO_3^- is reduced to nitrous oxide (N_2O). Nitrate reduction under low O_2 conditions with methane as an electron donor has been known for many years (Costa et al., 2000; Guerrero-Cruz et al., 2021; Kits et al., 2015). Nitrate reduction by methanotrophs has important implications for climate change and nitrogen cycling, as N_2O is a more potent greenhouse gas than methane and is difficult to biologically or chemically convert to nitrate (Stein, 2020; Stein & Klotz, 2011).

In addition to denitrification, type I methanotrophs can "ferment" methane via the RuMP pathway and a pyrophosphate (PPi)-dependent glycolysis. Growth of *Methylomicrobium alcaliphilum* 20Z in chemostat cultures under low oxygen conditions resulted in the production of organic acids indicative of fermentation (formate, acetate, lactate, and, under batch conditions with an N_2 headspace, succinate and 3-hydroxybutyrate) as well as production of H_2. Roughly 50% of the ^{13}C-methane consumed under these low oxygen conditions was excreted as organic acids (Kalyuzhnaya et al., 2013). These results were later investigated in a metabolic modeling study of *M. alcaliphilum* 20Z, where it was predicted that acetate produced from the phosphoketolase pathway was the main method of ATP generation under low O_2 levels. It should be noted that several organic acid byproducts were included in the biomass term of this model (Akberdin et al., 2018). While the term "fermentation" is used to describe this type of growth, O_2 is still required to oxidize methane.

An alternative to direct fermentation of methane is the catabolism of carbon storage compounds. Many microorganisms use storage compounds like glycogen and PHB for supplemental energy or carbon under stress conditions where exogenous resources are not present in a sufficient amount to meet the demands of cellular processes. These conditions include O_2 scarcity, which is likely to be experienced by methanotrophs living at oxic-anoxic zones on a regular basis (Roslev & King, 1994). The type of storage compound that is accumulated by the organism depends both on its metabolic capabilities and on environmental conditions like substrate availability (Wilkinson, 1959, 1963). In methanotrophs, it is known that type II methanotrophs preferentially accumulate PHB (Pieja, Rostkowski, et al., 2011), synthesis of which shares several steps with the ethylmalonyl-CoA (EMC) pathway that is used by these

organisms to drive the serine pathway for methane assimilation. Type I methanotrophs accumulate glycogen, which is readily produced via a combination of gluconeogenesis and the RuMP pathway for methane assimilation.

There are reports of production of organic acids by type II methanotrophs under starvation conditions dating back many decades. One early report in *Methylosinus trichosporium* OB3b, a model alphaproteobacterial methanotroph (Stein et al., 2010), detailed the accumulation of acetone with the concomitant degradation of PHB. Interestingly, degradation of PHB was seen only under conditions where OB3b was incubated with compounds that are now known to interact with its MMOs but cannot support growth, suggesting that PHB consumption is used to power methane oxidation after a period of carbon starvation (Thomson et al., 1976). In other organisms, PHB consumption has been shown to support replication, not just energy production, although this has not been reported for methanotrophs (early reports summarized in Wilkinson, 1959).

Several additional studies reinforce the premise of PHB catabolism for energy generation rather than cell division in type II methanotrophs. A study in *Methylocystis parvus* OBBP demonstrated that PHB breakdown did not lead to cell replication, and little PHB was consumed when carbon and nitrogen limitation conditions were applied. Supplementation with formate, a C_1 electron donor, delayed PHB consumption, while supplementation with glyoxylate, a C_2 donor, did not (Pieja, Sundstrom, et al., 2011). Degradation of PHB under starvation conditions to acetone, acetate, butyrate (butanoate), isopropanol, 2,3-butanediol, and succinate in *Methylocystis parvus* MTS was shown in both short-term (two week) and long-term (90 day) experiments, although cell counts were not determined (M. Vecherskaya et al., 2001; Margarita

Vecherskaya et al., 2009). The authors suggest that which metabolites were excreted depended on whether starvation conditions were anaerobic or microaerobic (Margarita Vecherskaya et al., 2009). PHB degradation has also been linked to denitrification (Dam et al., 2013).

In addition to consumption under anoxic conditions, several studies have demonstrated the cyclical accumulation and consumption of PHB under nutrient replete growth (Pieja, Sundstrom, et al., 2011; Ren et al., 2009). In a study in *M. trichosporium* OB3b, PHB consumption was proposed to power N_2 fixation (Zhang et al., 2019). A transcriptomics study of *M. trichosporium* OB3b also showed that both PHB synthesis and degradation genes were expressed at the same time (Matsen et al., 2013).

There are also earlier reports of organic acid production by gammaproteobacterial methanotrophs, with the carbon source for these generally being attributed not to methane fermentation, but instead to the breakdown of carbon storage byproducts like glycogen (Kalyuzhnaya et al., 2013). Methane fermentation and glycogen or PHB degradation both release organic byproducts to the environment, potentially supporting associated heterotrophic communities and influencing microbial community structure at oxic-anoxic interfaces. Methane conversion to these byproducts also has important implications for global methane cycling.

This paper aims to address the role of carbon storage compounds in methanotroph growth under both oxic and anoxic conditions. The driving questions are as follows:

1. How does consumption of storage compounds in type I and type II methanotrophs compare to other possible acclimation strategies for low O_2 conditions, like partial denitrification? Does production of different fermentative byproducts depend on the degree of O_2 scarcity?

2. Is the degradation of these storage compounds likely to result in high levels of organic acids being secreted from the methanotrophs? If so, could this be part of the mechanism for carbon transfer between methanotrophs and heterotrophs?
3. Can the stored energy and carbon theoretically be used for growth, or is it more likely (as is generally accepted for at least alphaproteobacterial methanotrophs) that the stored compounds are used to fuel a restart of the energy-intensive methane oxidation process after starvation? Does the same trend hold for both PHB and glycogen consumption?
4. What are the predicted effects/purpose of co-consumption of methane and PHB or glycogen under nutrient replete conditions?
5. It was long thought that both alpha- and gammaproteobacterial methanotrophs could produce PHB, but more recent studies have shown PHB is only accumulated by the alphaproteobacterial methanotrophs. Could alphaproteobacterial methanotrophs theoretically use glycogen as a carbon storage compound instead of PHB? If not, is there an energetic constraint, or rather a flux constraint, as little carbon should be flowing through gluconeogenesis vs. the ethylmalonyl-CoA (EMC) pathway?
6. Methanotrophs consume the greenhouse gas methane while producing CO_2 and sometimes nitrous oxide. Under what conditions are methanotrophs predicted to decrease greenhouse gas burden, and when are they expected to contribute to climate change?

7. How does copper limitation impact respiration in alphaproteobacterial methanotrophs?

This chapter uses elementary flux mode analysis to compare the central carbon metabolism of type I and type II methanotrophs. Emphasis is placed on the ways in which central carbon metabolism structure influences the carbon storage compounds that are utilized by methanotrophs, and how O_2 limitation impacts the breakdown of these storage products, which supplies multi-carbon nutrients for other microorganisms in the environment. The role of methanotrophs in greenhouse gas cycling is also examined.

This work also details the steps required to build and analyze a core-scale metabolic model of organisms with metabolisms that are not easily captured by automated model building tools such as KBase (Edirisinghe et al., 2016). While protocols have been developed for building metabolic models, they tend to focus on high-level modeling processes or refinement of genome-scale models (Thiele & Palsson, 2010). This work shows the process of building a detailed core metabolic model with demonstrations of how model construction influences predictions. Literature reviews are followed by in-depth explanations of reaction incorporation and development.

Methods

Two core-scale metabolic models were constructed: one for type II methanotrophs, and one for type I methanotrophs. These models include reactions for central carbon, nitrogen, and energy metabolism, including fermentative pathways. The alphaproteobacterial model additionally includes the EMC pathway and reactions for PHB production and degradation. The

gammaproteobacterial model includes the Entner-Doudoroff glycolytic pathway and the phosphoketolase pathway as well as glycogen synthesis and breakdown. Details on these pathways and their inclusion in their respective models are provided in the "Biochemistry" section and in the supplemental files. Global Warming Potential (GWP) calculations are included within the model, allowing for predictions of greenhouse gas release by methanotrophs under different cultivation conditions. The integration of GWP into model reactions is based on a technique developed in Beck et al., 2022 for analysis membrane occupancy costs (Beck et al., 2022, manuscript in progress). More information on these reactions is in the GWP section.

Reactions included in the model were designed using the MetaCyc, KEGG, and BRENDA databases as well as information from literature. Where possible, metabolite names are based on MetaCyc conventions. Transport reactions include the uptake of methane, O_2, nitrate, ammonium, N_2, and phosphate. Nitrate and phosphate transport are both ATP-dependent. Reversible reactions are present for water and proton transport. Excretion reactions are present for methanol, formate, acetate, acetone, ethanol, succinate, and pyruvate. The type II model includes PHB formation and uptake reactions. The type I model includes glycogen formation and uptake.

The biomass terms of the models are comprised of the central carbon metabolites that are precursors for the macromolecules of the cell. They are based on the biomass term developed in Carlson, 2007 on the theory proposed in Neidhardt et al., 1990 (R. P. Carlson, 2007; R. Carlson & Srienc, 2004; Neidhardt et al., 1990a; Varma & Palsson, 1994). Where possible, the biomass term reflects the cellular composition of *M. trichosporium* OB3b (Yang et al., 2013). Where no values had been determined for OB3b, values from *Escherichia coli* were used (Neidhardt et al.,

1990a). The biomass term is in units of moles, and where experimental values were given in terms of ratios or cell dry weights, appropriate conversions were made using the molar mass of the compounds and the standard conversion of 24 grams cell dry weight = 1 carbon mole (Cmol) of biomass. The degree of reduction was adjusted to 4.2 moles of electrons per Cmol biomass on an ammonium basis for the nitrogen species using the NADPH balance to adjust electrons. The type II model uses PHB as a carbon storage compound, while the type I model uses glycogen.

ATP maintenance adjustments were made using the detailed measurements in Rostkowski et al., 2013 for growth of OB3b on nitrate and methane. Roughly 3.4 moles of ATP are required per Cmol of biomass. All predictions in this paper are for growth on nitrate, however, growth measurements are available for ammonium and N_2 cultivation, as well, making nitrogen source comparisons a good possibility for future directions (Rostkowski et al., 2013). For ease of comparison, the biomass terms for both models use the same overall ATP requirement.

These models were compared using elementary flux mode analysis (EFMA). EFMA determines all of the possible minimal pathways (modes) for flux through a metabolic network. Each mode can be considered a possible phenotype that could be expressed by the organism. Optimization criteria for maximization of biomass and efficient use of limiting resources were used to determine which phenotypes are most likely to be expressed under different stress conditions. Model construction and EFMA was performed in CellNetAnalyzer (von Kamp et al., 2017). Tradeoff curve analysis code was modified from Beck, 2020 (A. E. Beck, 2020).

Both the type I and the type II models are also available in Escher-FBA. Escher-FBA is an online modeling tool that allows for fast and easy visualization of flux predictions without the

need for coding or modeling programs (Rowe et al., 2018). It should be noted that both the type I and the type II models follow EFMA conventions, not FBA conventions, for the reaction directionality. Escher-FBA is also a simplified modeling program and does not currently filter out two-reaction loops as CellNetAnalyzer does, which can substantially impact predictions made within the web application. Future updates to Escher-FBA may reduce this problem by implementing loopless FBA techniques, which have been developed for other prediction tools (Rowe et al., 2018; Schellenberger et al., 2011).

Biochemistry

Methane Oxidation: Literature Review

Figure 2.1. Methane monooxygenase reactions as written in the type I and type II models. QH2 refers to quinol, and Q refers to quinone.

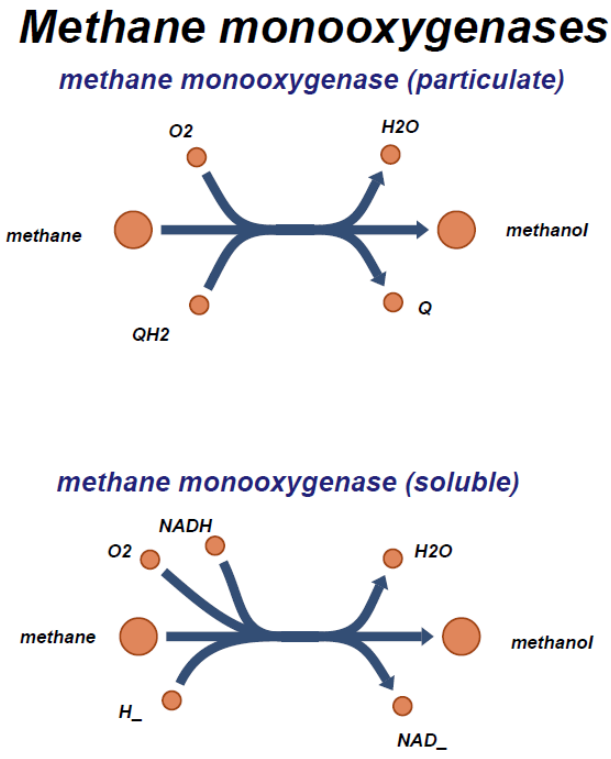

Figure 2.1 Continued.

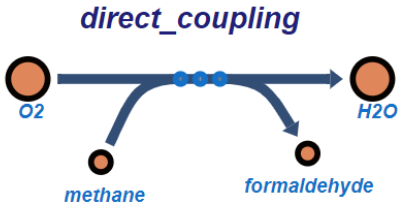

Methane assimilation begins with the energy-requiring oxidation of methane to methanol by one of two methane monooxygenases: the membrane-bound particulate methane monooxygenase (pMMO) or the cytoplasmic soluble methane monooxygenase (sMMO). sMMO is proposed to use NADH as an electron source, and while the electron source of pMMO has not been definitively determined, though it is thought to be a quinol (D.-W. Choi et al., 2003; Hakemian et al., 2008). Other methods of electron transfer to pMMO have been proposed, including direct coupling of methanol dehydrogenase to pMMO, which uses the electrons produced in the oxidation of methanol to power further methane oxidation (Akberdin et al., 2018; Tonge et al., 1977). sMMO is also less specific for methane and can oxidize a wider range of substrates, although these cannot be used by methanotrophs for energy or growth (Semrau et al., 2018). The lower energy requirement and higher specificity make pMMO the most metabolically efficient methane monooxygenase under ideal culturing environments (Semrau et al., 2010).

The majority of methanotrophs express pMMO, some express both sMMO and pMMO (Hakemian & Rosenzweig, 2007), and at least one methanotroph (a marine methanotroph) expresses only sMMO (Vekeman et al., 2016). In the methanotrophs that can express both sMMO and pMMO, expression is tightly controlled by a mechanism referred to as the “copper

switch" (Park et al., 1991; Semrau et al., 2018; Stanley et al., 1983). The active site of pMMO contains copper, and, as a result, its expression is dependent on copper availability. At low copper to biomass ratios, sMMO is the sole methane monooxygenase expressed. At high copper to biomass concentrations, only pMMO is expressed (D.-W. Choi et al., 2003). The copper switch has extensive effects on gene expression and metabolism (Gu & Semrau, 2017; Matsen et al., 2013).

Methanobactin is a chalkophore used by methanotrophs to acquire copper from the environment. It has an incredibly high binding affinity for copper (10^{16} M^{-1}) and similar metals and has even been shown to inhibit copper-requiring metabolism in other microorganisms (Balasubramanian et al., 2011; Balasubramanian & Rosenzweig, 2008; Chang et al., 2018; McCabe et al., 2017; Stein, 2020). It is excreted in the unbound form, then reacquired as a methanobactin-copper complex by the methanotroph via active transport, although soluble copper can also be taken up via porins (Balasubramanian et al., 2011). When copper is provided in an insoluble form, methanobactin is required to trigger the copper switch between sMMO and pMMO, indicating that it is especially useful for pMMO expressing methanotrophs grown on insoluble copper sources (Knapp et al., 2007). Methanobactin also has peroxidase activity and may help reduce oxidative stress (D.-W. Choi et al., 2003; D. W. Choi et al., 2008). sMMO expression may be triggered even in the presence of copper if other metals are present in high enough concentrations to prevent copper binding to methanobactin (Kalidass et al., 2014).

The number of copper atoms required for pMMO activity has been debated for years, with estimates generally ranging between 2 and 20 copper atoms per enzyme. (Lieberman & Rosenzweig, 2004; Semrau et al., 2010). Several reasons have been proposed for the

discrepancy in estimates: the number of copper atoms in pMMO may vary between different methanotroph species (Hakemian et al., 2008); preparations of membrane-bound enzymes are difficult and differences in wash protocols may result in the retention of excess metal ions (Lieberman & Rosenzweig, 2004); binding of methanobactin to pMMO preparations, which increases pMMO activity, increases the copper atom count (D.-W. Choi et al., 2003; Hakemian & Rosenzweig, 2007). pMMO is also proposed to sometimes contain a diiron center, which may catalyze the actual reaction of methane oxidation (Semrau et al 2010). Zinc has also been detected in pMMO preparations (Semrau et al., 2010) and in methanobactin solutions when little copper is present (H. J. Kim et al., 2005), but it is likely that this binding is not relevant to pMMO function *in vivo*.

Methane Oxidation: Model Construction. In the presented work, two reactions are included for pMMO: one using the direct coupling method of reduction, and one using the quinol pool as a source of reductants. The direct coupling method for pMMO was better able to replicate experimental values of biomass yields for the type II methanotrophs and thus is the focus of modeling predictions (discussed in the ATP maintenance section). For the sMMO reaction, only NADH was investigated as a reductant. A value of 3 copper atoms per pMMO reaction is used (Hakemian et al., 2008). No iron atoms were included in the metal content of pMMO, based on the findings of Hakemian, et al. for *Methylosinus trichosporium* OB3b (Hakemian et al., 2008).

Table 2.1. Methane oxidation reactions incorporated into the models on the basis of the literature review. QH2 is used as an abbreviation for a generic quinol, and Q is used to represent a generic quinone.

Model Reactions: Methane Oxidation				
Model	Enzyme	Reaction	Copper cost	Iron cost
Both	Particulate methane monooxygenase (pMMO)	methane + QH2 + O2 = methanol + Q + H2O	3	0
Both	Soluble methane monooxygenase (sMMO)	methane + NADH + H+ + O_2 = methanol + NAD+ + H_2O	0	2
Both	Direct coupling of pMMO and methanol dehydrogenase	methane + O2 = formaldehyde + H2O	3	1

Methanol Oxidation: Literature Review

Figure 2.2. The methanol dehydrogenase reaction in the type I and type II models. Cytc is used as an abbreviation for an oxidized cytochrome c, and cytcE is an abbreviation for a reduced cytochrome c. H_pmf refers to protons that contribute to the proton motive force.

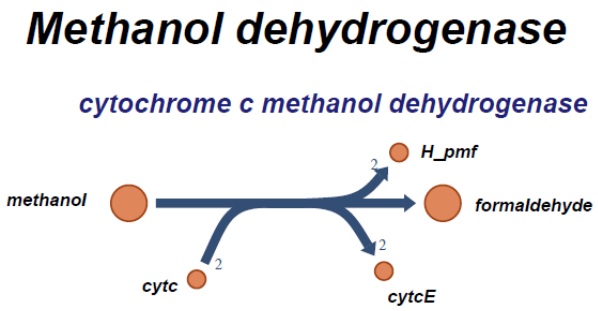

After the initial step of methane oxidation to methanol, methanol is oxidized to formaldehyde by methanol dehydrogenase. Methanol dehydrogenase is pyrroloquinoline quinone (PQQ)-dependent with cytochrome c as its electron acceptor. Methanol dehydrogenase is located in the periplasm and generates protons that contribute to the proton motive force. See Anthony, 1992, Anthony et al., 1994, and Anthony and Williams, 2003 for overviews of research into the

fundamental workings of methanol dehydrogenase (C. Anthony et al., 1994; Christopher Anthony, 1992; Christopher Anthony & Williams, 2003).

There are two classes of methanol dehydrogenase in methanotrophs: one with calcium in its active site (Mxa-MeDH) and one with a rare earth element (REE) in the active site (Xox-MeDH) (Farhan Ul Haque et al., 2015; Hibi et al., 2011; Nakagawa et al., 2012; Pol et al., 2014). Cerium and lanthanum have both been investigated for their role in methanol dehydrogenase activity (Farhan Ul Haque et al., 2015; Good et al., 2019). The REE-dependent version of methanol dehydrogenase appears to be more catalytically active (Hibi et al., 2011), likely because the lanthanides can be stronger Lewis acids than calcium (Cotruvo, 2019). Its expression, however, is subject both to copper levels, with low Cu levels promoting expression of Xox MeDH, and concentration of the REE, with copper concentration appearing to be the most important factor in both MeDH and genome-wide gene expression (Farhan Ul Haque et al., 2015; Gu & Semrau, 2017). While some versions of Xox-MeDH produce formate from methanol (Pol et al., 2014), studies in both *Methylobacterium extorquens* AM1 (Good et al., 2019) and *Methylosinus trichosporium* OB3b (Gu & Semrau, 2017) show production of formaldehyde by Xox-MeDH. Expression of Xox-MeDH is thus unlikely to negatively impact biomass production, which in methanotrophs begins at formaldehyde.

Methanol Oxidation: Model Construction. A cytochrome c-dependent, proton-pumping methanol dehydrogenase is included in the model. As the stoichiometric reactions are typically the same for both types of methanol dehydrogenase and either can support growth in OB3b (Farhan Ul Haque et al., 2016), no REE-dependence is included in this model. The iron cost for methanol dehydrogenase is one atom based on the information for EC 1.1.2.7 in BRENDA.

Table 2.2. Methanol oxidation reactions incorporated into the models on the basis of the literature review. Cytc is used as an abbreviation for an oxidized cytochrome c, and cytcE is an abbreviation for a reduced cytochrome c. H_pmf refers to protons that contribute to the proton motive force.

Model Reactions: Methanol Oxidation				
Model	Enzyme	Reaction	Copper cost	Iron cost
Both	Methanol dehydrogenase (MeDH)	methanol + 2 cytc = formaldehyde + 2 cytcE + 2 H_pmf	0	1

Formaldehyde oxidation: Literature Review

There are three pathways for formaldehyde oxidation in methanotrophs: a formaldehyde dehydrogenase, part of dissimilatory methane metabolism that converts formaldehyde directly to formate; the assimilatory tetrahydromethanopterin (H_4MPT) and tetrahydrofolate (THF) pathways, which use different cofactors to carry out a four step oxidation of formaldehyde to formate; and the ribulose monophosphate pathway, which is used by gammaproteobacterial methanotrophs to funnel methane into glycolysis (Hanson & Hanson, 1996; Matsen et al., 2013; Naizabekov & Lee, 2020).

Formaldehyde dehydrogenase and formate dehydrogenase

Figure 2.3. Formaldehyde dehydrogenase and formate dehydrogenase reactions in the type I and type II models. Cytc is used as an abbreviation for an oxidized cytochrome c, and cytcE is an abbreviation for a reduced cytochrome c. H_pmf refers to protons that contribute to the proton motive force.

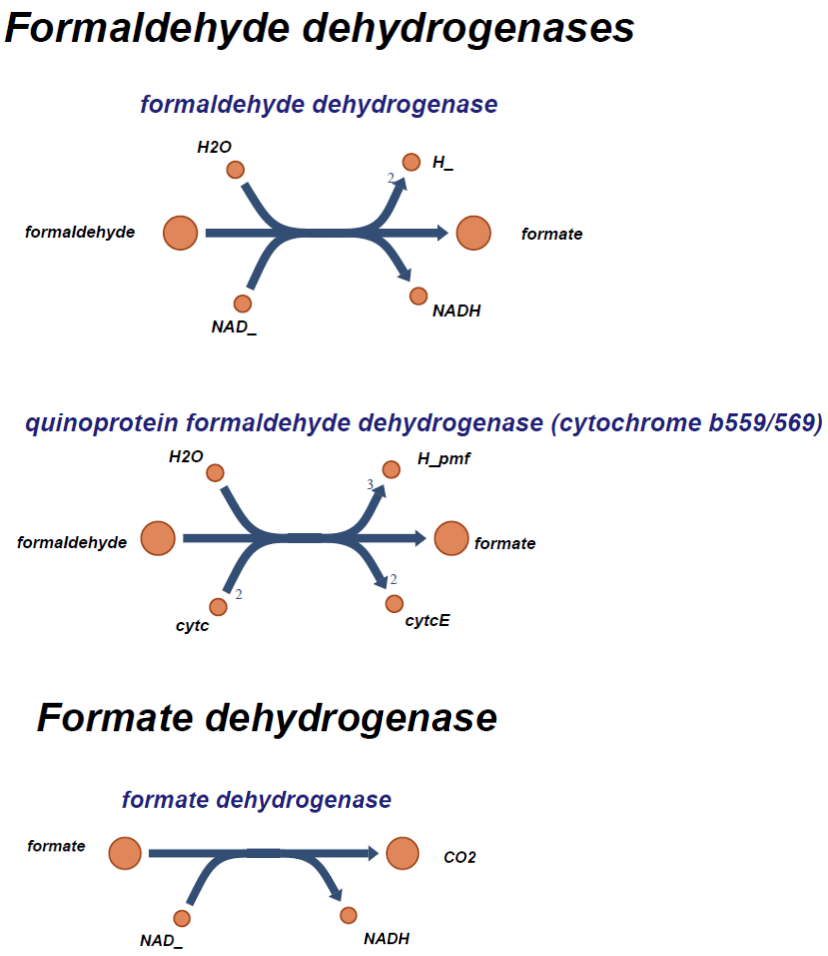

In dissimilatory methane metabolism, after the conversion of methanol to formaldehyde by methanol dehydrogenase, it is thought that formaldehyde dehydrogenase converts formaldehyde into formate (Hanson & Hanson, 1996). There are two main types of formaldehyde dehydrogenases described in methanotrophs: one cytoplasmic, and one membrane-bound. The cytoplasmic formaldehyde dehydrogenase is NAD-dependent, while the membrane

bound is cytochrome-dependent. The cytochrome-dependent formaldehyde dehydrogenase has been reported experimentally in OB3b (Patel et al., 1980), but in the genome study by Matsen et al., only generic aldehyde dehydrogenases were found, two of the three of which were NAD-dependent (Matsen et al., 2013). Previous studies in *Methylococcus capsulatus* Bath have shown that expression of the two versions is linked to copper concentration, likely to balance electron flow depending on the different cofactors for the MMOs being expressed (Hakemian & Rosenzweig, 2007; Zahn et al., 2001). Others, however, have found that enzymes other than formaldehyde dehydrogenase may be responsible for the NAD-dependent activity in *M. capsulatus* Bath (Adeosun et al., 2004). The cytochrome-dependent formaldehyde dehydrogenase contributes to the proton motive force.

An NAD-dependent formate dehydrogenase from OB3b has been purified and characterized by two groups (Jollie & Lipscomb, 1991; Yoch et al., 1990). The sequence encoding this enzyme was also found in the genome study by Matsen et al. (Matsen et al., 2013). Other methanotrophs have multiple formate dehydrogenases, although it has been shown in *Methylobacterium extorquens* AM1 that only one formate dehydrogenase is necessary for growth on formate, and none are required for growth on methanol (Chistoserdova et al., 2000).

H4MPT and THF-based formaldehyde oxidation

Figure 2.4. Tetrahydromethanopterin (H4MPT) and tetrahydrofolate (THF) pathways for formaldehyde oxidation.

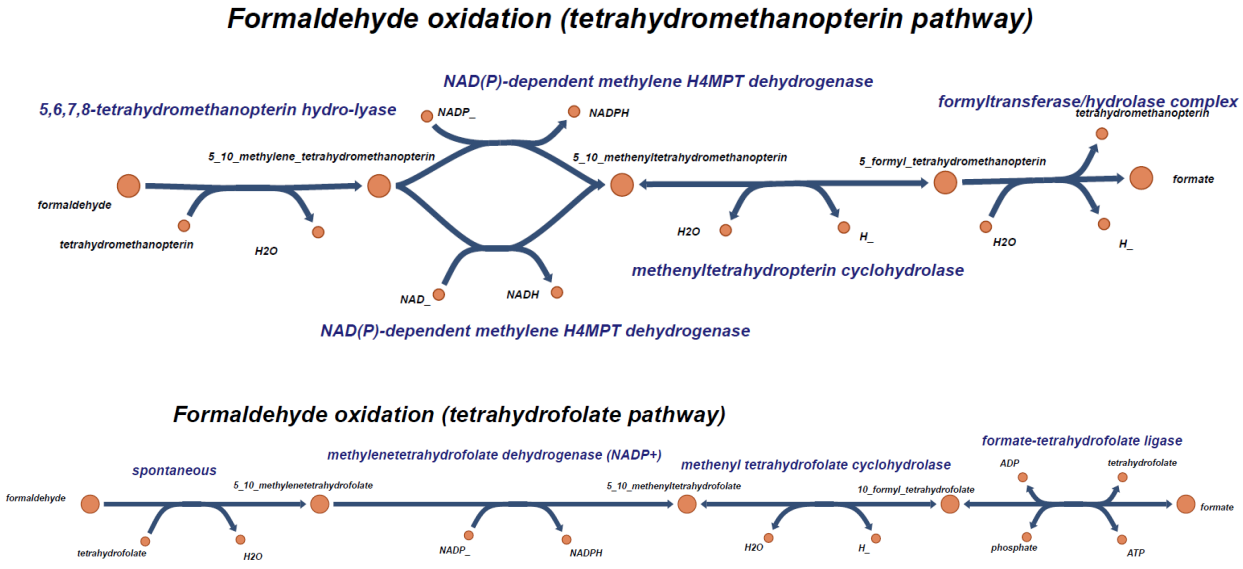

Many methanotrophs encode both the tetrahydromethanopterin (H4MPT) and the tetrahydrofolate (THF) pathways for formaldehyde oxidation (Chistoserdova et al., 1998; Matsen et al., 2013). Both of these cofactor-dependent pathways are linear and result in the production of formate (Vorholt, 2002). The H4MPT pathway has been shown to be the most active pathway in several methanotrophs during growth on methane (Crowther et al., 2008; Matsen et al., 2013; Pomper et al., 1999). This is likely due to thermodynamic differences between the two methyl group carriers, with H4MPT transferring methyl groups more easily, and because of energy differences between the two pathways, as the H4MPT pathway can generate NADH (Maden, 2000; Vorholt, 2002). The H4MPT pathway does require an additional ATP, however (Crowther et al., 2008). 5,10-methylenetetrahydrofolate, an intermediate of the THF pathway that can be

generated using either majority H_4MPT- or THF-dependent enzymes, is the donor of the 1C group from methane into the serine pathway in type II methanotrophs (Crowther et al., 2008).

Ribulose monophosphate pathway

Figure 2.5: Ribulose monophosphate (RuMP) pathway in the type I model.

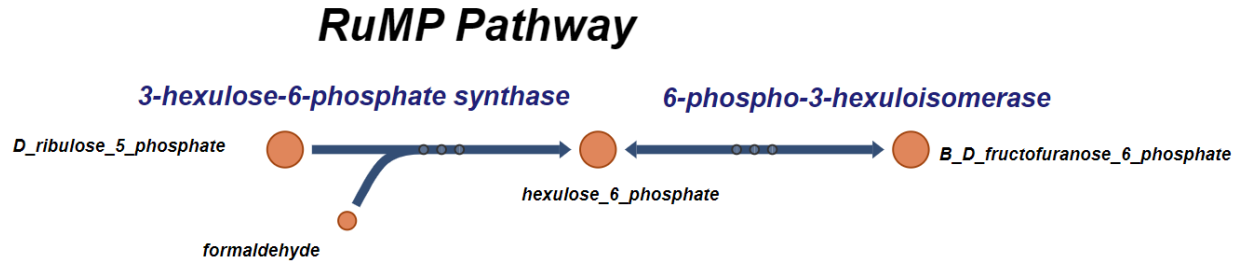

The ribulose monosphosphate (RuMP) pathway is present only in type II methanotrophs and is used for methane assimilation in these organisms. There are two steps: the condensation of formaldehyde with ribulose-5-phosphate to form a phosphorylated six carbon hexose, and the conversion of that hexose to fructose 6-phosphate (Khmelenina et al., 2019). From there, assimilation proceeds via glycolytic pathways.

Formaldehyde Oxidation: Model Incorporation. While there is continued debate over which version of formaldehyde dehydrogenase is encoded by different methanotrophs and over the relevance of this type of formaldehyde dehydrogenase in methanotroph metabolism (Klein et al., 2022; Vorholt, 2002), for completeness both possible reactions are included in the model. Only the NAD-dependent formate dehydrogenase is included in the model, as it is thought to be the most common form of formate dehydrogenase in methanotrophs (Hanson & Hanson, 1996). Both models contain the H_4MPT and THF pathways for formaldehyde oxidation. It should be noted that this does allow for formaldehyde assimilation via the serine pathway in type I methanotrophs (the presence of this pathway is described below). Modes that used the serine

pathway for formaldehyde assimilation were removed from analysis of the type I growth on methane, as the RuMP pathway is the major method of methane assimilation in gammaproteobacterial methanotrophs. Only the type I model includes the reactions for the RuMP pathway.

Table 2.3. Reactions for formaldehyde metabolism in type I and type II models. Cytc is used as an abbreviation for an oxidized cytochrome c, and cytcE is an abbreviation for a reduced cytochrome c. H_pmf refers to protons that contribute to the proton motive force.

Model Reactions: Formaldehyde Oxidation				
Model	Enzyme	Reaction	Copper cost	Iron cost
Both	Formaldehyde dehydrogenase	formaldehyde + NAD+ + H2O = formate + NADH + 2 H+	0	0
Both	Formaldehyde dehydrogenase (cytochrome)	formaldehyde + 2 cytc + H2O = formate + 2 cytcE + 3 H_pmf	0	0
Both	formate dehydrogenase	formate + NAD+ = NADH + CO2	0	4
Both	5,6,7,8-tetrahydromethanopterin hydro-lyase	formaldehyde + tetrahydromethanopterin = H2O + 5,10-methylene-tetrahydromethanopterin	0	0
Both	NAD(P)-dependent methylene H4MPT dehydrogenase	5,10-methylene-tetrahydromethanopterin + NAD+ = 5,10-methenyltetrahydromethanopterin + NADH	0	0
Both	NAD(P)-dependent methylene H4MPT dehydrogenase	5,10-methylene-tetrahydromethanopterin + NADP+ = 5,10-methenyltetrahydromethanopterin + NADPH	0	0
Both	methenyltetrahydropterin cyclohydrolase	5,10-methenyltetrahydromethanopterin + H2O = 5-formyl-tetrahydromethanopterin + H+	0	0
Both	formyltransferase/hydrolase complex	5-formyl-tetrahydromethanopterin + H2O = formate + tetrahydromethanopterin + H+	0	0

Table 2.3 continued.

Both	spontaneous	formaldehyde + tetrahydrofolate = 5,10-methylenetetrahydrofolate + H2O	0	0
Both	methylenetetrahydrofolate dehydrogenase (NADP+)	5,10-methylenetetrahydrofolate + NADP+ = 5,10-methenyltetrahydrofolate + NADPH	0	0
Type II	methenyl tetrahydrofolate cyclohydrolase	5,10-methenyltetrahydrofolate + H2O = 10-formyl-tetrahydrofolate + H+	0	0
Both	formate-tetrahydrofolate ligase	ATP + formate + tetrahydrofolate = ADP + 10-formyl-tetrahydrofolate + phosphate	0	0
Type I	3-hexulose-6-phosphate synthase	D-ribulose_5-phosphate + formaldehyde = hexulose_6-phosphate	0	0
Type I	6-phospho-3-hexuloisomerase	hexulose_6-phosphate = B-D-fructofuranose_6-phosphate	0	0

Serine Pathway: Literature Review

Figure 2.6. Serine pathway for formaldehyde assimilation in type II methanotrophs. The ethylmalonyl-CoA (EMC) pathway is used to replenish the glyoxylate supply if biomass precursors are pulled off of the serine pathway. The type I model does not include phosphoenolpyruvate carboxylase or methylene tetrahydrofolate cyclohydrolase.

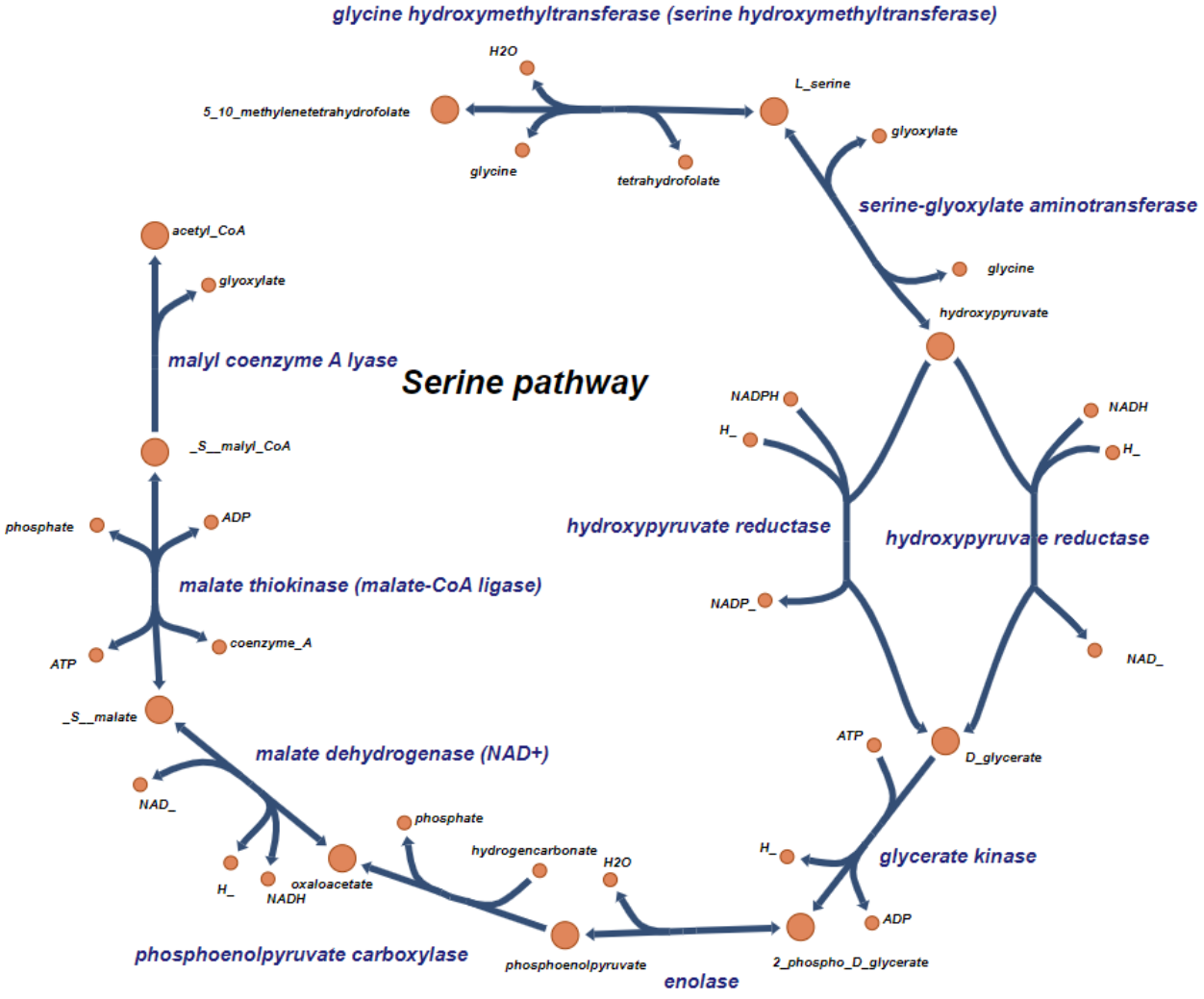

Figure 2.7. Ethylmalonyl-CoA (EMC) pathway and propanoyl-CoA degradation in the type II model. The EMC converts two carbon compounds to four carbon compounds, generating glyoxylate and propanoyl-CoA. Glyoxylate is used to power the serine pathway. Propanoyl-CoA is degraded to succinyl-CoA and can enter the citric acid cycle. QH2 is used as an abbreviation for a generic quinol, and Q is used to represent a generic quinone.

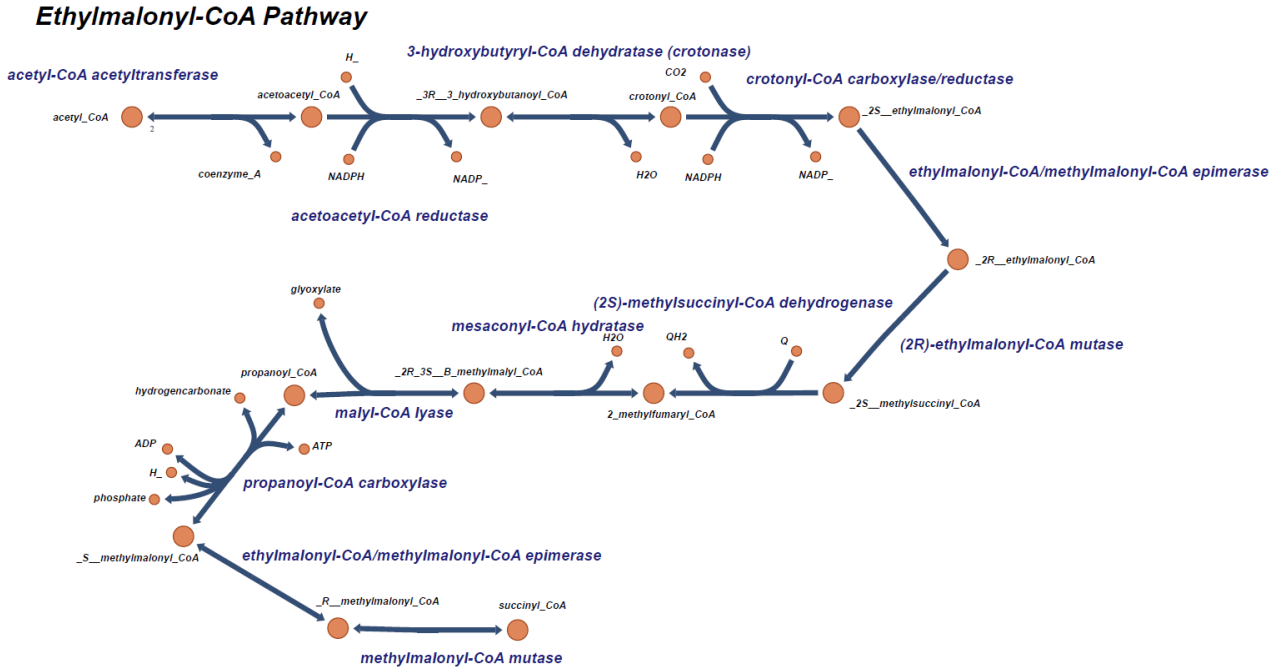

Type II methanotrophs use the serine pathway for formaldehyde assimilation into biomass (Khmelenina et al., 2019). The pathway begins with the conversion of glyoxylate to glycine, with glycine then accepting a methyl group from an intermediate of the THF pathway. 2-phosphoglycerate, phosphoenolpyruvate, oxaloacetate, malate, and acetyl-CoA are all intermediates of the serine pathway, making it a central hub for generation of biomass precursors (Christopher Anthony, 2011). In most type II methanotrophs, including OB3b, the glyoxylate required for the serine pathway is regenerated via the ethylmalonyl-CoA (EMC) pathway (Matsen et al., 2013; Peyraud et al., 2009; Yang et al., 2013). Some alphaproteobacterial methanotrophs use the glyoxylate shunt instead of the EMC pathway, which is less energy intensive and requires fewer enzymes but results in less CO_2 fixation overall (Christopher

Anthony, 2011; Crowther et al., 2008). The glyoxylate shunt has also been the focus of metabolic engineering experiments in type II methanotrophs (Schada von Borzyskowski et al., 2018).

Type I methanotrophs also encode the serine pathway (S. Y. But et al., 2017). A recent series of studies examined the properties of key serine pathway enzymes from various methanotrophs (Khmelenina et al., 2019). These studies generally support the idea of the serine pathway as a major biosynthetic pathway in type II methanotrophs but as a formaldehyde-detoxification method in type I methanotrophs (But et al., 2017, 2019; But et al., 2020). Interestingly, the serine-glyoxylate aminotransferase of *M. capsulatus* Bath was shown to be able to transfer an amino group from alanine to glyoxylate, rather than the typical serine to glyoxylate transfer, which forms glycine. It is proposed that this reaction, in combination with the reaction of alanine-pyruvate aminotransferase, could represent a link in gammaproteobacterial methanotrophs between the key intermediate pyruvate and the serine pathway and TCA cycle (S. Y. But et al., 2019). The alanine-glyoxylate transfer activity was lower than that of the standard reaction and may not be physiologically relevant (S. Y. But et al., 2019).

Serine Pathway: Model Incorporation. The EMC pathway was included in the type II model as the method of glyoxylate generation. Isocitrate lyase was not included in either model, as it is known to be present in few methylotrophs and is not essential for growth of type I methanotrophs (Christopher Anthony, 2011). Alternative methods of glyoxylate generation in type I methanotrophs are also not included, but represent an interesting possibility for future studies (S. Y. But et al., 2019).

Most type I methanotrophs do not encode phosphoenolpyruvate carboxylase, so this enzyme is not included in the type I model (although there are some exceptions, and alternate enzymes may exist—these are reviewed in Khmelenina et al., 2019). No gammaproteobacterial methanotrophs encode methylene tetrahydrofolate cyclohydrolase, so it is likewise excluded (Khmelenina et al., 2019) from the type I model, which reduces serine pathway function. To prevent loops while running predictions for glycogen degradation in type I methanotrophs, conversion of glycolytic intermediates to formate using the serine pathway was prevented. These reactions would theoretically be possible, however, and could be analyzed in the future.

Table 2.4: Serine pathway reactions in the type I and type II models. Ethylmalonyl-CoA pathway reactions can be found in the supplemental file.

Model Reactions: Serine Pathway				
Model	Enzyme	Reaction	Copper cost	Iron cost
Both	glycine hydroxymethyltransferase (serine hydroxymethyltransferase)	glycine + 5,10-methylenetetrahydrofolate + H2O = L-serine + tetrahydrofolate	0	0
Both	serine-glyoxylate aminotransferase	glyoxylate + L-serine = glycine + hydroxypyruvate	0	0
Both	hydroxypyruvate reductase	hydroxypyruvate + NADH + H+ = D-glycerate + NAD+	0	0
Both	hydroxypyruvate reductase	hydroxypyruvate + NADPH + H+ = D-glycerate + NADP+	0	0
Both	glycerate kinase	D-glycerate + ATP = 2-phospho-D-glycerate + ADP + H+	0	0
Both	2,3-bisphosphoglycerate-independent phosphoglycerate mutase	2-phospho-D-glycerate = 3-phospho-D-glycerate	0	0
Both	enolase	2-phospho-D-glycerate = phosphoenolpyruvate + 1 H2O	0	0
Type II	phosphoenolpyruvate carboxylase	phosphoenolpyruvate + hydrogencarbonate = oxaloacetate + phosphate	0	0
Both	malate dehydrogenase	oxaloacetate + NADH + H+ = (S)-malate + NAD+	0	0

Table 2.4 continued.

Both	malate thiokinase (malate-CoA ligase)	(S)-malate + ATP + coenzyme_A = (S)-malyl-CoA + ADP + phosphate	0	0
Both	malyl coenzyme A lyase	(S)-malyl-CoA = acetyl-CoA + glyoxylate	0	0

Citric Acid Cycle and Anaplerotic Reactions: Literature Review

Figure 2.8: Citric acid cycle and related reactions in both the type I and the type II models. QH2 is used as an abbreviation for a generic quinol, and Q is used to represent a generic quinone.

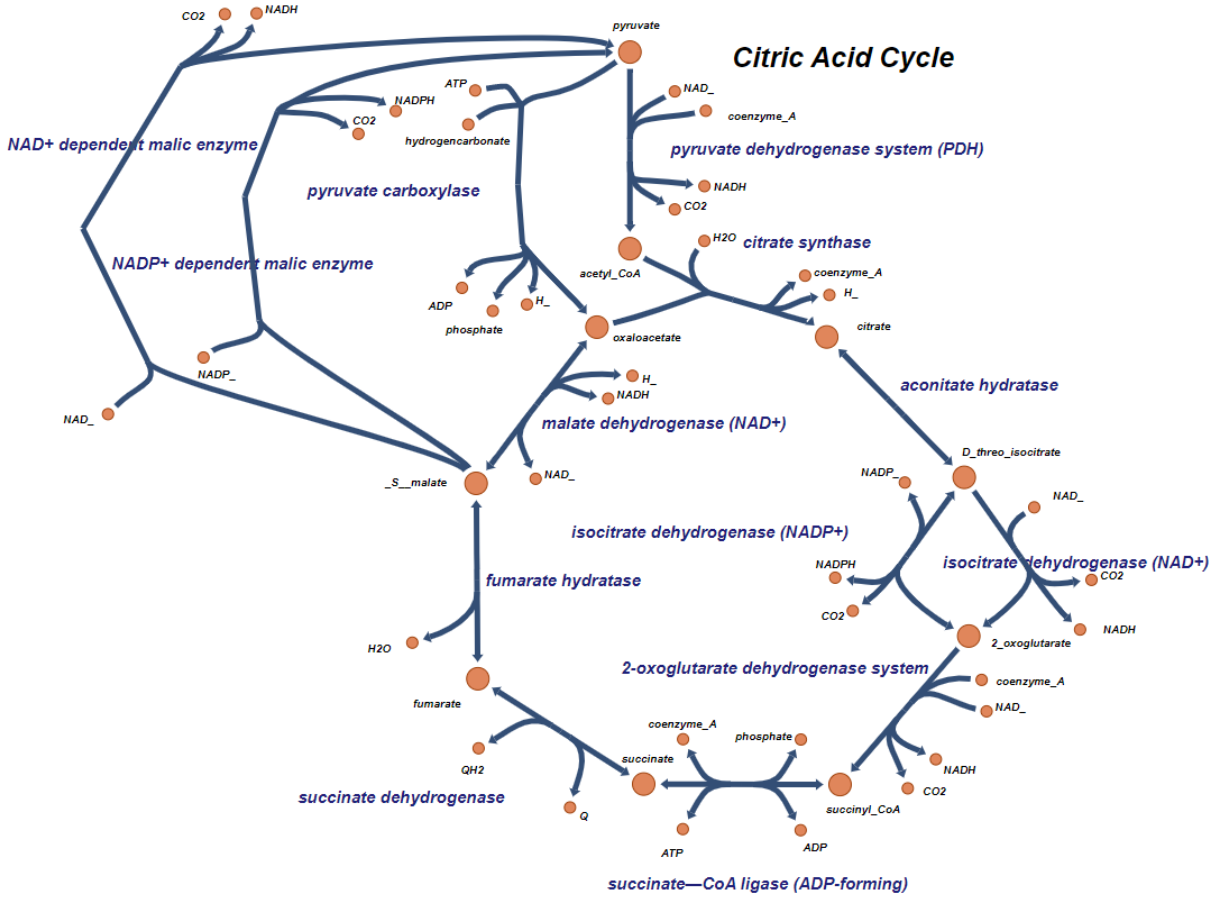

The role and presence of the complete citric acid cycle (TCA) in methanotrophs has long been debated (Khmelenina et al., 2019; Van Dien & Lidstrom, 2002; Wood et al., 2004). It was previously hypothesized that missing enzymes in the TCA cycle may contribute to obligate methanotrophy in some organisms. However, the complete set of genes for the TCA has been

found in OB3b (Matsen et al., 2013), and a functionally complete TCA has been demonstrated in *Methylomicrobium buryatense* 5GB1 (Fu et al., 2017).

Citric Acid Cycle and Anaplerotic Reactions: Model Incorporation. All TCA cycle reactions are included in both models. Both models additionally included an NAD-dependent and an NADP-dependent malic enzyme (Matsen et al., 2013). Only the alphaproteobacterial model includes phosphoenolpyruvate carboxylase. While genes for a presumed 2-oxoacid ferredoxin oxidoreductase were identified in OB3b, that reaction is not currently included in the model but could be used for future studies. Pyruvate carboxylase is included in both models on the basis of its presence in OB3b and in the KEGG annotation for *Methylomonas koyamae* LM6 (D.-H. Lee et al., 2020; Matsen et al., 2013).

Table 2.5: TCA cycle reactions in type I and type II methanotrophs. QH2 represents a generic reduced quinol, and Q represents a generic oxidized quinone.

Model Reactions: Citric Acid Cycle				
Model	Enzyme	Reaction	Copper cost	Iron cost
Both	pyruvate dehydrogenase system (PDH)	pyruvate + coenzyme_A + NAD+ = acetyl-CoA + CO2 + NADH	0	0
Both	citrate synthase	acetyl-CoA + oxaloacetate + H2O = citrate + coenzyme_A + H+	0	0
Both	aconitate hydratase	citrate = D-threo-isocitrate	0	0
Both	isocitrate dehydrogenase (NADP+)	D-threo-isocitrate + NADP+ = 2-oxoglutarate + CO2 + NADPH	0	0
Both	isocitrate dehydrogenase (NAD+)	D-threo-isocitrate + NAD+ = 2-oxoglutarate + CO2 + NADH	0	0
Both	2-oxoglutarate dehydrogenase system	2-oxoglutarate + coenzyme_A + NAD+ = succinyl-CoA + NADH + CO2	0	0
Both	succinate—CoA ligase (ADP-forming)	ADP + phosphate + succinyl-CoA = ATP + succinate + coenzyme_A	0	0
Both	succinate dehydrogenase	succinate + Q = fumarate + QH2	0	0
Both	fumarate hydratase	fumarate + H2O = (S)-malate	0	0
Both	NADP+ dependent malic enzyme	(S)-malate + NADP+ = pyruvate + CO2 + NADPH	0	0

Table 2.5 continued.

Both	NAD+ dependent malic enzyme	(S)-malate + NAD+ = pyruvate + CO2 + NADH	0	0
Both	pyruvate carboxylase	pyruvate + hydrogencarbonate + ATP = oxaloacetate + ADP + phosphate + H+	0	0

Polyhydroxybutyrate Synthesis and Degradation: Model Incorporation

Figure 2.9: Polyhydroxybutyrate (PHB) synthesis and degradation reactions in the type II model.

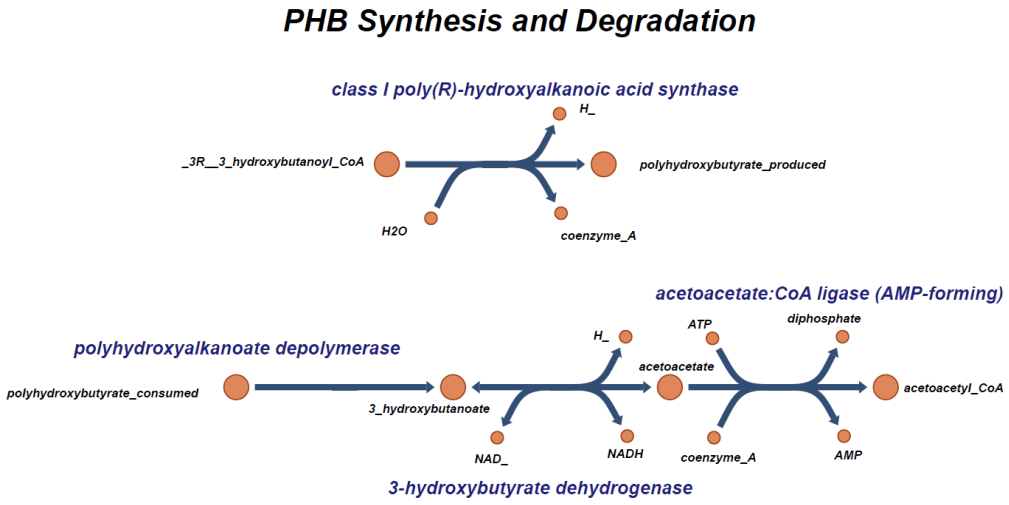

Figure 2.10. Fermentative metabolism in the type I and type II metabolic models. Acetone synthesis proceeds from polyhydroxybutyrate degradation and is blocked in the type I model.

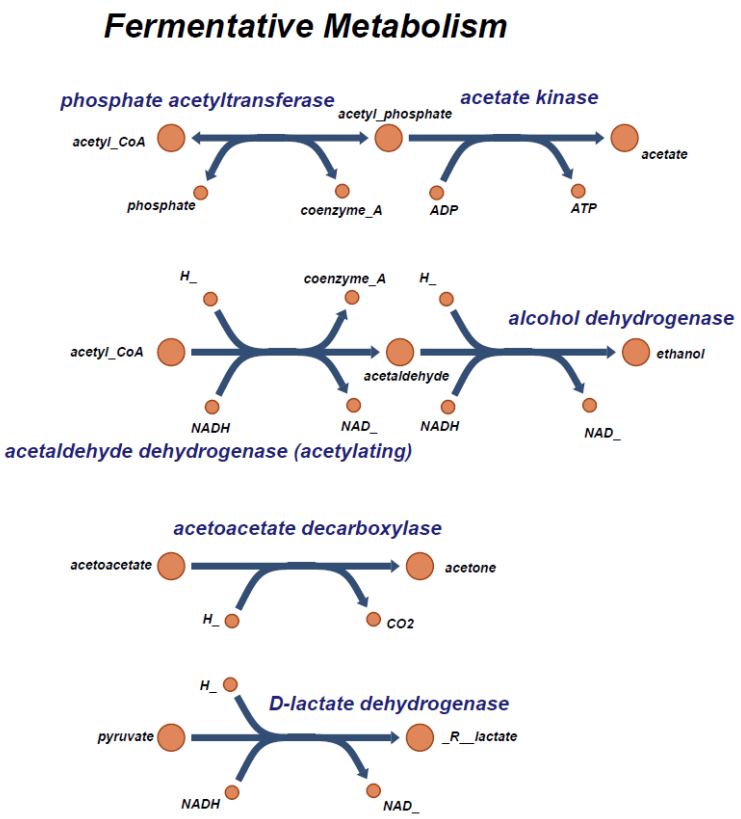

PHB synthesis requires several enzymes of the EMC pathway (acetyl-CoA acetyltransferase and acetoacetyl-CoA reductase) in addition to polyhydroxyalkanoate synthase. In the type II model, PHB is broken down first by the removal of a hydroxybutanoate monomer from the PHB polymer, then by conversion of that molecule to acetoacetate and then to acetoacetyl-CoA, which can re-enter the EMC pathway. Fermentation byproducts that can be produced by the model are acetone, acetate, ethanol, lactate, pyruvate, and succinate. Acetone production proceeds from acetoacetate, which is not a metabolic intermediate in the gammaproteobacterial model, so acetone production is infeasible in the type I model.

Table 2.6. Polyhydroxybutyrate synthesis and degradation reactions in the type I and type II models.

Model Reactions: Polyhydroxybutyrate Synthesis and Degradation				
Model	Enzyme	Reaction	Copper cost	Iron cost
Type II	class I poly(R)-hydroxyalkanoic acid synthase	(3R)-3-hydroxybutanoyl-CoA + H2O = polyhydroxybutyrate_produced + coenzyme_A + H+	0	0
Type II	polyhydroxyalkanoate depolymerase	polyhydroxybutyrate_consumed = 3-hydroxybutanoate	0	0
Type II	3-hydroxybutyrate dehydrogenase	NAD+ + 3-hydroxybutanoate = acetoacetate + NADH + H+	0	0
Type II	acetoacetate:CoA ligase (AMP-forming)	ATP + acetoacetate + coenzyme_A = AMP + diphosphate + acetoacetyl-CoA	0	0

Table 2.7. Fermentative metabolism in type I and type II models. Acetone production is infeasible in type I methanotrophs.

Model Reactions: Fermentation				
Model	Enzyme	Reaction	Copper cost	Iron cost
Both	phosphate acetyltransferase	acetyl-CoA + phosphate = acetyl_phosphate + coenzyme_A	0	0
Both	acetate kinase	acetyl_phosphate + ADP = acetate + ATP	0	0
Both	acetaldehyde dehydrogenase	acetyl-CoA + NADH + H+ = acetaldehyde + coenzyme_A + NAD+	0	0
Both	alcohol dehydrogenase	acetaldehyde + NADH + H+ = ethanol + NAD+	0	0
Both	acetoacetate decarboxylase	acetoacetate + H+ = acetone + CO2	0	0
Both	D-lactate dehydrogenase	pyruvate + NADH + H+ = (R)-lactate + NAD+	0	0

Glycolytic Pathways

Figure 2.11. Embden-Meyerhof-Parnas (EMP) glycolysis. In the type II model, reaction directions were adjusted to force flux through the gluconeogenic direction only.

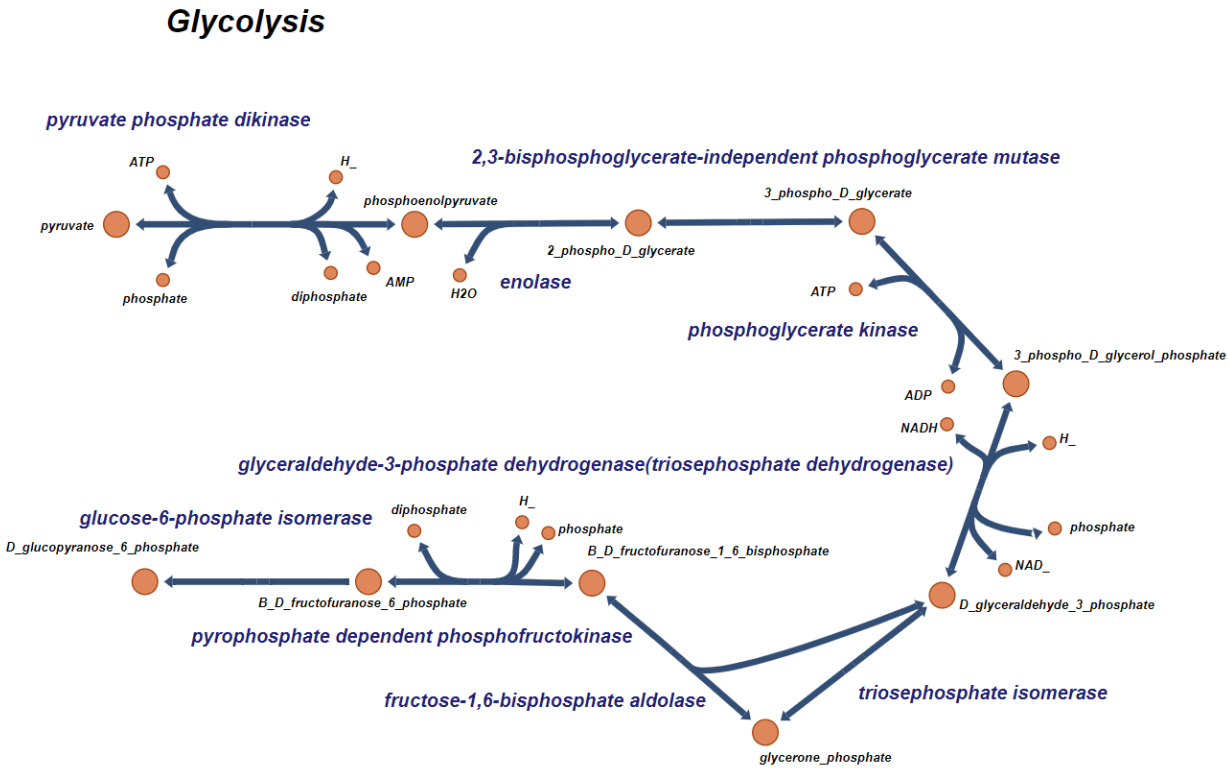

EMP Glycolysis: Model Incorporation. Both alpha- and gammaproteobacterial methanotrophs encode several PP_i-dependent enzymes in addition to the standard Embden-Meyerhof-Parnas (EMP) glycolysis enzymes. The reversible PP_i-phosphofructokinase (PP_i-PFK) is included in both models (Khmelenina et al., 2018; O. N. Rozova et al., 2012). Pyruvate phosphate dikinase (PPDK) is also commonly found in both types of methanotrophs and was included in both models. This makes glycolysis fully reversible (Khmelenina et al., 2018). PP_i-dependent phosphoenolpyruvate carboxykinase was not included in either model.

A proton-translocating pyrophosphatase is included in both models (Kalyuzhnaya et al., 2013). An ATP diphosphatase is also included in both models to supply PP_i where it is not

already generated by steps of central carbon metabolism (this is more likely in the type II model, where gluconeogenesis rather than glycolysis is required at a higher rate). If multiple enzymes can carry out one reaction (for example, the conversion of phosphoenolpyruvate to pyruvate could be carried out either by PPDK or phosphoenolpyruvate), the PP_i-dependent reaction was used. This prevented the generation of ATP from PP_i in metabolic loops. A reversible glycolysis caused too many loops in the type II model, and as a result, glycolysis was altered to run only in the gluconeogenic direction by making glucose 6-phosphate isomerase irreversible.

Table 2.8. Emden-Meyerhof-Parnas glycolysis in type I and type II models. To prevent loops in the type II model, glucose-6-phosphate dehydrogenase was made irreversible in the gluconeogenic direction.

Model Reactions: Emden-Meyerhof-Parnas Glycolysis				
Model	Enzyme	Reaction	Copper cost	Iron cost
Both	glucose-6-phosphate isomerase	D-glucopyranose_6-phosphate = B-D-fructofuranose_6-phosphate	0	0
Both	pyrophosphate dependent phosphofructokinase	B-D-fructofuranose_6-phosphate + diphosphate = B-D-fructofuranose_1,6-bisphosphate + phosphate + H+	0	0
Both	fructose-1,6-bisphosphate aldolase	B-D-fructofuranose_1,6-bisphosphate = glycerone_phosphate + D-glyceraldehyde_3-phosphate	0	0
Both	triosephosphate isomerase	glycerone_phosphate = D-glyceraldehyde_3-phosphate	0	0
Both	glyceraldehyde-3-phosphate dehydrogenase (triosephosphate dehydrogenase)	D-glyceraldehyde_3-phosphate + NAD+ + phosphate = 3-phospho-D-glycerol_phosphate + NADH + H+	0	0
Both	phosphoglycerate kinase	3-phospho-D-glycerol_phosphate + ADP = 1 3-phospho-D-glycerate + 1 ATP	0	0
Both	pyruvate phosphate dikinase	phosphoenolpyruvate + AMP + diphosphate + H+ = pyruvate + ATP + phosphate	0	0

Entner-Doudoroff Glycolysis: Literature Review. Key enzymes of the Entner-Doudoroff (EDD) pathway have recently been characterized in *M. alcaliphilum* 20Z (Olga N. Rozova et al., 2021). The EDD pathway is hypothesized to be important in regulating the levels of free glucose in the cell and in degradation of glycogen for energy or carbon in gammaproteobacterial methanotrophs (Olga N. Rozova et al., 2021).

Figure 2.12. Entner-Doudoroff (EDD) glycolysis in the type I model.

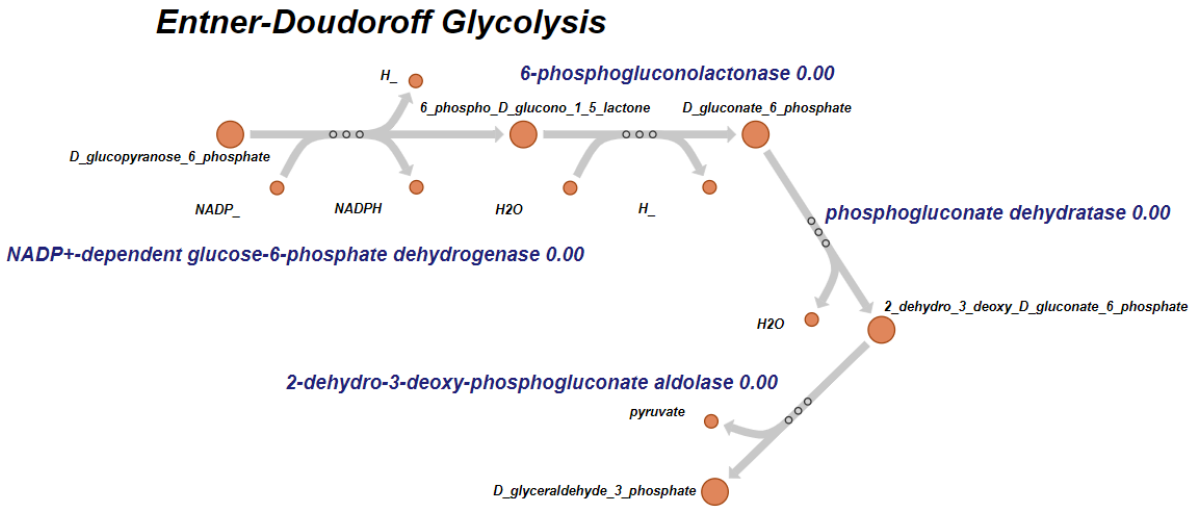

Entner-Doudoroff Glycolysis: Model Incorporation. This pathway is included only in the gammaproteobacterial model. It was previously shown that the EMP pathway was favored over the EDD pathway in *M. alcaliphilum* 20Z and in *Methylotuvimicrobium buryatense* 5GB1C (He et al., 2020; Kalyuzhnaya et al., 2013). In *M. buryatense* 5GB1C, however, the EDD pathway is still essential for growth (He et al., 2020).

Table 2.9. Entner-Doudoroff glycolysis in the type I model.

Model Reactions: Entner-Doudoroff Glycolysis				
Model	Enzyme	Reaction	Copper cost	Iron cost
Type I	NADP+-dependent glucose-6-phosphate dehydrogenase	D-glucopyranose_6-phosphate + NADP+ = 6-phospho_D-glucono-1,5-lactone + NADPH + H+	0	0
Type I	6-phosphogluconolactonase	6-phospho_D-glucono-1,5-lactone + H2O = D-gluconate_6-phosphate + H+	0	0
Type I	phosphogluconate dehydratase	D-gluconate_6-phosphate = 2-dehydro-3-deoxy-D-gluconate_6-phosphate + H2O	0	0
Type I	2-dehydro-3-deoxy-phosphogluconate aldolase	2-dehydro-3-deoxy-D-gluconate_6-phosphate = D-glyceraldehyde_3-phosphate + pyruvate	0	0

Phosphoketolase Pathway: Literature Review and Model Incorporation. Phosphoketolase cleaves sugars to acetyl phosphate and either D-glyceraldehyde 3-phosphate or erythrose 4-phosphate. This enzyme typically participates in heterolactic fermentation, but it is also present in both alpha- and gammaproteobacterial methanotroph genomes, where it has been proposed to play a role in fermentation and acetyl-CoA production (Akberdin et al., 2018; Olga N. Rozova et al., 2015). The phosphoketolase pathway was only included in the type I model, as its incorporation in the type II model created loops.

Figure 2.13. Phosphoketolase pathway-specific reactions in the type I model.

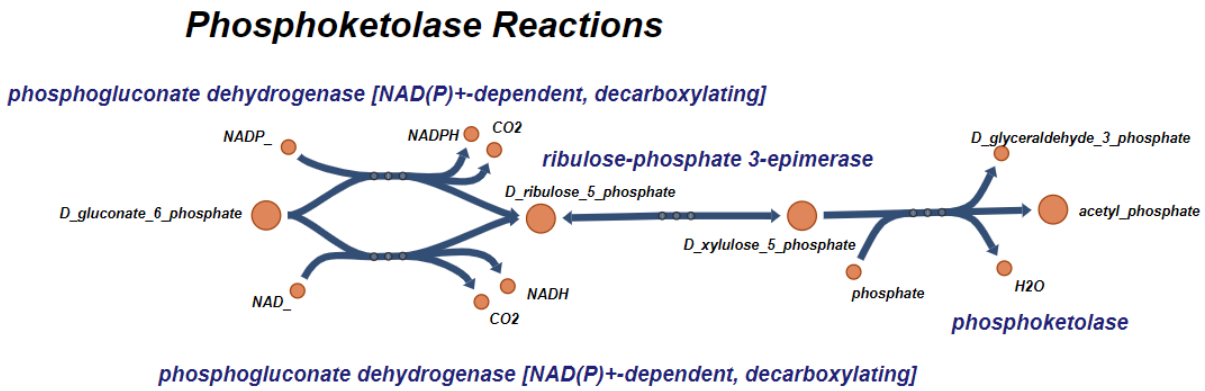

Table 2.10. The phosphoketolase pathway in the type I model.

Model Reactions: Phosphoketolase Pathway				
Model	Enzyme	Reaction	Copper cost	Iron cost
Type I	phosphogluconate dehydrogenase [NAD(P)+-dependent, decarboxylating]	D-gluconate_6-phosphate + NADP+ = D-ribulose_5-phosphate + CO2 + NADPH	0	0
Type I	phosphogluconate dehydrogenase [NAD(P)+-dependent, decarboxylating]	D-gluconate_6-phosphate + NAD+ = D-ribulose_5-phosphate + CO2 + NADH	0	0
Type I	phosphoketolase	D-xylulose_5-phosphate + phosphate = D-glyceraldehyde_3-phosphate + acetyl_phosphate + H2O	0	0
Type I	phosphoketolase	B-D-fructofuranose_6-phosphate + phosphate = D-erythrose_4-phosphate + acetyl_phosphate + H2O	0	0

Glycogen Formation: Literature Review and Model Incorporation

Figure 2.14. Glycogen synthesis and degradation reactions in type I model.

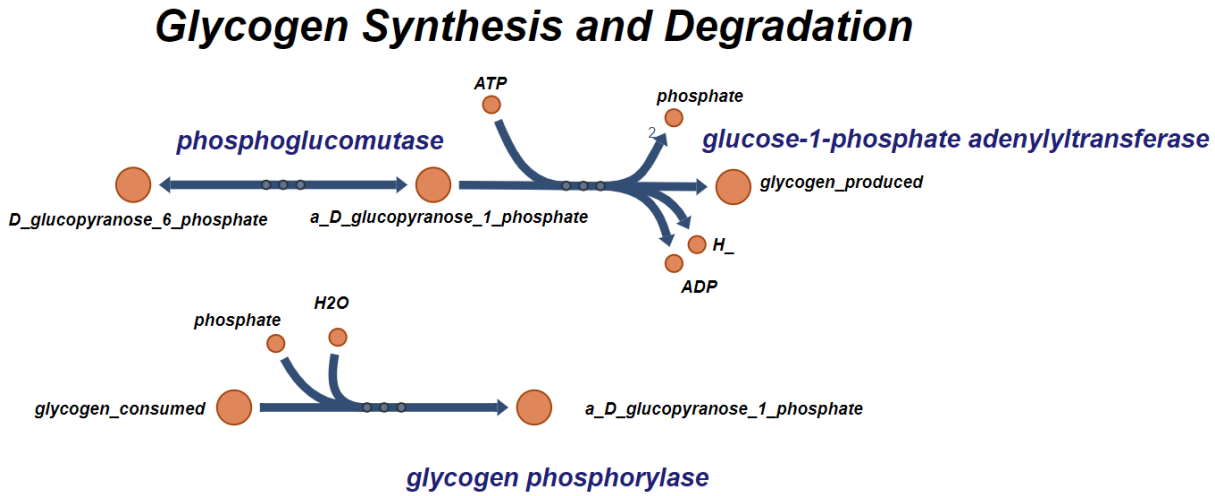

Glycogen formation has been characterized in an alkaliphilic methanotroph. In *M. alcaliphilum* 20Z, glycogen formation occurs either via sucrose or via ADP-glucose (S. Yu But et al., 2020). In the gammaproteobacterial model, glycogen synthesis proceeds via ADP-glucose. To simplify the model, glycogen degradation requires only EC 2.4.1.1, which uses excess energy

from glycogen bond lysis to phosphorylate the glucose monomer. Fermentation pathways are detailed in Table 2.7.

Table 2.11. Glycogen synthesis and degradation in the type I model.

Model Reactions: Glycogen Synthesis and Degradation				
Model	Enzyme	Reaction	Copper cost	Iron cost
Type I	phosphoglucomutase	D-glucopyranose_6-phosphate = a-D-glucopyranose_1-phosphate	0	0
Type I	glucose-1-phosphate adenylyltransferase	a-D-glucopyranose_1-phosphate + ATP = glycogen_produced + ADP + 2 phosphate + H+	0	0
Type I	glycogen synthase	glycogen_consumed = glycogen_produced	0	0
Type I	glycogen phosphorylase	glycogen_consumed + phosphate + H2O = a-D-glucopyranose_1-phosphate	0	0

Electron Transport Chain: Model Incorporation

Figure 2.15. Electron transport reactions in the type I and type II models. Cytc is used as an abbreviation for an oxidized cytochrome c, and cytcE is an abbreviation for a reduced cytochrome c. QH2 is used as an abbreviation for a generic quinol, and Q is used to represent a generic quinone. H_pmf refers to protons that contribute to the proton motive force.

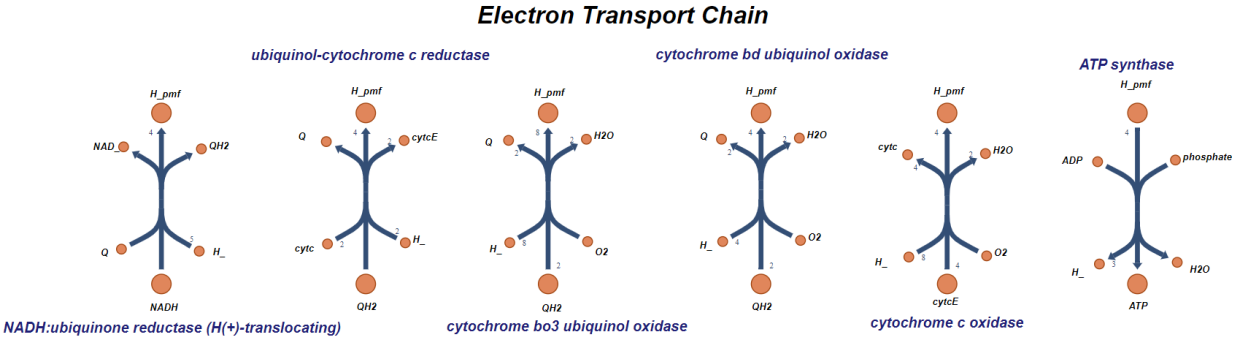

The electron transport chain (ETC) of both methanotroph models is based on the KEGG annotation for *Methylosinus trichosporium* OB3b. There is one NADH:ubiquinone reductase, one quinol-cytochrome reductase, two quinol oxidases, and one cytochrome oxidase. Interestingly, alternative enzymes in the ETC often have different copper requirements (as

determined in a variety of organisms; info from metacyc), possibly allowing for flexibility under copper limiting conditions with potential tradeoffs in energetic efficiency.

Table 2.12. Electron transport chain in the type I and II models. QH2 refers to quinol, and Q refers to quinone. H_pmf are protons that contribute to the proton motive force. Reduced cytochromes are cytcE, and oxidized cytochromes are cytc.

Model Reactions: Electron Transport Chain and Additional Energy Metabolism				
Model	Enzyme	Reaction	Copper cost	Iron cost
Both	NADH:ubiquinone reductase (H(+)-translocating)	1 NADH + 1 Q + 5 H+ = 1 NAD+ + 1 QH2 + 4 H_pmf	0	0
Both	ubiquinol-cytochrome c reductase	1 QH2 + 2 H+ + 2 cytc = 1 Q + 4 H_pmf + 2 cytcE	2	0
Both	cytochrome c oxidase	4 cytcE + 1 O2 + 8 H+ = 4 cytc + 4 H_pmf + 2 H2O	0	0
Both	cytochrome bd ubiquinol oxidase	2 QH2 + 1 O2 + 4 H+ = 2 Q + 2 H2O + 4 H_pmf	0	0
Both	cytochrome bo3 ubiquinol oxidase	2 QH2 + 1 O2 + 8 H+ = 2 Q + 2 H2O + 8 H_pmf	1	0
Both	H+-exporting diphosphatase	diphosphate + H2O = 2 phosphate + H_pmf	0	0
Both	ATP diphosphatase	ATP + H2O = AMP + diphosphate + H+	0	0
Both	ATP synthase	1 ADP + phosphate + 4 H_pmf = 1 ATP + 3 H+ + 1 H2O	0	0
Both	adenylate kinase	ATP + AMP = 2 ADP	0	0
Both	ATP maintenance	1 ATP + 1 H2O = 1 ATP_main + 1 ADP + 1 H+ + 1 phosphate	0	0
Both	transhydrogenase	NAD+ + NADPH = NADH + NADP+	0	0

Nitrogen Metabolism: Literature Review

Figure 2.16. Dissimilatory and assimilatory nitrogen metabolism in the type I and type II models.

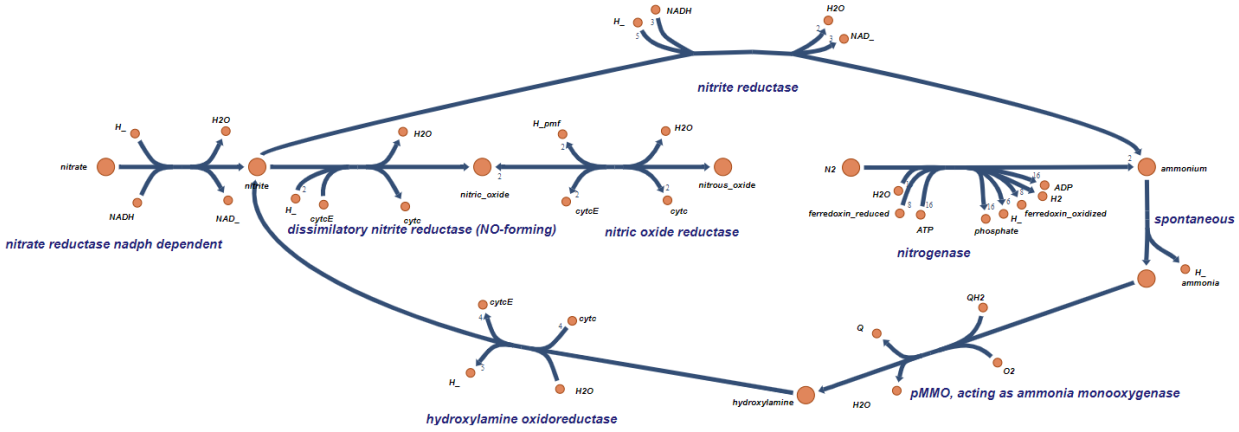

Methanotrophs can grow using a variety of nitrogen sources, including ammonium, nitrate, and urea. Growth on ammonium is particularly interesting for methanotrophs, as MMOs have a similar structure to ammonia monooxygenases (AMOs) and growth is sometimes (but not always) inhibited by competition between ammonium and methane at the MMO active site (Rostkowski et al., 2013; Tays et al., 2018). The reaction of ammonium with O_2 produces hydroxylamine, which is likely detoxified by an enzyme similar to hydroxylamine oxidoreductase (Stein, 2020). Methanotrophs are thus capable of nitrification, but they do not use this pathway to grow (Stein & Klotz, 2011).

In addition to nitrification, methanotrophs can also carry out aerobic denitrification with N_2O as the end product (Dam et al., 2013; Stein & Klotz, 2011). These reactions are all included in both models. A comparison of denitrification-related genes in methanotrophs can be found in Stein & Klotz 2011. Both alpha- and gammaproteobacterial methanotrophs can fix N_2 (Auman et al., 2001).

Nitrogen Metabolism: Model Incorporation. Both metabolic models include the GS-GOGAT system for ammonium assimilation. Both models include a reaction for the conversion of hydroxylamine to nitrite based on EC 1.7.2.6. Aerobic denitrification is included in both models. Nitrate reduction does not contribute to the proton motive force in these models (Kits et al., 2015), although nitric oxide reduction does. The nitrite reductase used in the model is nirK, which is copper-dependent. Nitrogenase is included in both models, as is an NAD-dependent hydrogenase, which was detected in *M. alcaliphilum* 20Z (Kalyuzhnaya et al., 2013). Reactions for polyamine synthesis are also included in both models (Nguyen & Lee, 2019).

Table 2.13. Nitrogen metabolism reactions in the type I and type II modelsQH2 refers to quinol, and Q refers to quinone. Reduced cytochromes are cytcE, and oxidized cytochromes are cytc.

Model Reactions: Nitrogen Metabolism				
Model	Enzyme	Reaction	Copper cost	Iron cost
Both	spontaneous	ammonium = ammonia + H+	0	0
Both	glutamine synthetase	ammonium + L-glutamate + ATP = L-glutamine + ADP + phosphate + H+1 QH2 + 2 H+ + 2 cytc = 1 Q + 4 H_pmf + 2 cytcE	2	0
Both	glutamate synthase	L-glutamine + 2-oxoglutarate + NADPH + H+ = 2 L-glutamate + NADP+	0	0
Both	nitrogenase	N2 + 8 ferredoxin_reduced + 16 ATP + 16 H2O = 2 ammonium + H2 + 16 ADP + 16 phosphate + 8 ferredoxin_oxidized + 6 H+	0	0
Both	hydrogenase	NAD+ + H2 = NADH + H+	0	0
Both	ferredoxin-NAD+ oxidoreductase	2 ferredoxin_oxidized + NADH = 2 ferredoxin_reduced + NAD+ + H+	0	0
Both	nitrate reductase	nitrate + NADH + H+ = nitrite + NAD+ + H2O	0	0
Both	nitrite reductase	nitrite + 3 NADH + 5 H+ = ammonium + 3 NAD+ + 2 H2O	0	0
Both	pMMO, acting as ammonia monooxygenase	ammonia + QH2 + O2 = hydroxylamine + Q + H2O	3	0

Table 2.13 continued.

Both	hydroxylamine oxidoreductase	4 cytc + hydroxylamine + H2O = 4 cytcE + nitrite + 5 H+	0	0
Both	dissimilatory nitrite reductase (NO-forming)	nitrite + cytcE + 2 H+ = nitric_oxide + cytc + H2O	2	
Both	nitric oxide reductase	2 nitric_oxide + 2 cytcE + 2 H_pmf = nitrous_oxide + 2 cytc + H2O	0	0
Both	glutamate 5-kinase	L-glutamate + ATP = g-L-glutamyl_5-phosphate + ADP	0	0
Both	glutamate-5-semialdehyde dehydrogenase	g-L-glutamyl_5-phosphate + NADPH + H+ = L-glutamate-5-semialdehyde + NADP+ + phosphate	0	0
Both	ornithine--oxo-acid transaminase	L-glutamate-5-semialdehyde + L-glutamate = L-ornithine + 2-oxoglutarate	0	0
Both	ornithine decarboxylase	L-ornithine + H+ = CO2 + putrescine	0	0

Global Warming Potential and Methanotroph Metabolism

Public policy and environmental remediation decisions must account for the climatic effects of greenhouse gas releases. Researchers use emissions metrics like global warming potential (GWP) to compare the impact of different greenhouse gases in standardized units. GWP measures how the release of a greenhouse gas effects energy trapping in the atmosphere. These effects are described in terms of CO_2 equivalents, which compare both the lifetime and the radiative properties of a particular gas to those of CO_2. GWP values for greenhouse gases also include the warming effects of breakdown products like ozone that can be produced as greenhouse gases decay. As an example, methane is a more potent greenhouse gas than CO_2, and the release of one metric ton of methane is considered equivalent to the release of 79.7 metric tons of CO_2 on a 20-year timescale. Methane breaks down faster than CO_2, however, so when the timescale is increased to 100 years, one metric ton of methane is considered equivalent to 27

metric tons of CO_2. GWP is commonly reported as GWP-20, GWP-100, and GWP-500, which are the 20-year, 100-year, and 500-year global warming potentials, respectively. The GWP that should be used depends on the prediction being made, but GWP-100 is commonly used to inform policy decisions (Forster et al., 2021).

Methanotrophs act as biological methane sinks. They are estimated to consume about 5% of atmospheric methane (Canadell et al., 2021; Knief, 2015). In consuming methane, however, methanotrophs produce CO_2 and sometimes nitrous oxide, which is a more potent greenhouse gas than either CO_2 or methane. Excess nitrate in the environment, typically from agricultural pollution via fertilizer runoff, can result in the microbial production of nitrous oxide (Stein, 2011). Nitrous oxide production has been shown for many methanotrophs and should be a consideration when growing methanotrophs for industrial use or for remediation, as methanotroph mediums often contain nitrate (Stein & Klotz, 2011; Whittenbury et al., 1970).

We have incorporated measures of GWP into both the type I and the type II metabolic models. The models can make predictions of greenhouse gas release under different cultivation conditions, which can help guide decisions about industrial cultivation and the use of methanotrophs for environmental remediation.

In the metabolic models, CO_2 equivalents were included as metabolites within reactions related to greenhouse gas flux. A transport reaction is used to tally production and consumption of greenhouse gases as CO_2 equivalents based on the GWP-20 and GWP-100 measures. CO_2 equivalents were also included for the consumption of PHB and glycogen, since these carbon storage compounds are derived from methane. CO_2 equivalents for these reactions were

calculated using model predictions for the minimum amount of methane required to form one mole of PHB or glycogen.

Table 2.14. Global warming potential (GWP) calculations as included in the type I and type II models. Both the 20 year and the 100 year GWP values are considered. CO2 equivalents are included as metabolites in units of moles. CO2 equivalents for PHB and glycogen were calculated using model predictions of the minimum cost of methane required to form one mole of each storage compound. Flux of CO_2 equivalents is tracked and used to calculate the overall GWP of each mode.

Model	Reaction
Type I	glycogen_consumed_ext + 349 CO2_eq_20 + 118 CO2_eq_100 = glycogen_consumed
Type II	polyhydroxybutyrate_consumed_ext + 145 CO2_eq_20 + 49.2 CO2_eq_100 = polyhydroxybutyrate_consumed
Both	nitrous_oxide = nitrous_oxide_ext + 273 CO2_eq_20 + 273 CO2_eq_100
Both	CO2 = CO2_ext + 1 CO2_eq_20 + 1 CO2_eq_100
Both	CO2_eq_100 = GWP100
Both	CO2_eq_20 = GWP20

Results and Discussion

Model Validation

Model predictions for biomass yield on methane were compared to experimental values for the growth of OB3b on nitrate as a nitrogen source (Rostkowski et al., 2013). Typically, idealized model predictions do not initially fit real-world growth data and the model must be adjusted by manipulating the ATP requirement of the model. This adjusted ATP value is referred to as “maintenance ATP” and is meant to represent the metabolic costs associated with cellular repair, growth inhibition, and other factors that require energy but are not easily captured in

stoichiometric models, which can result in incorrect predictions prior to model calibration (Thiele & Palsson, 2010). In EFMA, ATP maintenance values are generally included as part of the biomass term, with different biomass terms being developed, for example, for growth on nitrate vs. growth on ammonium, conditions which would be expected to place different energy requirements on methanotrophs due to competition between methane and ammonium at the active site of the MMOs.

Cell growth requires not only ATP, but also electrons. The degree of reduction is another energy value within the biomass term that can be adjusted in order to improve modeling predictions. Degree of reduction refers to the moles of electrons per mole of carbon in a compound. For a compound with the equation $C_WH_XO_YN_Z$, carbon has 4 available electrons, hydrogen has 1, oxygen has -2, and the electrons for nitrogen vary based on the reference state (5 for nitrate, -3 for ammonia, and 0 for N_2) (Doran, 1997). The degree of reduction for key metabolic intermediates of methanotroph metabolism is shown in Table 2.15.

Table 2.15. Degree of reduction values for metabolic intermediates in the type I and type II models. Degree of reduction is calculated for an ammonia basis.

Compound	Formula in Model	Degree of Reduction, Ammonia Basis (electrons per carbon mole)
Methane	CH_4	8
Methanol	CH_4O	6
Formaldehyde	CH_2O	4
Formate	CHO_2	2
CO_2	CO_2	0
Hexulose 6-phosphate	$C_6H_{11}O_9P$	4
Pyruvate	$C_3H_3O_3$	3.33
Glycogen	$C_6H_8O_4$	4
Acetyl-CoA	$C_{23}H_{34}N_7O_{17}P_3S$	6.6
Serine	$C_3H_7NO_3$	6
Polyhydroxybutyrate	$C_4H_7O_3$	4.5

In this work, degree of reduction in the biomass term is adjusted by manipulating the NADPH requirement, where NADPH acts as an electron donor and $NADP^+$ is a byproduct of biomass formation (Neidhardt et al., 1990b). The degree of reduction of the biomass term used in predictions presented here is 4.2 moles of electrons per carbon moles of biomass on an ammonium basis, which is a generic value determined using the average elemental composition of microbial biomass ($CH_{1.8}O_{0.5}N_{0.2}$) (Doran, 1997).

For the type II model, before calibration to experimental data, it was found that the predicted yields of biomass on methane during growth on nitrate were consistently lower than experimental yields. Interestingly, the model displays a large tolerance to changes in ATP maintenance. Removing polymerization and maintenance ATP completely from the biomass term did not increase the predicted biomass yield. Increasing ATP maintenance did eventually decrease the overall yield, but only at a high ratio of ATP/Cmol biomass (Table 2.16). It is hypothesized that the high degree of reduction of methane allows for a large amount of ATP production (roughly 5.5 ATP/ methane, based on model predictions, vs. roughly 4.33 ATP/glucose in *Escherichia coli*), and that this excess ATP is readily funneled into biomass production. Methanotrophs also have highly flexible electron transport chains and encode electron transport chain enzymes that allow for a high P/O ratio, which increases ATP yield (Figure 2.15) (Akberdin et al., 2018; DiSpirito et al., 2004).

To check model function, we compared the effects of adjusting the degree of reduction of the biomass term on yield predictions. Increasing the degree of reduction decreased overall biomass yield (Figure 2.17, Table 2.16). It should be noted that methanotrophs form extensive

lipid membranes under conditions of copper excess, which is predicted to raise the degree of reduction of biomass above the value of 4.2 that is used here (Semrau et al., 2010).

Improving efficiency of energy generation is one way to increase biomass yield, making electron transport chain stoichiometry a key component of metabolic models (Taymaz-Nikerel et al., 2010). Because the electron donor of particulate methane monooxygenase is debated, we tested the possibility of direct coupling between pMMO and methanol dehydrogenase, where the electrons generated in the oxidation of methanol are used to provide reducing power to pMMO (Akberdin et al., 2018). This reaction essentially allows pMMO to use reduced cytochromes as electron donors instead of quinol, reducing the energy required for methane oxidation. The simplified reaction is below:

Equation 2.1: $CH_4 + O_2 = CH_2O + H_2O$

Changing the electron donor for pMMO from the quinol pool to methanol dehydrogenase increased the predicted yield of biomass on methane (Figure 2.17, Table 2.16). The yield of ATP on methane also increased to 6 moles of ATP per mole of methane, the same value that has been determined in other modeling studies (Akberdin et al., 2018). Similar adjustments could be used to investigate the possibility of alternative enzymes in the electron transport chain or the proton-pumping capacity of the various membrane-bound enzymes in methanotroph metabolism; any adjustment that improves energy efficiency should increase ATP and biomass yields. These alternatives represent a possible avenue for future work.

Figure 2.17. Comparisons of experimental and predicted methane uptake rates for growth of *Methylosinus trichosporium* OB3b on methane, O_2, and nitrate. The experimental values were determined based on Rostkowski et al., 2013. Model predictions were consistently higher than experimental values; introducing direct coupling in electron transfer between pMMO and methanol dehydrogenase increased expected biomass yields on methane.

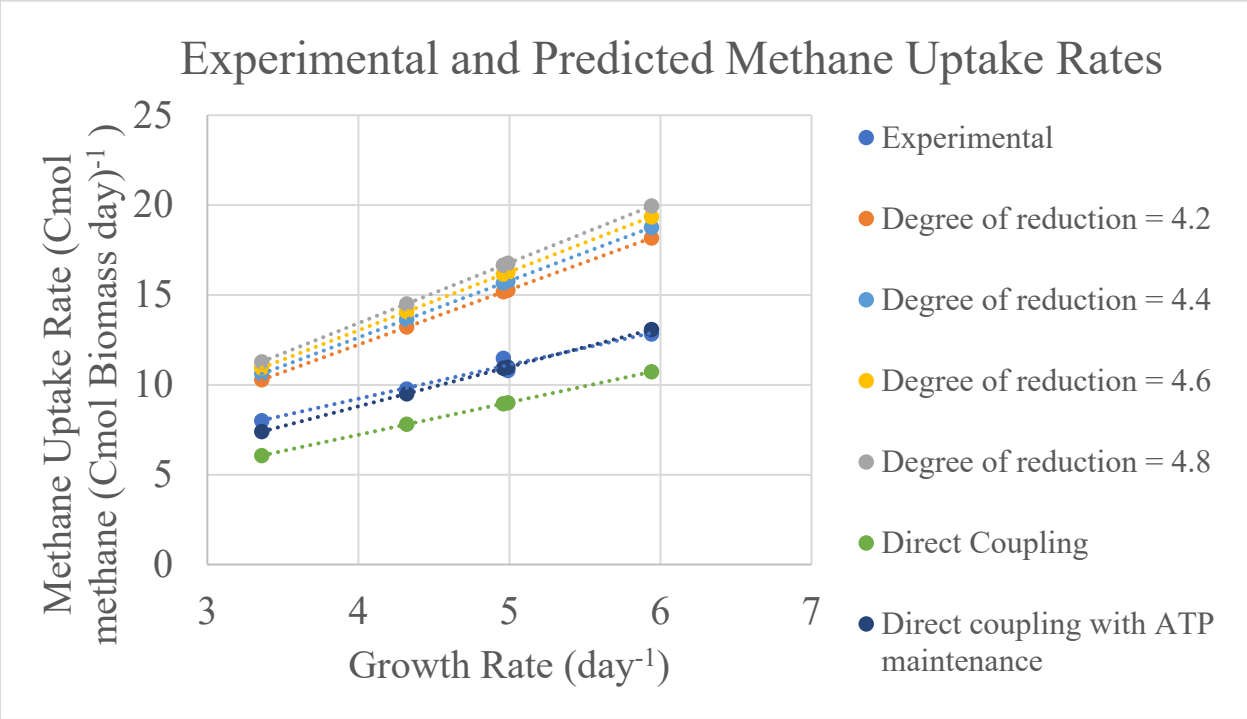

Table 2.16. Predicted methane costs per carbon mole (Cmol) of biomass as determined by changes to the biomass term or to model structure.

Biomass Term Adjustments	**Minimum Predicted Methane Cost (Cmol methane/Cmol biomass)**
Degree of reduction = 4.2	3.06
Degree of reduction = 4.4	3.12
Degree of reduction = 4.6	3.26
Degree of reduction = 4.8	3.36
Degree of reduction = 4.2; ATP cost 0 ATP per Cmol biomass	3.06
Degree of reduction = 4.2; ATP cost 5 ATP per Cmol biomass	3.06
Degree of reduction = 4.2; ATP cost 10 ATP per Cmol biomass	3.61
Degree of reduction = 4.2; ATP cost 50 ATP per Cmol biomass	10.88
Degree of reduction = 4.2; direct coupling	1.80
Degree of reduction = 4.2; direct coupling with ATP maintenance	2.20

While adjusting the electron donor for pMMO improved biomass yields, it lowered the predicted O_2/methane consumption ratio away from the experimentally supported value of 1.5 moles of O_2 per mol of methane for optimal growth of type II methanotrophs (Fig 2.17) (Pieja, Sundstrom, et al., 2011; Zhang et al., 2019). The predicted value with direct coupling for pMMO reduction is closer to the optimal growth values for *M. alcaliphilum* 20Z of 1.3 O_2/methane (Fig 2.18). It is possible that other changes to the model would increase the biomass yield while preserving the O_2/methane uptake ratio, which should be investigated in future studies. A mix of electron donors for pMMO is one possibility that merits more focus. Other work that has investigated the electron donor of pMMO has revealed similar problems matching experimental data exactly to a particular electron donor within the model (Akberdin et al., 2018).

Figure 2.18. Comparison of biomass yields and O_2/methane uptake ratios for type II methanotrophs with the direct coupling mode of pMMO reduction. The x-axis shows the ratio of O2 to methane consumption. The y-axis shows the yield of biomass on methane. Modes are color-coded according to the ratio of methane that flows through the pMMO reaction vs. the sMMO reaction, which uses NADH as an electron donor. Yields are higher with the direct coupling method. The predicted optimal O_2:methane ratio is 1.3 mol O_2:mol methane.

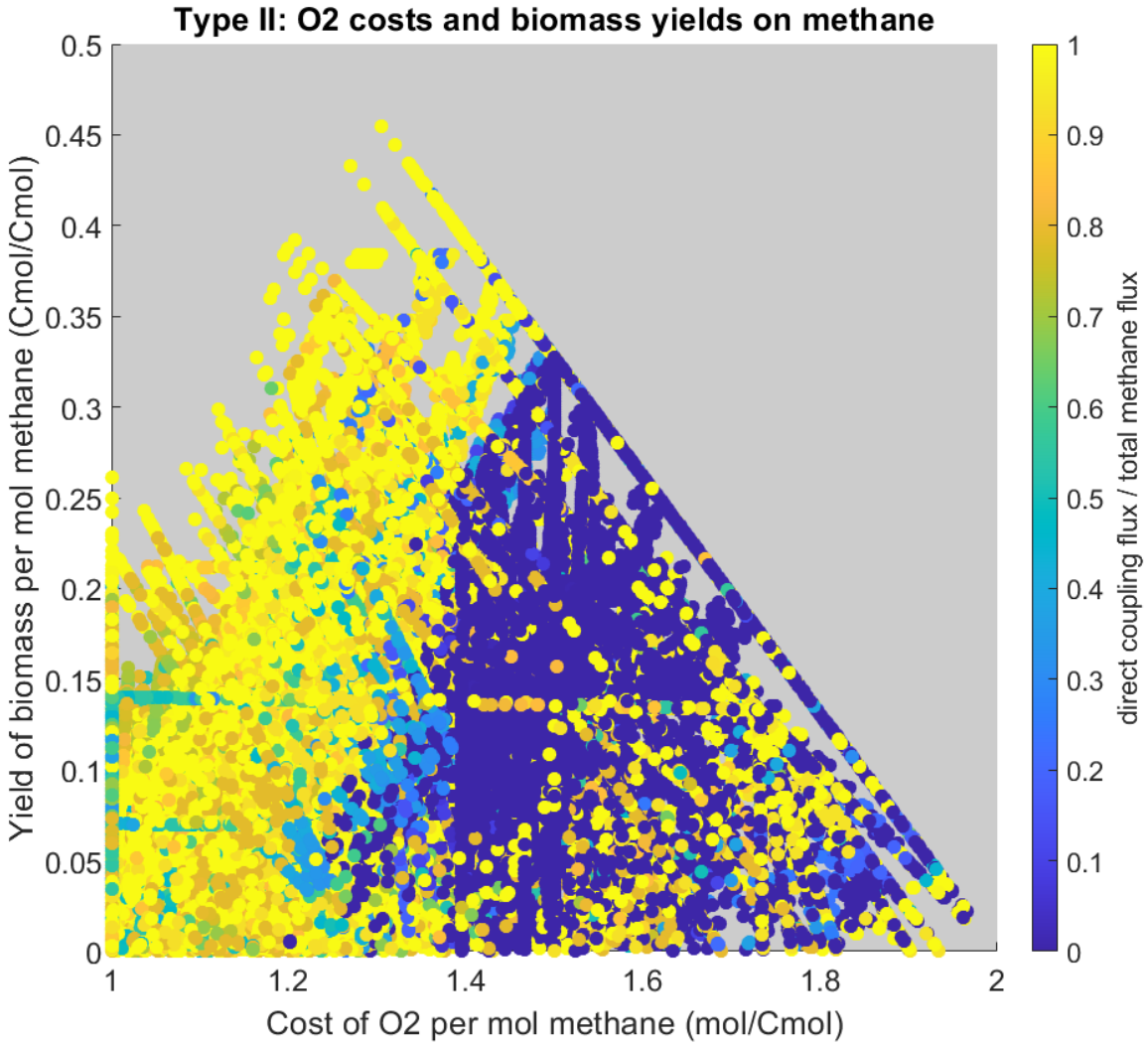

Comparison of Denitrification and PHB Degradation

Methanotrophs have been shown to degrade PHB under low O_2 conditions. In some experiments, the degradation of PHB led to production of reduced carbon byproducts like

acetone and acetate. Predictions were run for PHB degradation for the generation of biomass or for the generation of energy in the form of ATP. Modes were sorted according to the cost of PHB and O_2 per biomass, with the assumption that competitive phenotypes in the environment would maximize production of biomass on carbon and O_2, which are anticipated to be limiting resources under these conditions.

It is thought that PHB degradation is used for the generation of reducing equivalents for methane oxidation. In these predictions, however, it was found that the biomass yield on PHB is similar to that on methane (0.4348 Cmol biomass/Cmol PHB, compared to 0.4327 Cmol biomass/mol methane) (Figure 2.19). It was also predicted that in the presence of nitrate, no fermentative byproducts are produced during PHB degradation. Instead, the phenotypes that are predicted to be expressed (those along the tradeoff curves) represent a gradual switch from fully aerobic respiration to the use of nitrate as an electron acceptor (Figure 2.19, Figure 2.20).

Figure 2.19. Predictions for biomass production during polyhydroxybutyrate (PHB) degradation. The x-axis is the cost of O_2 per carbon mole of biomass produced, and the y-axis is the cost of PHB per carbon mole of biomass produced. The tradeoff curve (red line) shows the optimal phenotypes expressed between O_2 sufficient and O_2 limiting conditions. Modes are color coded according to the amount of nitrate that is directed towards denitrification (as opposed to biomass production).

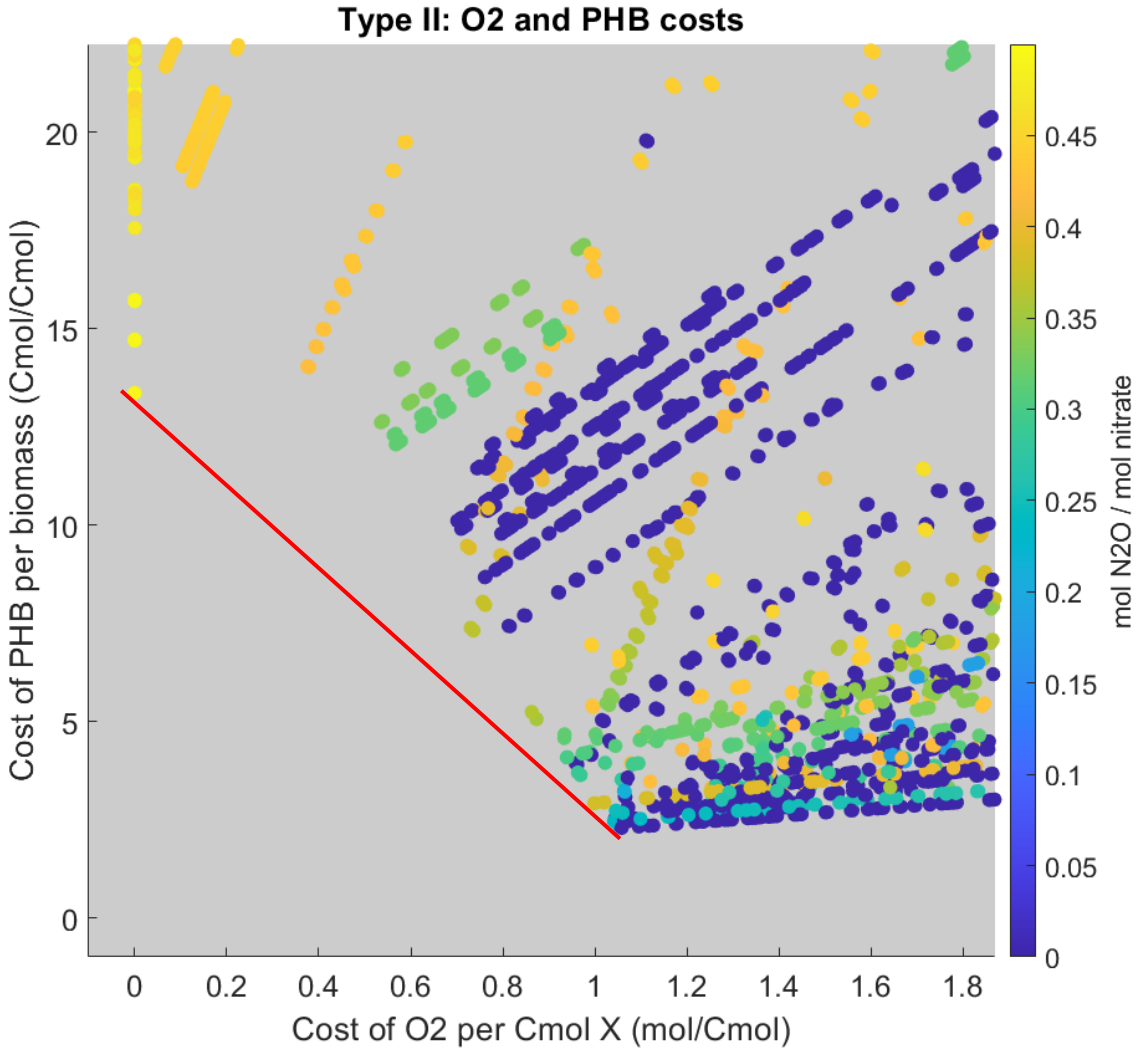

Predictions for PHB consumption leading to ATP production mirror the biomass predictions. There are only two points on the tradeoff curve: one for aerobic respiration, and one for denitrification (Figure 2.20). When denitrification is removed from the predictions, however, fermentation of PHB is predicted. Acetate is the sole byproduct excreted under the lowest O_2

conditions (Figure 2.21). Under the lowest possible O_2 availability for these conditions, nearly all PHB is converted to acetate. Figure 2.20 and Figure 2.21 show the same modes, but denitrification is removed in Figure 2.21, changing the shape of the tradeoff curve. In Figure 2.21, three points lie along the tradeoff curve, with more fermentative byproducts being produced as O_2 becomes more limited. ATP yield on PHB is comparable to ATP yield on methane (5.12 ATP/Cmol PHB vs. 6 ATP/mol methane).

Figure 2.20. Predictions for ATP production during polyhydroxybutyrate (PHB) degradation in the presence of nitrate. The x-axis is the cost of O2 per mole of ATP produced, and the y-axis is the cost of PHB per mole of ATP produced. The tradeoff curve (red line) shows the optimal phenotypes expressed between O_2 sufficient and O_2 limiting conditions. Modes are color coded according to the flux through the partial denitrification pathway, which is expressed as the cost of nitrate per ATP. When biomass is not being produced, all nitrate that is taken up by the cell is used for denitrification.

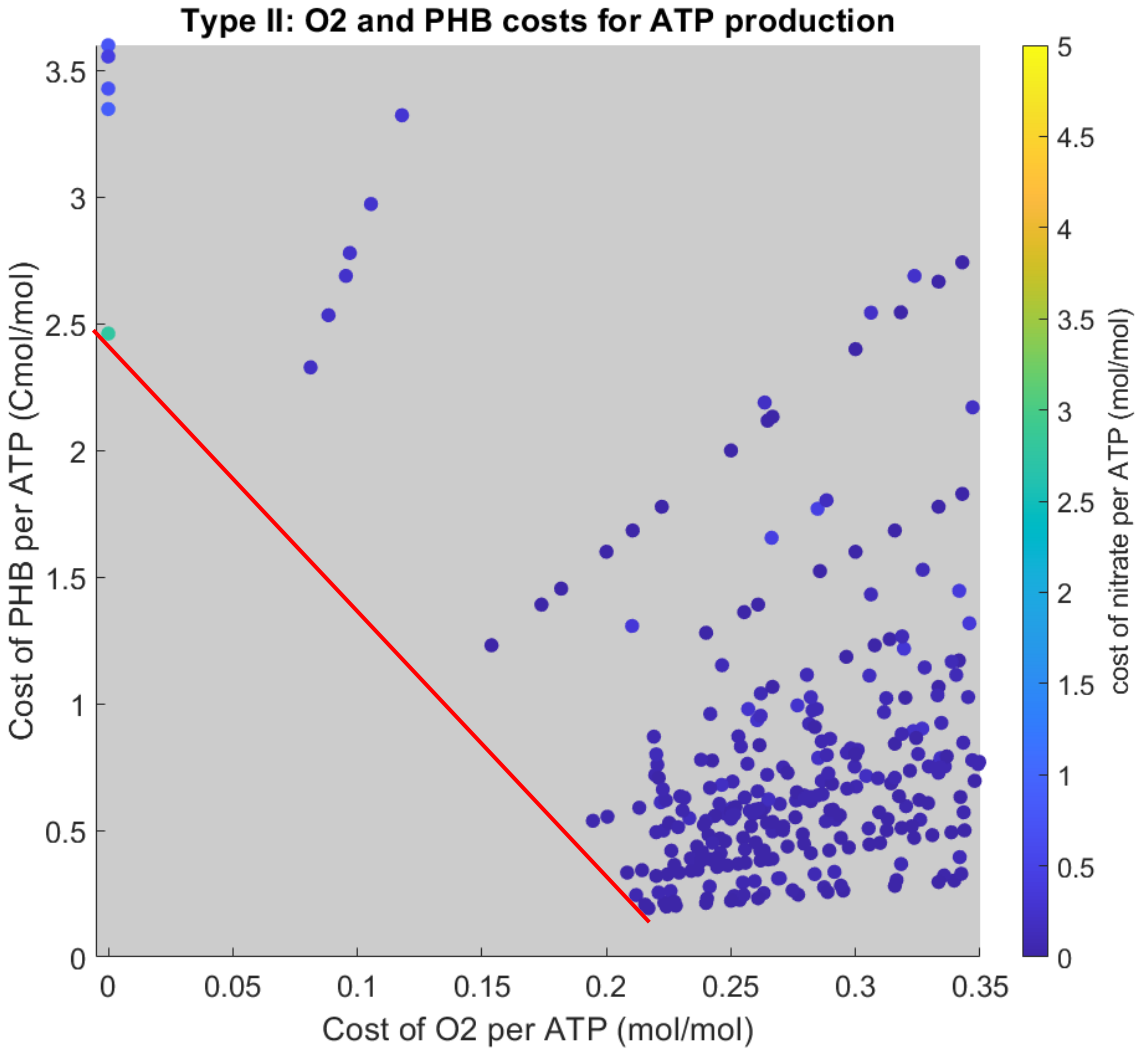

Figure 2.21. Predictions for ATP production during polyhydroxybutyrate (PHB) degradation in the absence of nitrate, when denitrification is not possible. The x-axis is the cost of O2 per mole of ATP produced, and the y-axis is the cost of PHB per mole of ATP produced. The tradeoff curve (red line) shows the optimal phenotypes expressed between O_2 sufficient and O_2 limiting conditions. Modes are color coded according to the yield of byproducts on PHB (Cmol/Cmol).

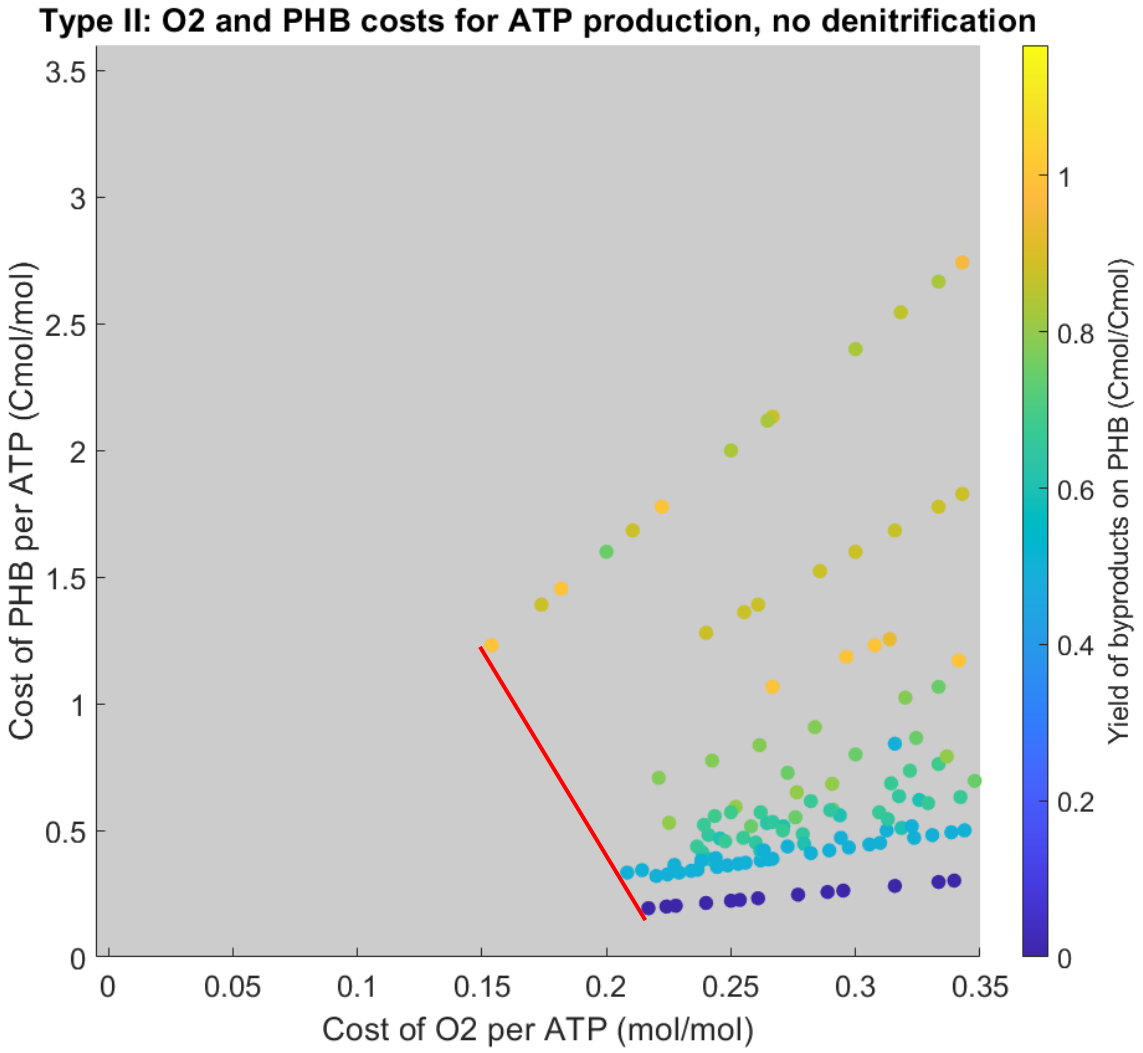

Comparison of Denitrification and Glycogen Degradation

Similar predictions were run to examine the role of glycogen degradation and denitrification in survival of type I methanotrophs under low O_2 conditions. Like the PHB degradation predictions, it was found that optimal phenotypes when comparing biomass yield

and O_2 consumption represent a walk between aerobic respiration and denitrification (Figure 2.22). No fermentation is predicted under low O_2 conditions when nitrate is present. This is also the case for predictions of ATP production on glycogen (Figure 2.23). Like the type II methanotrophs, however, fermentation is predicted under low O_2 conditions when denitrification is removed (Figure 2.24). The major byproducts that are produced are acetate and succinate, with the shift towards succinate being observed under lower O_2 conditions. Figure 2.25 shows this shift in terms of the amount of ATP that is produced via oxidative phosphorylation vs. fermentation. Biomass yield on glycogen is comparable to biomass yield on methane (0.4423 Cmol biomass/Cmol glycogen vs. 0.4263 Cmol biomass/Cmol methane).

Figure 2.22. Predictions for biomass production during glycogen (PHB) degradation. The x-axis is the cost of O_2 per carbon mole of biomass produced, and the y-axis is the cost of glycogen per carbon mole of biomass produced. The tradeoff curve (red line) shows the optimal phenotypes expressed between O_2 sufficient and O_2 limiting conditions. Modes are color coded according to the amount of nitrate that is directed towards denitrification (as opposed to biomass production).

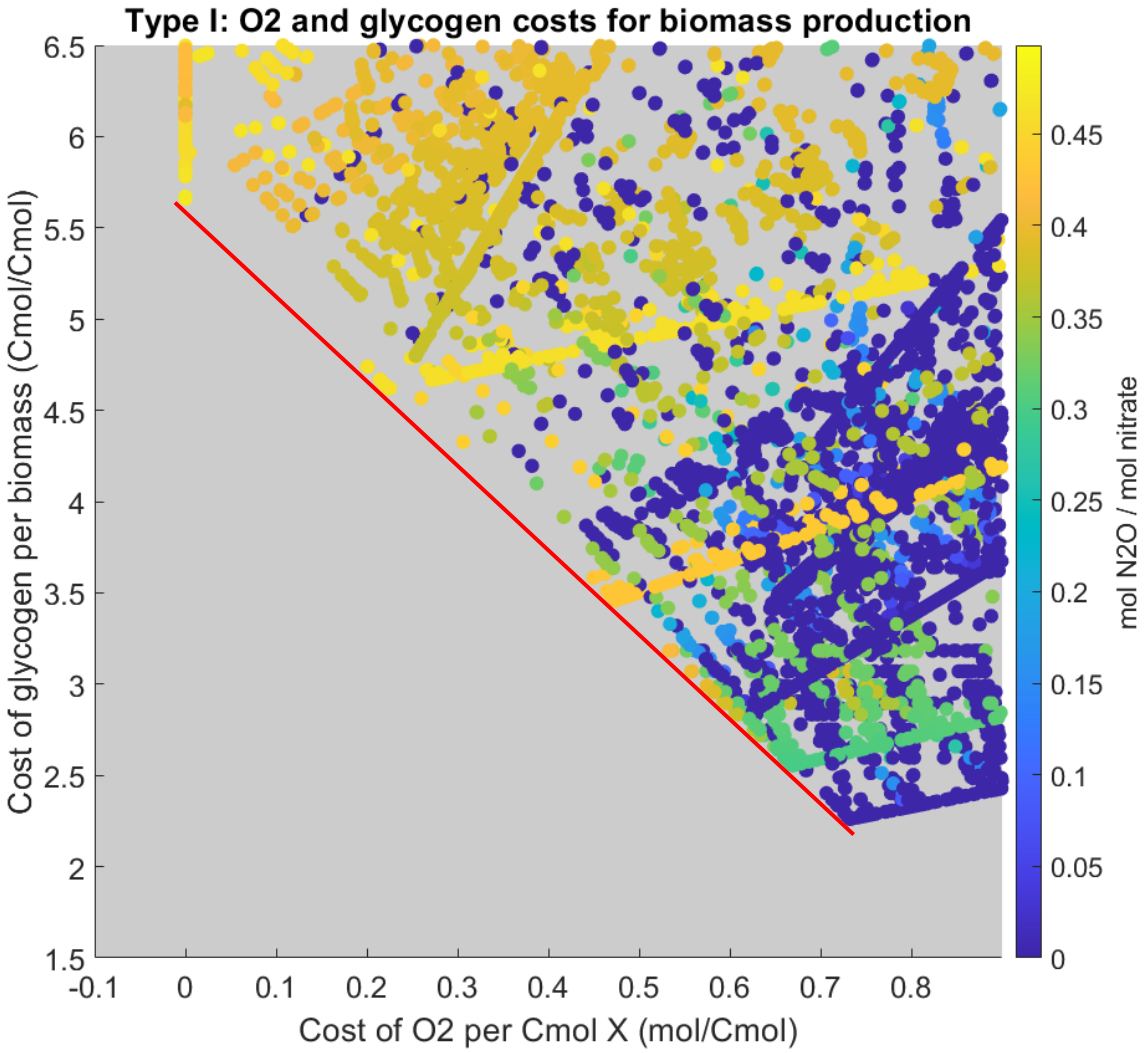

Figure 2.23. Predictions for ATP production during glycogen degradation in the presence of nitrate. The x-axis is the cost of O_2 per mole of ATP produced, and the y-axis is the cost of glycogen per mole of ATP produced. The tradeoff curve (red line) shows the optimal phenotypes expressed between O_2 sufficient and O_2 limiting conditions. Modes are color coded according to the flux through the partial denitrification pathway, which is expressed as the cost of nitrate per ATP. When biomass is not being produced, all nitrate that is taken up by the cell is used for denitrification.

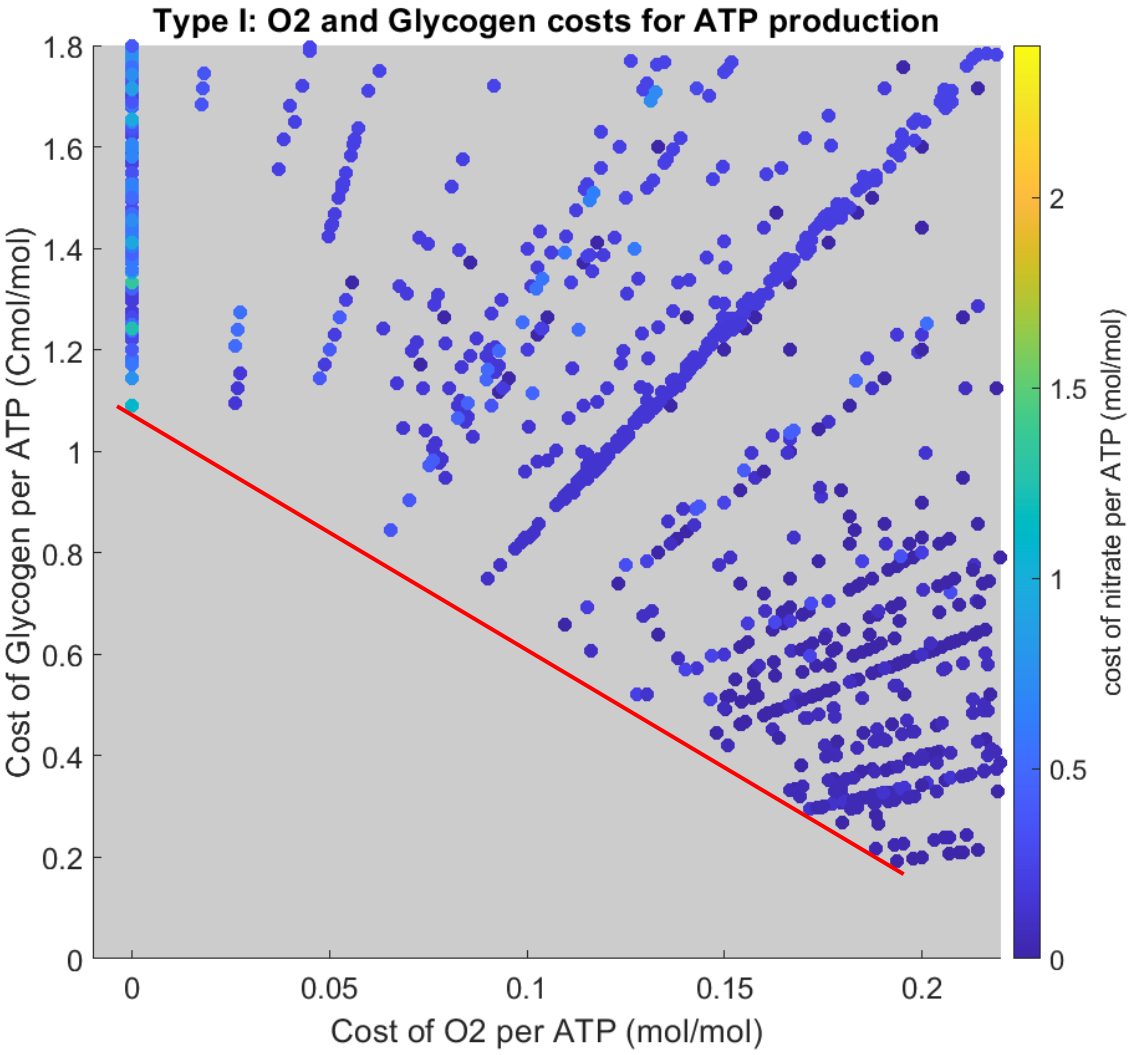

Figure 2.24. Predictions for ATP production during glycogen degradation in the absence of nitrate, when denitrification is not possible. The x-axis is the cost of O_2 per mole of ATP produced, and the y-axis is the cost of glycogen per mole of ATP produced. The tradeoff curve (red line) shows the optimal phenotypes expressed between O_2 sufficient and O_2 limiting conditions. Modes are color coded according to the yield of byproducts on PHB (Cmol/Cmol).

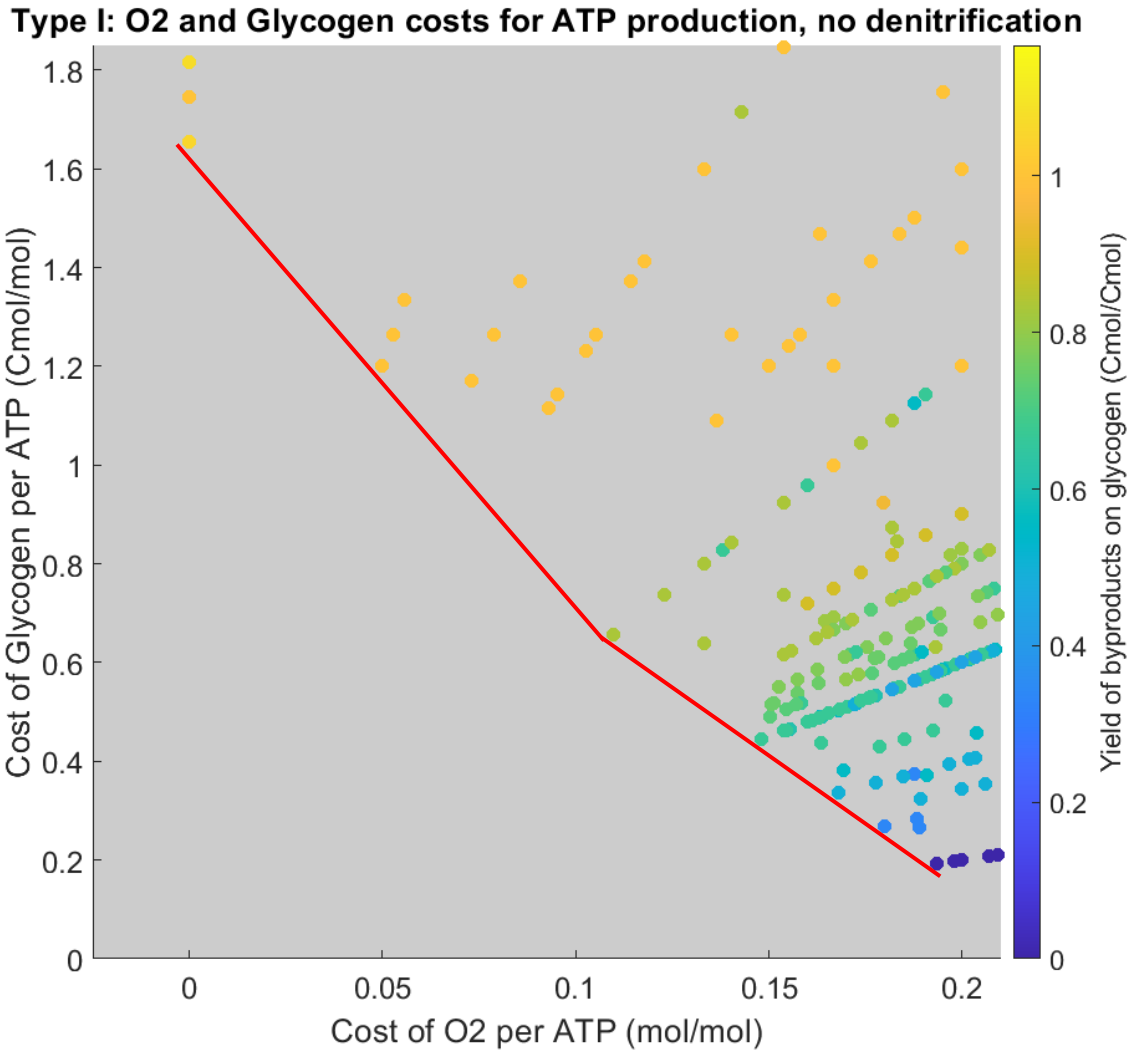

Figure 2.25. Predictions for ATP production during glycogen degradation in the absence of nitrate, when denitrification is not possible. The x-axis is the cost of O_2 per mole of ATP produced, and the y-axis is the cost of glycogen per mole of ATP produced. The tradeoff curve (red line) shows the optimal phenotypes expressed between O_2 sufficient and O_2 limiting conditions. Modes are color coded according to the amount of ATP that is produced via oxidative phosphorylation per glycogen that is consumed (mol/Cmol). The modes that are shown here are the same as in Figure 2.24, with different color coding.

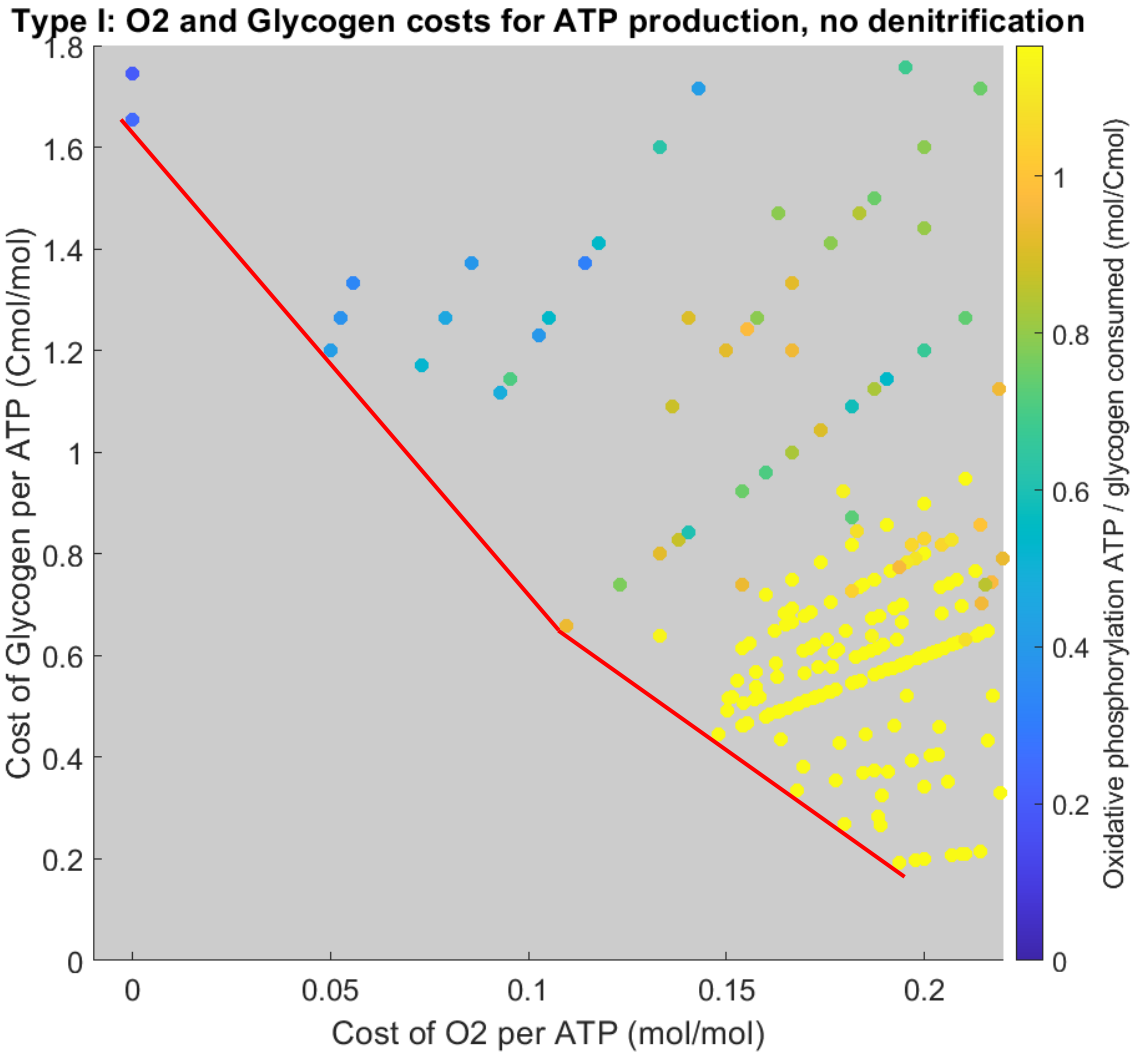

Glycogen Predictions in Type II Methanotrophs

Glycogen synthesis reactions were added to the type II model in order to investigate whether type II methanotrophs can produce glycogen in yields comparable to PHB accumulation. Figure 2.26 and Figure 2.27 compare the accumulation of PHB or glycogen to biomass yield. These predictions are for growth on methane, which means that all modes require biomass to be produced, so the yield of each storage compound is slightly lower than the theoretical maximum (for example, the yield of PHB when biomass is being produced is 0.7677 Cmol PHB/Cmol methane, compared to 0.8 Cmol PHB/Cmol methane when no biomass is produced in addition to the PHB). It was found that glycogen yields on methane are comparable to PHB yields: 0.7466 Cmol glycogen/Cmol methane vs. 0.7677 Cmol PHB/Cmol methane.

Figure 2.26. Comparison of polyhydroxybutyrate (PHB) accumulation and biomass yields during growth on methane in type II methanotrophs. The y-axis is the yield of PHB on methane (Cmol/Cmol), and the x-axis is the yield of biomass on methane (Cmol/Cmol). Modes are color coded according to the yield of PHB on methane (same value as the y-axis). These predictions were run for growth conditions, so all modes shown here produce biomass.

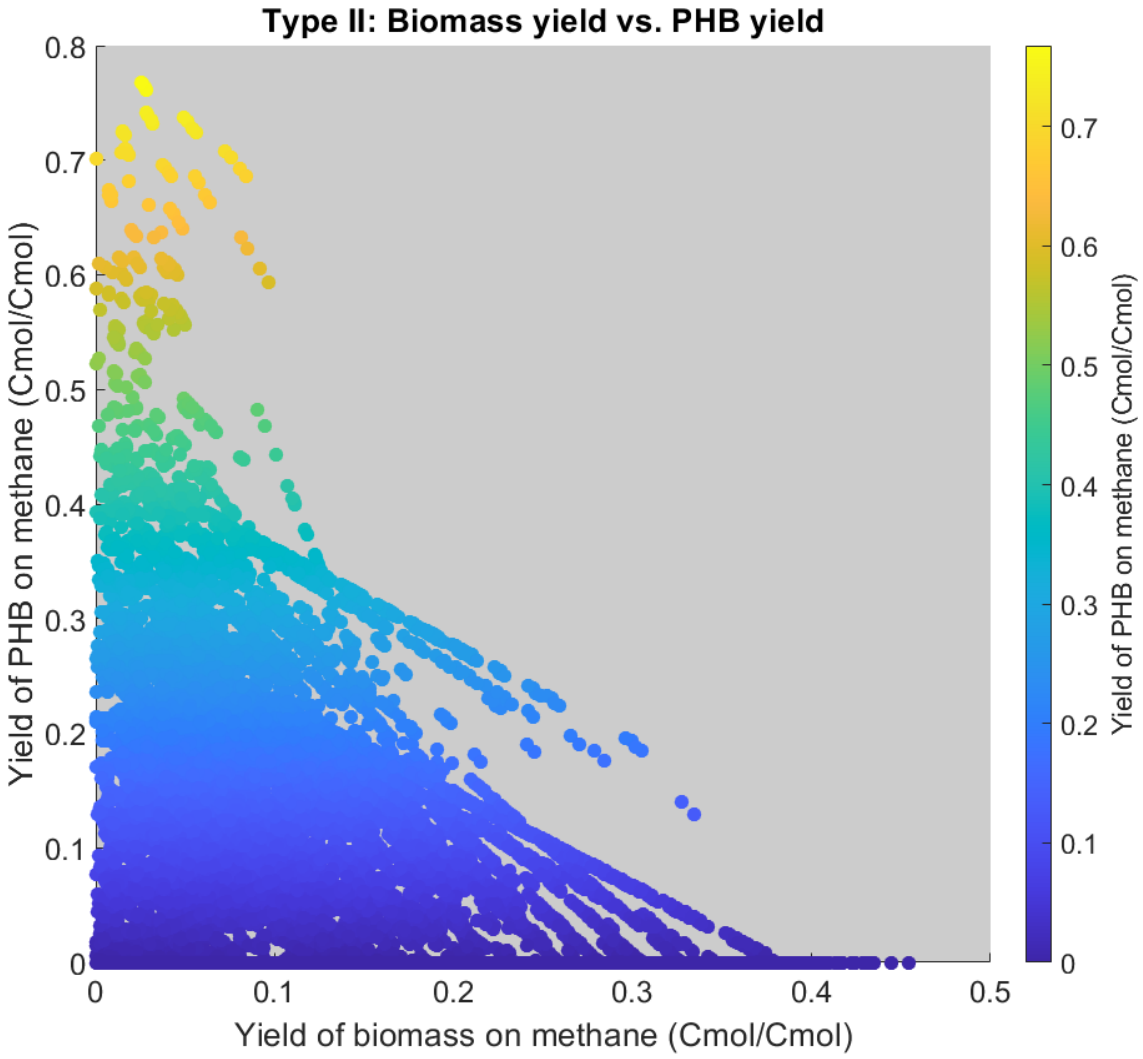

Figure 2.27. Comparison of glycogen accumulation and biomass yields during growth on methane in type II methanotrophs. The y-axis is the yield of glycogen on methane (Cmol/Cmol), and the x-axis is the yield of biomass on methane (Cmol/Cmol). Modes are color coded according to the yield of glycogen on methane (same value as the y-axis). These predictions were run for growth conditions, so all modes shown in this figure produce biomass.

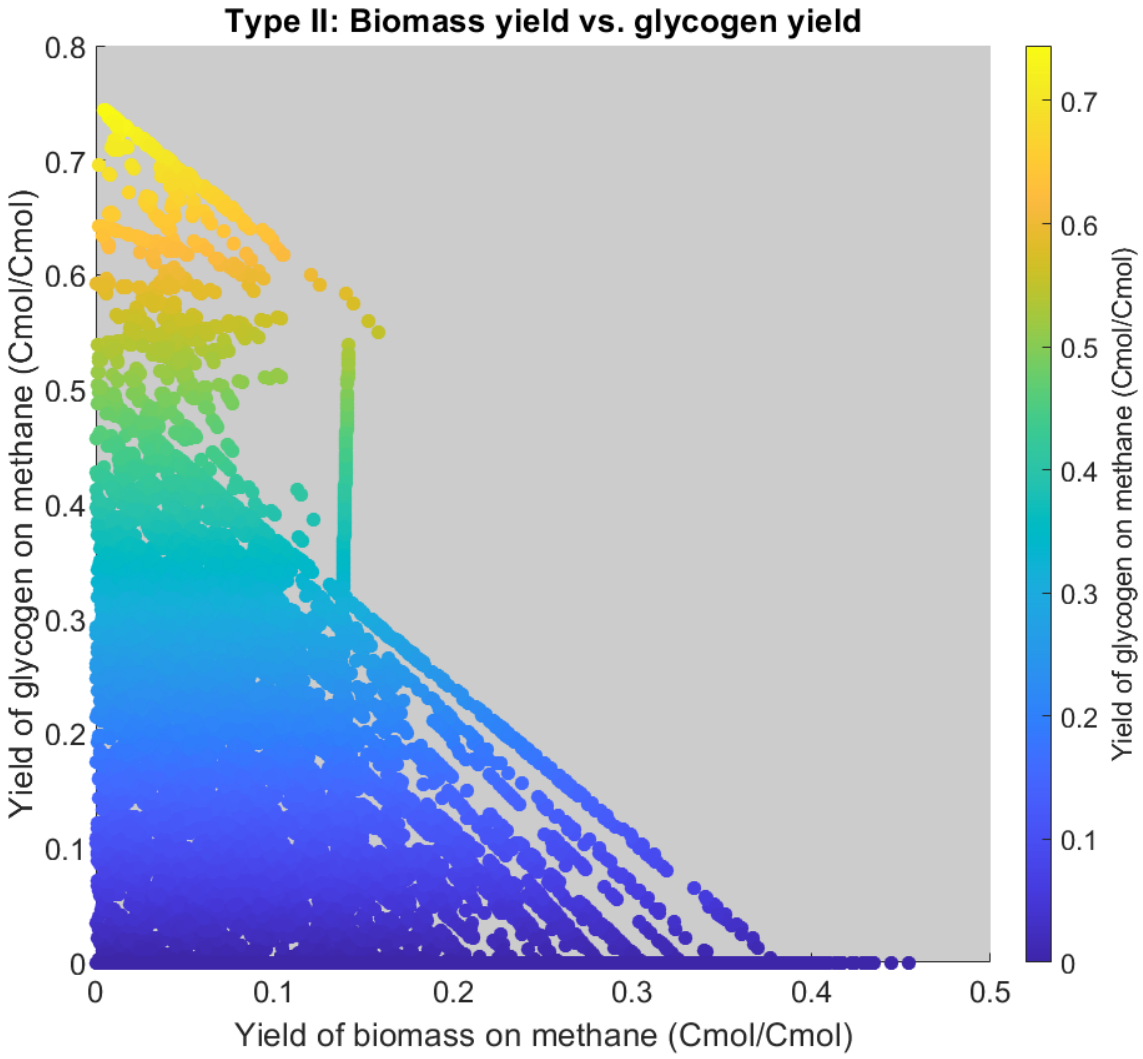

Global Warming Potential Evaluations

Type II methanotroph metabolism was evaluated in terms of global warming potential (GWP). These predictions are once again plotted in terms of competing costs, with the

assumption that carbon and O_2 are limiting resources during methanotroph growth. Figure 2.28 shows the CO_2-equivalents consumed during type II growth on O_2 and methane without denitrification. The modes on the right-hand side of the tradeoff curve are phenotypes that are predicted to be expressed when O_2 availability is high. These phenotypes use O_2 as an electron acceptor. The modes on the left-hand side of the tradeoff curve display a shift towards a type of "fermentative" metabolism, where succinate, methanol, and formate are excreted as reduced byproducts. Methane oxidation is an energy intensive process, and in the modes experiencing the lowest possible O_2 availability under which methane can be oxidized, methane oxidation to methanol and formate apparently represents an efficient method of disposing of excess energy. Reports of byproduct excretion by type II methanotrophs during growth on methane are scarce. In at least one study, however, *Methylocystis* sp. Rockwell was shown to produce formate during growth on methanol, which the authors suggested was a strategy to balance electrons during unfavorable growth conditions (Tays et al., 2018). Methanol excretion may not be favored as a "fermentation" strategy under real-world conditions as methanol is often inhibitory to methanotroph growth, but these predictions support formate production as a method to reduce energy burden.

Figure 2.29 illustrates the switch between overall consumption of greenhouse gases to production of greenhouse gases that occurs at lower O_2 availability conditions. Type II methanotrophs will always reduce greenhouse gas burden when growing on methane under O_2 replete conditions (Figure 2.28). When denitrification is allowed, however, nitrous oxide is produced under lower O_2 conditions (below a methane:O_2 ratio of 1.2), and type II methanotrophs are predicted to substantially contribute to climate change (Figure 2.29). No

byproducts are excreted by any mode along this tradeoff curve, in contrast to the modes where denitrification is blocked.

Figure 2.28. CO_2 equivalents (on a global warming potential basis of 100 years) during type II methanotroph growth on methane when denitrification is blocked. The y-axis is the cost of methane per biomass (Cmol/Cmol), and the x-axis is the cost of O_2 per methane (mol/Cmol). Modes are color coded according to the production or consumption of CO_2 equivalents.

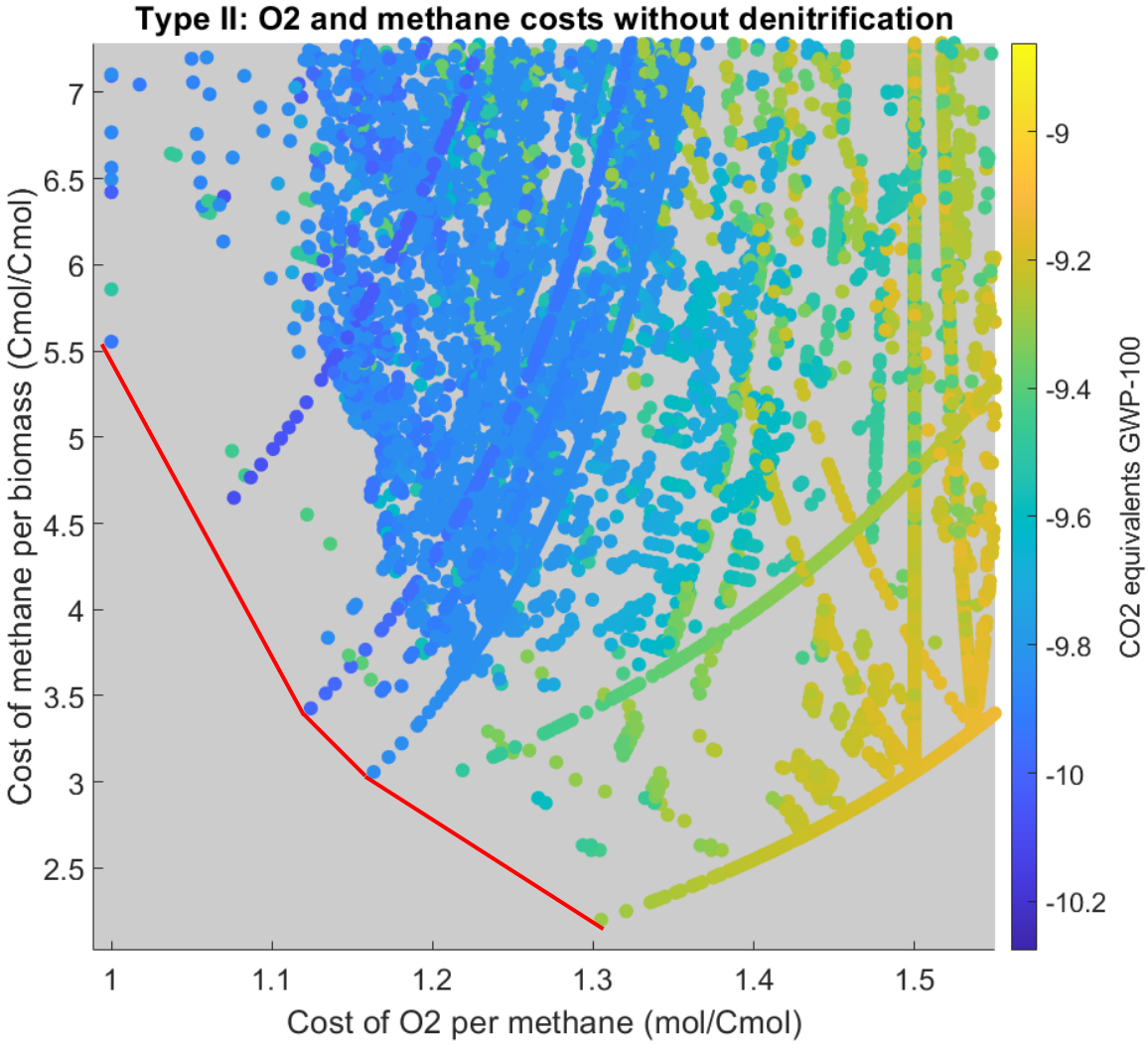

Figure 2.29. CO_2 equivalents (on a global warming potential basis of 100 years) during type II methanotroph growth on methane when denitrification is allowed. The y-axis is the cost of methane per biomass (Cmol/Cmol), and the x-axis is the cost of O_2 per methane (mol/Cmol). Modes are color coded according to the production or consumption of CO_2 equivalents.

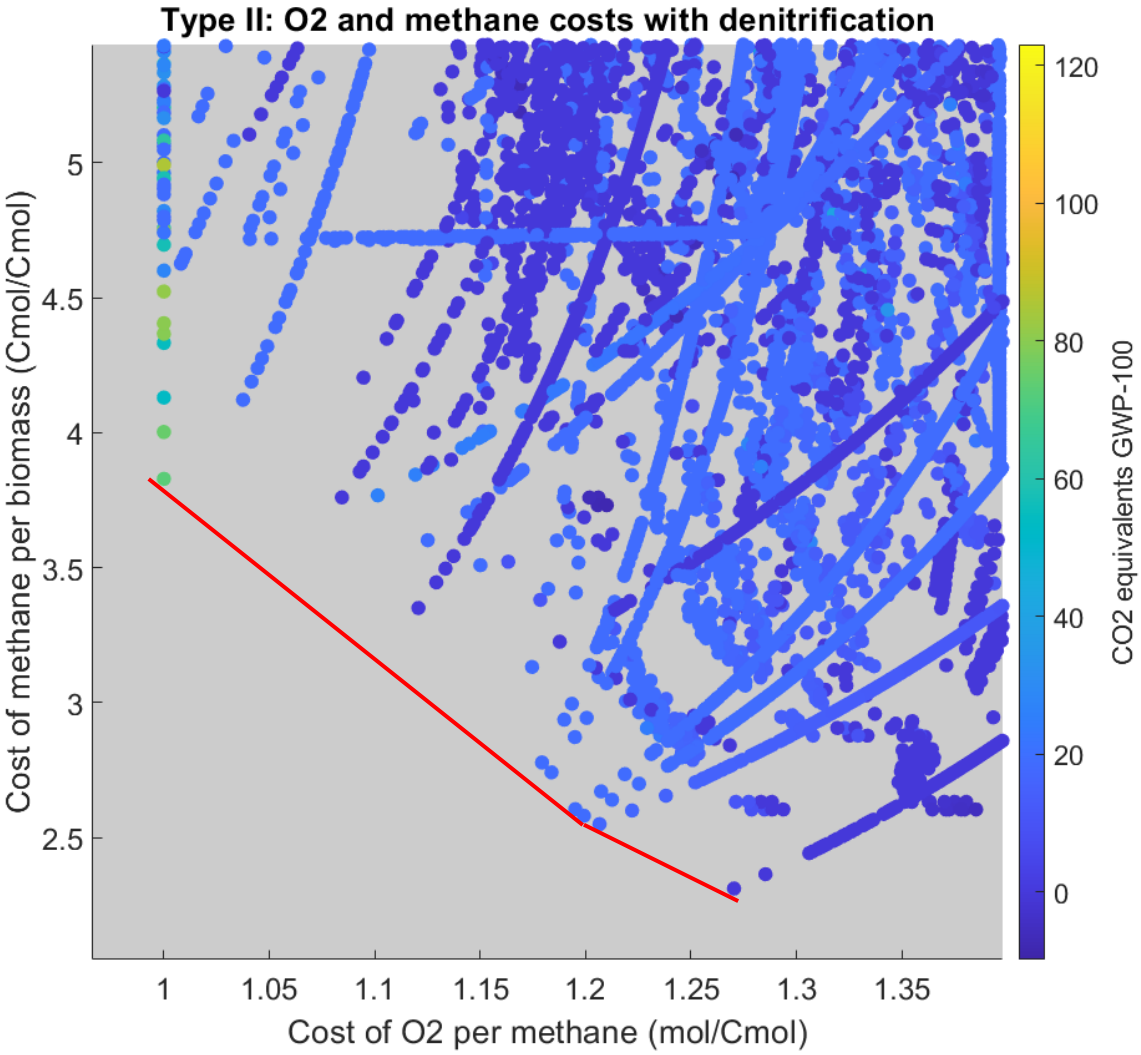

Role of Copper in Type II Methanotroph Respiration

Copper is required by several enzymes in the methanotroph electron transport chain. It is also required by nirK, the nitrite reductase used in the type II model. Figure 2.30 shows the relationship between copper availability, denitrification, and aerobic respiration. Copper costs

are calculated according to enzyme use rather than flux. For example, if pMMO is expressed in a certain mode, then the copper cost for that mode is 3 (plus the cost of any other copper enzymes that may be used). Alternatively, copper costs can be scaled to the flux through each reaction, in a method that is similar to parsimonious flux balance analysis. Figure 2.30 shows that nirK expression is constrained under low copper availability, reducing the production of nitrous oxide emissions.

Figure 2.30. CO_2 equivalents (on a global warming potential basis of 100 years) during type II methanotroph growth on methane. The y-axis is the moles of CO_2 equivalents (GWP-100) produced per mole of methane consumed. The x-axis is the copper cost of each mode, with copper costs scaled to each reaction rather than to flux. Modes are color coded according to production of nitrous oxide.

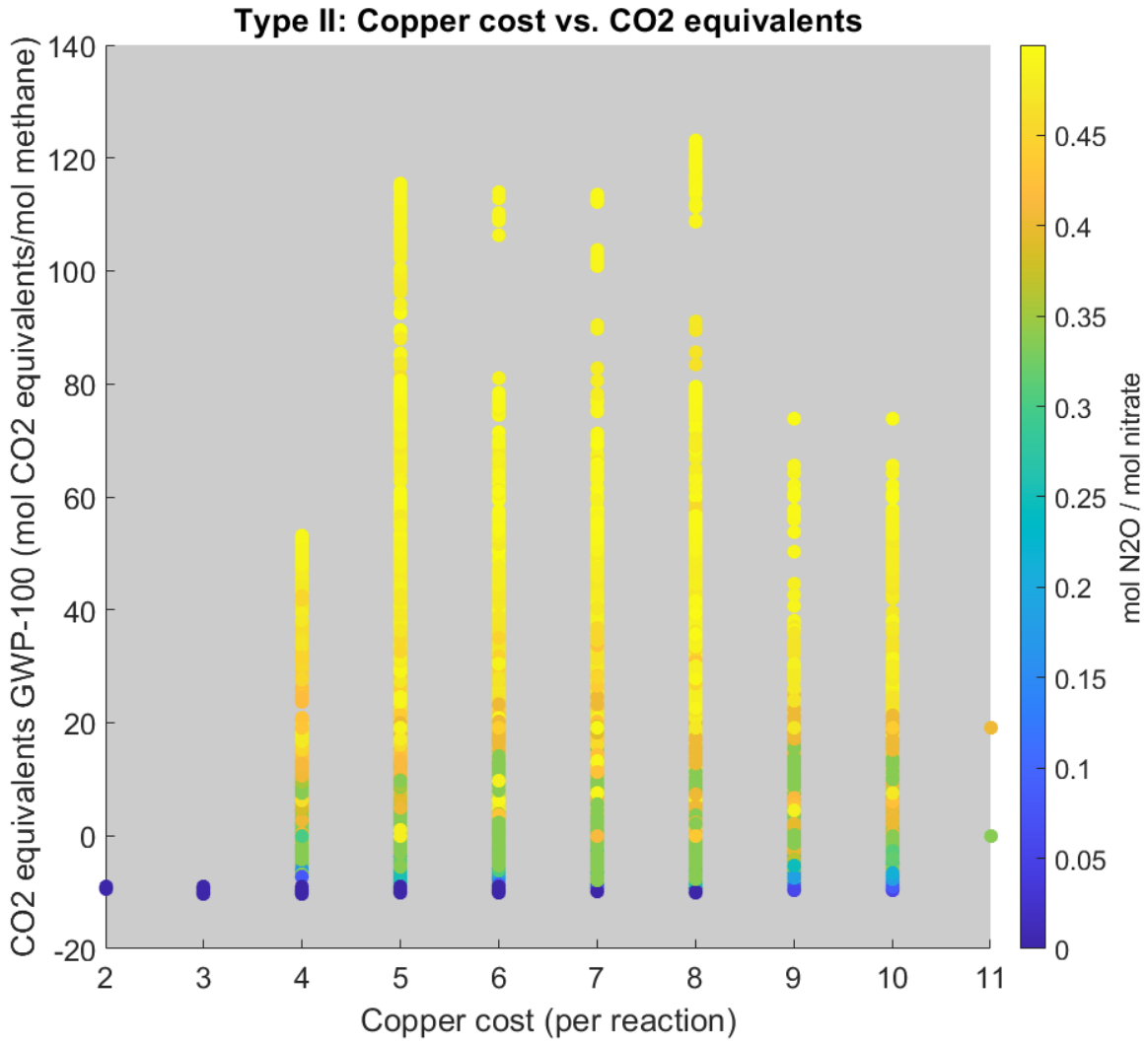

Conclusions

Role of Carbon Storage Compounds in Acclimation to Low O_2 Conditions

Both type I and type II methanotrophs can ferment carbon storage compounds under low O_2 conditions. Denitrification is energetically preferred over fermentation, however, and it is predicted that nitrate will prevent fermentative metabolism. In type I methanotrophs, the byproducts that are produced during glycogen degradation depend on the degree of O_2 limitation, with acetate production seen first, then succinate production under the lowest O_2 cost modes. In type II methanotrophs, acetate is the only reduced byproduct that is predicted during PHB degradation.

Carbon Storage Compounds and Community Crossfeeding

Under low O_2 conditions when denitrification is prevented, methanotrophs convert the majority of the carbon storage compounds that are degraded to organic acids. These compounds could play a major role in community crossfeeding under low O_2 conditions.

Growth or Energy Production from Carbon Storage Compounds?

Both models predict that storage compound degradation could be used either for production of biomass or production of ATP. The predicted biomass yields on glycogen and PHB are comparable to yields on methane; ATP yields on PHB are slightly lower than yields on methane. Experimental evidence suggests that carbon storage compound degradation during starvation is used by cells to restart methane oxidation, but this is likely a regulatory mechanism that methanotrophs have developed to adapt to shifting methane concentrations, rather than a metabolic constraint.

Purpose of Co-consumption of Methane and Storage Compounds

Experimental evidence also shows that carbon storage compounds are often consumed in conjunction with methane oxidation during nutrient replete growth. Based on modeling predictions, this consumption could be used either to provide energy or metabolic intermediates for central carbon metabolism.

Glycogen Accumulation in Type II Methanotrophs

The type II model predicts that glycogen can be accumulated by type II methanotrophs to nearly the same levels as PHB. Type II methanotrophs do not accumulate glycogen; this is not a metabolic constraint, but rather is likely a flux constraint, as a large amount of flux is directed through the serine pathway and the EMC pathway, which share several reactions with PHB formation and degradation.

Greenhouse Gas Production and Consumption by Type II Methanotrophs

Methanotrophs grown in O_2 replete conditions are predicted to always reduce greenhouse gas burden, as they consume methane and produce CO_2, a less potent greenhouse gas. Under O_2 limiting conditions, however, denitrification is predicted to produce large amounts of nitrous oxide. Methanotrophs grown under O_2 limitation in the presence of nitrate are expected to contribute to climate change.

Copper and Respiration in Type II Methanotrophs

Reducing copper availability may help reduce greenhouse gas emissions under low O_2 conditions. In methanotrophs encoding nirK, low copper conditions prevent the denitrification pathway from proceeding, eliminating nitrous oxide production. Methanotrophs are often

investigated as a method of biological remediation for sites that are contaminated with organic solvents, as MMOs can act on some of these short-chain compounds and convert them into a less dangerous form (S. W. Lee et al., 2006). Based on these predictions, sites with high copper and high nitrate concentrations should be avoided, as methanotroph growth under these conditions can lead to production of nitrous oxide.

Summary of Work

This work demonstrates the steps required to build and analyze detailed core metabolic models. The role of carbon storage compound degradation in methanotroph survival under O_2 limited conditions is compared to the use of nitrate as an electron acceptor. Nitrate reduction is preferred to fermentation. When denitrification is prevented, however it is predicted that both reduced carbon compounds like formate, acetate, and succinate are likely to be excreted into the environment both during growth on methane and during catabolism of glycogen or PHB. These compounds provide an opportunity for community crossfeeding.

The models were also used to investigate the role of methanotrophs in greenhouse gas production. Under low O_2 conditions, denitrification results in methanotrophs contributing to climate change. Nitrate and copper concentrations could be controlled to prevent the production of nitrous oxide from methanotrophs.

Chapter Acknowledgements

Thanks to Dr. Ashley Beck for her guidance and instruction on model development and modeling techniques.

CHAPTER THREE

COMPATIBLE SOLUTES PRODUCTION IN AN ALKALI-TOLERANT MICROALGA

Contribution of Authors and Co-Authors

Author: Adrienne D. Arnold

Contributions: Conceived and directed the research, performed analysis, conducted literature review, wrote the manuscript

Co-Author: Charles J. Holcomb

Contributions: Performed analysis

Co-Author: Dr. Ross P. Carlson

Contributions: Conceived and directed the research

Manuscript Information

Adrienne D. Arnold, Charles J. Holcomb, and Ross P. Carlson

[TBD]

Status of Manuscript:
__X__ Prepared for submission to a peer-reviewed journal
____ Officially submitted to a peer-reviewed journal
____ Accepted by a peer-reviewed journal
____ Published in a peer-reviewed journal

Introduction

Green microalgae are phototrophic eukaryotes. They are often studied for their industrial potential, as green algae can accumulate starch and lipids up to 50% of cell dry weight under ideal conditions (Narala et al., 2016). Starch and lipids are biofuel precursors that can be converted into renewable energy. The use of algae to produce biofuels has significant advantages over traditional biofuel production methods. Algae can be grown in wastewater and in locations with non-arable land, so that biofuel production does not compete with food supplies (Narala et al., 2016). They do not require extensive structures like roots and stems, meaning that more CO_2 that is fixed goes towards high-value biomass (Benedetti et al., 2018). Algae also grow quickly, allowing for faster recovery from crop failures (Subramanian et al., 2013).

Production of biofuels from microalgae takes advantage of a survival mechanism utilized by photosynthetic algae to endure dark conditions. During the day, when light can be used to drive photosynthesis and power carbon fixation, algae accumulate carbon reserves. At night, resources are scarce for phototrophs, so storage compounds are broken down to supply both carbon and energy for algal cells (Raven & Beardall, 2016; Vitova et al., 2014). Starch and lipids are both used for carbon and energy storage, but they fill different roles for the algae. Starch is a polyglucan compound that can be broken down under oxic or anoxic conditions. Lipids are more energy dense than starch and therefore store more energy while taking up less space in the cell (Vitova et al., 2014). They are broken down via the β oxidation pathway, however, and thus can only be degraded when O_2 is present. Storage compounds have also been implicated in algal adaptation to other types of stress, like high salinity (Liska et al., 2004; Oren, 2017). Multiple cultivation factors influence accumulation, degradation, and interconversion of starch and lipids,

and the elucidation these factors is an active area of research that continues to improve biofuel precursor production from algae (Johnson & Alric, 2013; Sato & Toyoshima, 2021; Subramanian et al., 2013).

Several methods are used to trigger overaccumulation of lipids and starch. Because the formation of a storage compound diverts carbon away from biomass, a two-stage cultivation technique is often used in industry. The first stage is cultivation under optimal growth conditions in order to obtain a high biomass yield. The second stage applies a stress that promotes accumulation of starch or lipids. The most typical triggers are nitrogen or phosphorous limitation, but many different stresses can cause accumulation of storage compounds, including high light, high heat, and high salinity (Cecchin et al., 2019; Sun et al., 2018; Vitova et al., 2014).

Chlorella sorokiniana SLA-04 is a green microalga isolated from Soap Lake, Washington, and grows well in high pH, high alkalinity environments. Cultivation in high pH, high alkalinity environments enhances CO_2 dissolution, reducing the need for costly CO_2 sparging and allowing algae to be grown away from CO_2 point sources like power plants. High pH cultivation also reduces the growth of many common algal predators, potentially reducing the risk of culture crashes (Vadlamani et al., 2017a, 2019). High alkalinity conditions are likely to also impose some stresses on the microalgae, however, including high osmotic pressure. Understanding the response of SLA-04 to stress conditions during cultivation is key to managing lipid and starch yields. This work will focus on the interplay between accumulation of carbon storage compounds and production of compatible solutes, with the goal of better understanding SLA-04 metabolism during growth in high salinity and high alkalinity conditions.

Adaptation to Osmotic Pressure

Cells must maintain an appropriate osmotic pressure relative to their environment in order to avoid water loss/desiccation and maintain turgor pressure. This poses a challenge for algae grown under conditions of high alkalinity or high salinity, where external osmotic pressure is high compared to the pressure inside cells. How do these cells remain hyperosmotic compared to the environment while avoiding the inhibitory effects of ion buildup on cytosolic enzymes (Hagemann, 2016)?

There are two strategies used by microorganisms for adaptation to high external osmotic pressure: the salt-in strategy, and the salt-out strategy. In the salt-in strategy, enzymes are modified to function under high ionic concentrations. This strategy is metabolically cheap but evolutionarily difficult, as the entirety of the enzymes expressed by the cell must have amino acid sequences that are compatible with the high salt concentration (Oren, 2001). In the salt-out strategy, which is used by all algae, cells accumulate high concentrations of soluble organic metabolites, referred to as compatible solutes, within the cytosol (Oren, 2007). These compounds balance intracellular and extracellular pressure without negatively impacting enzyme function. The salt-out strategy is metabolically expensive, however, as both carbon and energy are required to synthesize compatible solutes (R. P. Carlson et al., 2016; Hagemann, 2016).

There are several categories of compatible solutes, each favored by different organisms for different purposes. Simple sugars like sucrose are commonly accumulated by green algae with low salt tolerance. These compatible solutes are also proposed to be protective from temperature stress, possibly making them beneficial for multiple stress conditions (Hagemann, 2016). Glycerol is accumulated by *Dunaliella* sp., which are the green algae with the highest

known salt tolerance. Glycerol is cheap to synthesize but can leak through most biological membranes, requiring microorganisms that use glycerol as a compatible solute to use strategies to reduce glycerol loss, including modified membranes or special transporters (Hagemann, 2016; Oren, 2017). Other common compatible solutes include proline, glucosylglycerol, and ectoine/hydroxyectoine (Hagemann, 2016).

Compatible solutes are accumulated under salt stress and thus are released by cells during a hypoosmotic shock, such as a rain event that dilutes the salt concentration in the environment (Sauer & Galinski, 1998). The sudden decrease in external salt concentration requires cells to quickly expel accumulated compatible solutes so that the cell can avoid a rapid influx of water, which can cause cell lysis. As a result, compatible solutes are often traded back and forth between members of the microbial community. Glycerol from *Dunaliella* sp., either that which leaks out of the cell or that which is released when salt concentration drops, is proposed to be an important source of carbon for heterotrophic organisms in extremely salty environments (Oren, 2017). Ectoine has been shown to be exchanged between algal and bacterial species (Fenizia et al., 2020). Because compatible solute production is metabolically expensive, uptake of compatible solutes from the environment is often preferred by cells over endogenous synthesis (Fenizia et al., 2020; Oren, 2001).

Compatible solutes and other compounds can also be harvested from microbial cultures in a process known as “milking.” For compatible solutes production, cultures are grown in high salinity media, then subjected to alternating hypoosmotic shocks which catalyze the release of compatible solutes into the media for collection and hyperosmotic shocks to renew stores of compatible solutes (Sauer & Galinski, 1998). Under ideal conditions, milking processes do not

result in substantial cell death. This could make milking a cheaper production strategy compared to traditional batch cultivation and harvesting procedures (Hejazi & Wijffels, 2004; Taubert et al., 2019).

Starch and lipid reserves have been linked to compatible solutes metabolism. In *Dunaliella tertiolecta*, during the light cycle, glycerol was produced from both the Calvin cycle and from intracellular starch, with the amount of glycerol produced from starch increasing with increased salinity. Glycerol could also be converted into starch stores once a suitable level of compatible solute had accumulated (Goyal, 2007). The expression of starch-related enzymes in *Dunaliella salina* also increased under high salt conditions, with the authors likewise suggesting that glycerol could be produced from a combination of carbon from starch and from the Calvin cycle (Liska et al., 2004). Salt stress studies in *Chlorella vulgaris* and *Chlamydomonas reinhardtii* have demonstrated increased lipid and glycerol accumulation under high salt conditions, and key enzymes in glycerol synthesis are involved in both processes (Abdellaoui et al., 2019; Morales-Sánchez et al., 2017).

In this study, we investigate the relationship of carbon storage compounds in SLA-04 to compatible solutes metabolism, with a focus on sucrose and glycerol. These two compatible solutes represent the opposite ends of salinity tolerance, with sucrose common to low salinity environments and glycerol used by the most saline-tolerant algae. Sucrose and glycerol are relatively inexpensive compounds to synthesize and require few additional enzymes beyond those regularly used in central carbon metabolism. The goal of this section is to analyze the metabolic costs of compatible solute synthesis and use these costs to determine whether a

preference for starch vs. lipid reserves in SLA-04 may be influenced by the osmotic pressure constraints of the environment.

Methods

A simplified core metabolic model was developed using the genome for *Chlorella sorokiniana* SLA-04. For the purpose of these predictions, this core model includes only central carbon metabolism and accumulation and degradation of carbon storage compounds rather than full biomass synthesis reactions. The genome was annotated using KEGG's GhostKOALA tool (Kanehisa et al., 2016). Reaction designations and metabolite names, where possible, are based on MetaCyc conventions. While reactions were not assigned to particular organelles for these predictions, draft organelle assignments are included in the model file and are based on predictions from TargetP and PredAlgo (Armenteros et al., 2019; Reijnders et al., 2014; Tardif et al., 2012). The metabolic model was developed in CellNetAnalyzer and analyzed using flux balance analysis in CobraToolbox (Becker et al., 2007; von Kamp et al., 2017).

Flux balance analysis (FBA) is a stoichiometric modeling technique that is commonly used to analyze larger metabolic models. Rather than generating all possible phenotypes that an organism can display, FBA predicts a single optimal phenotype based on flux constraints that are present within the model. FBA is less computationally expensive than other modeling techniques like elementary flux mode analysis. The input requirement for optimization criteria, however, potentially introduces bias into the results.

FBA predictions are presented here using phenotypic phase plane analysis. In this method of analysis, the fluxes of two reactions are fixed, and a third reaction is optimized for each of the flux conditions. The figures presented here set the fluxes of two reactions from 5% of their

maximum possible flux to 100% of their maximum possible flux, with a 5% increase between predictions. As a result, four hundred predictions are used to make each figure. Not all predictions result in a feasible combination of fluxes, so some figures will appear to show more predictions than others, as infeasible predictions are represented by blank space. Pre-determining which reactions should be varied and which reaction should be optimized can introduce bias. However, phenotypic phase plane analysis illustrates how an organism may respond to changing conditions over a large range of fluxes. This expands the scenarios that are analyzed for each prediction and provides more information than a single phenotypic prediction, which helps to reduce bias.

Results and Discussion

Yield of Compatible Solutes Under High Light Conditions

High light conditions have been shown to induce accumulation of lipids and starch in microalgae, with lipids often favored, as they are more energy dense and therefore are more effective electron sinks (Subramanian et al., 2013). Phenotypic phase plane analysis was used to compare lipid and starch accumulation under different levels of light availability (Figure 3.1). As expected based on experimental reports, starch accumulation is favored under low light conditions, while the highest levels of TAG accumulation occur at high light conditions. Sucrose and glycerol production were also compared for different levels of light availability (Figure 3.2). Similar to the TAG and starch comparisons, glycerol has a higher degree of reduction than sucrose and is also favored under higher light conditions. High light conditions are also expected to increase temperature, however, and the protective effects of glycerol vs. sucrose against heat stress are not captured by the stoichiometric model.

Figure 3.1. Starch and triacylglycerol (TAG) accumulation under different levels of light availability. The x-axis shows light flux, the y-axis shows TAG flux, and predictions are color coded by starch production flux. All fluxes are in units of mol/day.

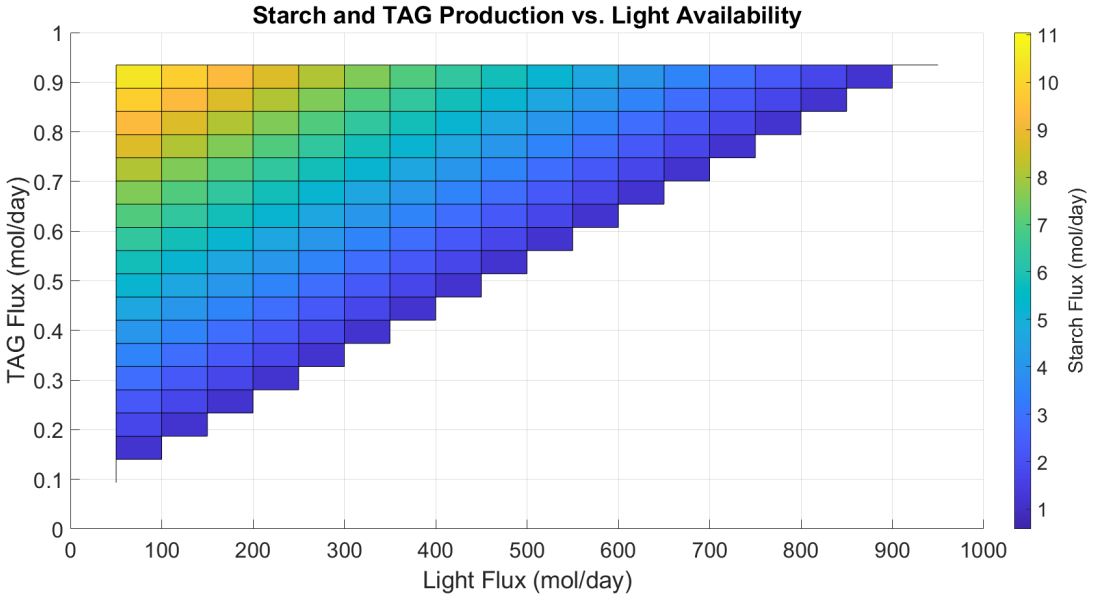

Figure 3.2. Sucrose and glycerol accumulation under different levels of light availability. The x-axis shows light flux, the y-axis shows glycerol flux, and predictions are color coded according to sucrose flux. All fluxes are in units of mol/day.

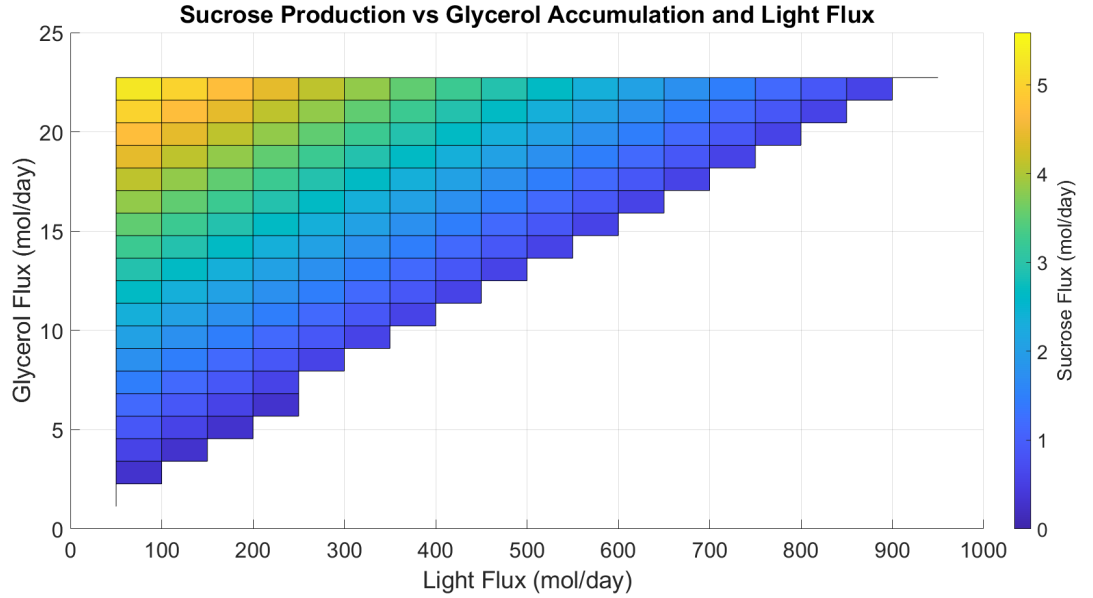

Compatible Solutes Production on Storage Compounds

Starch is easily converted to sucrose, and experimental results during growth of *Dunaliella* sp. under high salt conditions have shown that starch reserves can also serve as a source of glycerol (Hagemann, 2016; Oren, 2007). Based on model predictions, it is also possible that TAG could be degraded by algae to produce sucrose or glycerol. Predictions were run comparing glycerol and sucrose synthesis from starch and TAG in the dark, when carbon storage compounds would be the only possible source of these compounds. O_2 can become limiting in algal cultures at night, so phenotypic phase planes were generated to compare the consumption of carbon storage compounds under different O_2 availabilities.

During starch consumption in the dark, sucrose can be produced at its maximum value under a wide range of O_2 consumption levels (roughly 70% of the maximum possible O_2 consumption) (Figure 3.3). Glycerol production only reaches maximum possible values at the highest O_2 consumption levels. It is predicted that glycerol will be favored over sucrose as a compatible solute under dark, O_2 limited conditions.

Figure 3.3. Glycerol production from starch reserves under different levels of O_2 availability. The x-axis shows O_2 consumption (a greater negative value represents a higher level of consumption, as model directionality was determined based on production of O_2 during oxygenic photosynthesis), the y-axis shows starch consumption, and predictions are color coded according to glycerol flux. All fluxes are in units of mol/day.

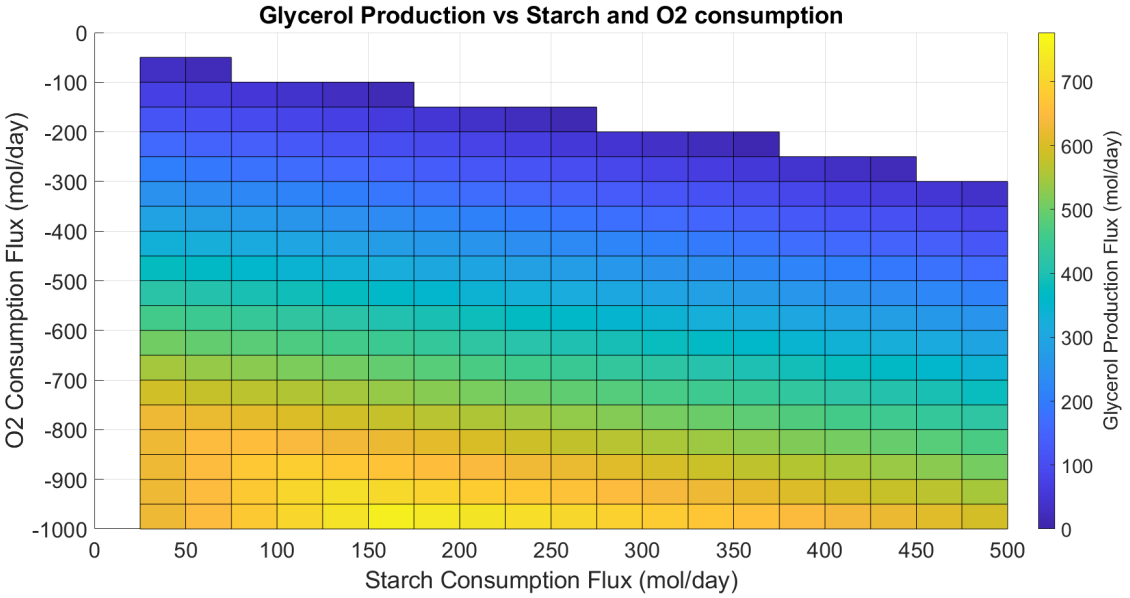

Figure 3.4. Sucrose production from starch reserves under different levels of O_2 availability. The x-axis shows O_2 consumption (a greater negative value represents a higher level of consumption, as model directionality was determined based on production of O_2 during oxygenic photosynthesis), the y-axis shows starch consumption, and predictions are color coded according to sucrose flux. All fluxes are in units of mol/day.

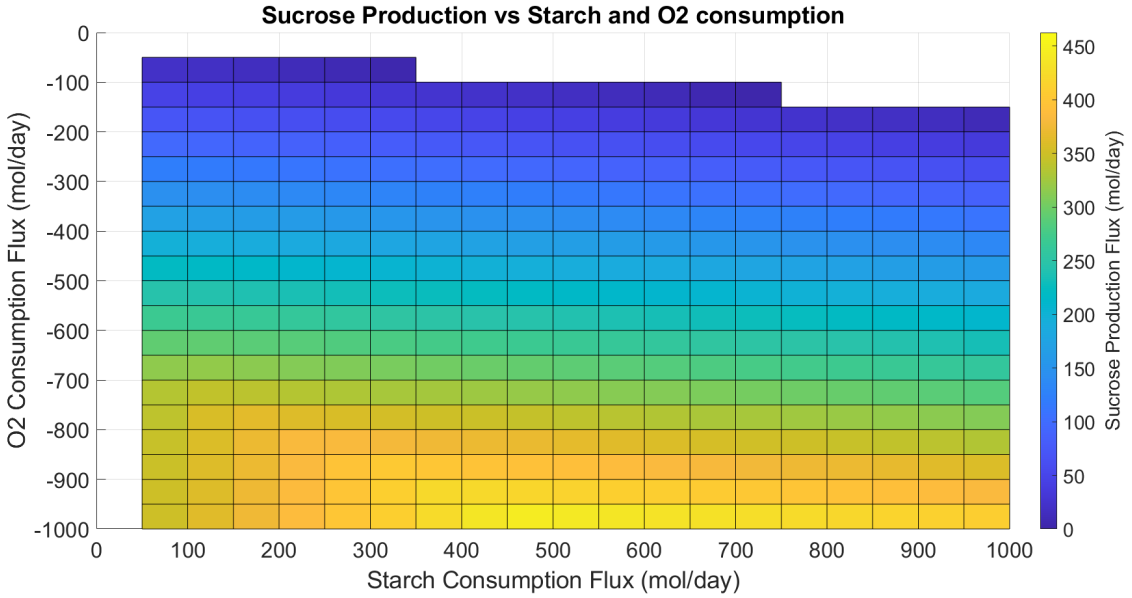

In contrast, production of glycerol and sucrose from TAG reserves peaked at lower O_2 availabilities, indicating that O_2 was required mostly for β oxidation and not as an electron acceptor for energy generation. It should also be noted that TAG degradation generates H_2O_2, which in the model is degraded to O_2, reducing overall values for O_2 consumption. Overall flux through glycerol and sucrose production was much lower during TAG degradation than during starch degradation, however. Due to the low yields of compatible solutes during TAG degradation, it is likely that starch would be preferred over TAG as a source of compatible solutes at night (Figure 3.5).

Figure 3.5. Sucrose production from triacylglycerol (TAG) reserves under different levels of O_2 availability. The x-axis shows O_2 consumption (a greater negative value represents a higher level of consumption, as model directionality was determined based on production of O_2 during oxygenic photosynthesis), the y-axis shows TAG consumption, and predictions are color coded according to sucrose flux. All fluxes are in units of mol/day.

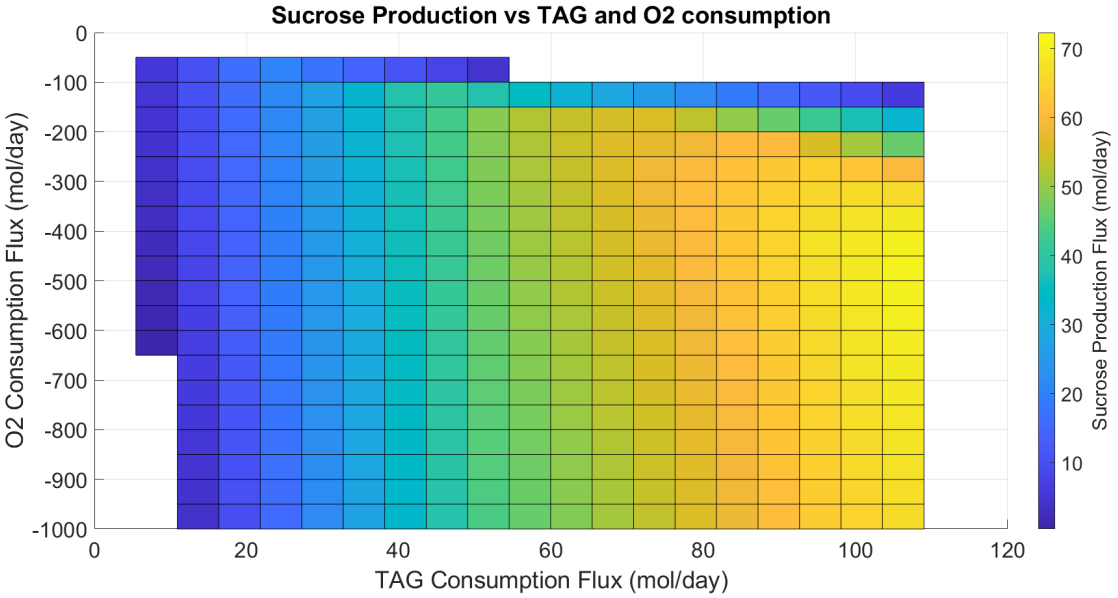

Starch Derived vs. Calvin Cycle Derived Glycerol

Glycerol can be derived from either the Calvin cycle or from starch degradation during algal growth in light conditions (Goyal, 2007). The metabolic model was used to investigate production of glycerol from CO_2 fixation via ribulose bisphosphate carboxylase/oxygenase (RuBisCO) and starch degradation. High levels of glycerol production can occur at low levels of CO_2 fixation, but starch consumption can be used to supplement glycerol production under high levels of CO_2 fixation. It is predicted that starch degradation may be used to supplement glycerol synthesis even under high light availability, when the Calvin cycle should be highly active.

Figure 3.6. Glycerol production from starch under different levels of ribulose bisphosphate carboxylase/oxygenase (RuBisCO) activity. The x-axis shows CO_2 fixation by RuBisCO, the y-axis shows glycerol production, and predictions are color coded according to starch consumption. All fluxes are in units of mol/day.

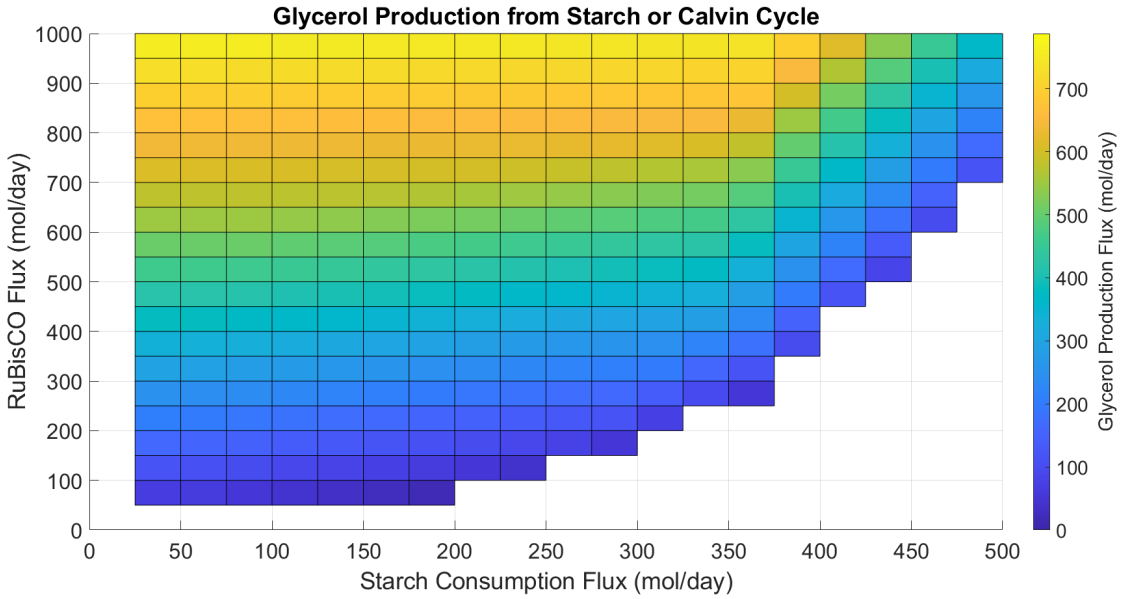

Conclusions

FBA predictions with phenotypic phase plane analysis were used to investigate SLA-04 metabolism under high osmotic pressure conditions, when compatible solutes are likely to be produced. The synthesis of sucrose and glycerol was compared during photosynthetic growth and during degradation of carbon storage compounds in the dark. Glycerol is predicted to be the favored as a compatible solute during growth in high light conditions, as it is a better electron sink than sucrose. Glycerol is also the favored compatible solute at night, when algae are likely to be limited for O_2. During the day, starch degradation to glycerol can supplement glycerol production from the Calvin cycle, providing an extra mechanism for SLA-04 to respond to salinity stress during the day. Starch degradation also results in higher production of both sucrose and glycerol than TAG degradation.

Starch reserves appear to be more beneficial for compatible solutes synthesis than TAG stores. This is an important consideration for biofuel production. While high alkalinity and high salinity conditions have many benefits for cultivation, including increased CO_2 dissolution and decreased risk of culture crashes, the synthesis of compatible solutes draws resources away from lipid biosynthesis. Algae cultivated at extreme osmotic pressure may also display a preference for starch accumulation over lipid accumulation.

Future Work

Future work will investigate compatible solutes synthesis in relation to biomass production. Additional compatible solutes like proline will be added to the analysis. The FBA technique minimization of metabolic adjustment will be used to compare metabolic shifts between carbon storage compound accumulation, biomass production, and synthesis of compatible solutes. Minimization of metabolic adjustment is based on the theory that microorganisms have adapted to shift quickly between changing stresses in the environment. As a result, the phenotypes that are expressed are predicted to be a tradeoff between two different conditions (Segrè et al., 2002). For example, during growth in high salinity conditions, algae need to adjust regularly to sudden shifts in osmotic pressure caused by dilution events like rainstorms. Minimization of metabolic adjustment could be used to predict which phenotypes represent the least disturbance to cellular metabolism as the organism oscillates between “high salinity” and “low salinity” conditions.

CHAPTER FOUR

GENOME-ENABLED EVALUATION OF MICROBIAL COMMUNITY INTERACTIONS USING KBASE

Contribution of Authors and Co-Authors

Author: Adrienne D. Arnold

Contributions: Conceived and directed the research, performed analysis, conducted literature review, wrote the manuscript

Co-Author: Dr. Ross P. Carlson

Contributions: Conceived and directed the research

Manuscript Information

Adrienne D. Arnold and Ross P. Carlson

[TBD]

Status of Manuscript:
__X__ Prepared for submission to a peer-reviewed journal
____ Officially submitted to a peer-reviewed journal
____ Accepted by a peer-reviewed journal
____ Published in a peer-reviewed journal

Algae/Prokaryote Associations

Microbial community interactions are important to algal growth, with algae-associated microbes being implicated both in culture crashes and in culture stability. Many algae are difficult or impossible to obtain as axenic cultures, suggesting a metabolic dependence on prokaryotic community members (Abby et al., 2014). The interactions between algae and bacteria can be complex and are the subject of much research (Ramanan et al., 2016).

Ongoing work on green alga *Chlorella sorokiniana* SLA-04 (referred to herein as SLA-04) is focused on elucidating the role of microbial community members in growth in raceway ponds and other xenic culturing conditions. Key questions to community assembly and structure include: are these microbes supplying key nutrients to SLA-04, perhaps in exchange for nutrients produced by the algae, thereby improving overall productivity? Are they subsisting on exudates or lysed cells from SLA-04, making them neutral or potentially beneficial partners, assisting algal growth via removal of inhibitory byproducts? Or are they predators of the algae and contributing to culture crashes? A benefit of high alkalinity and high pH cultivation is that many known algal grazers, such as the eukaryotic protist *Daphnia magna*, cannot survive at the highest pH values (Vadlamani et al., 2017a). Other prokaryotic microbes remain in SLA-04 cultures even under these extreme conditions, however, and determining their relationship to SLA-04 is a crucial step in the design of stable communities with higher productivity and reduced susceptibility to culture crashes.

This work presents a relatively quick, straightforward, and reproducible approach for screening the genomes of prokaryotes associated with SLA-04 for metabolic capabilities. The methodology uses KBase, the United States Department of Energy's online knowledgebase for

systems biology analysis (Bowen et al., 2018). The goal of this tutorial is to provide non-modeling experts with a framework for developing reasonable hypotheses of possible metabolic interactions in microbial communities.

Procedure

As of December 2021, KBase has several tools available for annotating prokaryotic genomes. It is not currently recommended that algal genomes be annotated or used to build metabolic models in KBase. A *Salinarimonas* species has been detected in high pH, high alkalinity SLA-04 cultures by 16S rRNA sequencing. *Salinarimonas* spp. are halotolerant gram-negative bacteria and have been found in alkaline lake environments similar to Soap Lake, WA, where SLA-04 was isolated (Liu et al., 2010; Vadlamani et al., 2017b; Zorz et al., 2019). The *Salinarimonas rosea* DSM 21201 genome was uploaded to KBase from NCBI. The genome quality and completeness were verified using the version 1.4.0 CheckM app with default metrics.

First, functional capabilities of *S. rosea* were visualized using the beta app DRAM (Distilled and Refined Annotation of Metabolism) (Shaffer et al., 2020). DRAM is a high throughput tool for genome annotation that is designed to help researchers use the genomes or metagenome assembled genomes (MAGs) of organisms to determine salient metabolic traits. A primary goal of DRAM is predicting the role of those organisms in their environments. Emphasis is placed on carbon, nitrogen, sulfur, and oxygen metabolism, and these traits are visualized in an easy-to-read format (Figure 1 and Figure 2; see also the narrative in KBase for all data and results discussed here). It should be noted that DRAM should not be used to definitively determine the absence of a pathway. Additional annotations and searches should be conducted before ruling out any pathways.

After analysis with DRAM, the *S. rosea* genome was annotated using both Prokka and RAST. Only RAST annotations can be used to construct metabolic models in KBase, but it is prudent to use both methods of annotation, as Prokka annotations generally provide more detail and can be used later in the pathway analysis process to double-check any enzymes that are missing from the RAST annotation. The TranSyT app can also be used to annotate transporters (Lagoa et al., 2021). Transporter annotations are notoriously difficult (Zengler & Zaramela, 2018), making the use of this app in addition to the standard RAST annotation beneficial for analysis of possible transporters. For this tutorial, annotation of transporters with TranSyT was conducted during the model refining process so that the new reactions could be directly added to an already-built model.

Figure 4.7. Central carbon metabolism and electron transport chain information on *S. rosea* from DRAM app in KBase. Enzymes or pathways that are marked as dark blue are 100% complete (shown as 1% in KBase), with all necessary subunits or enzymes present, while those marked yellow are expected to be absent in the organism. *S. rosea* appears to be aerobic, with the citric acid cycle, EMP glycolysis, and the pentose phosphate pathway either complete or nearly complete.

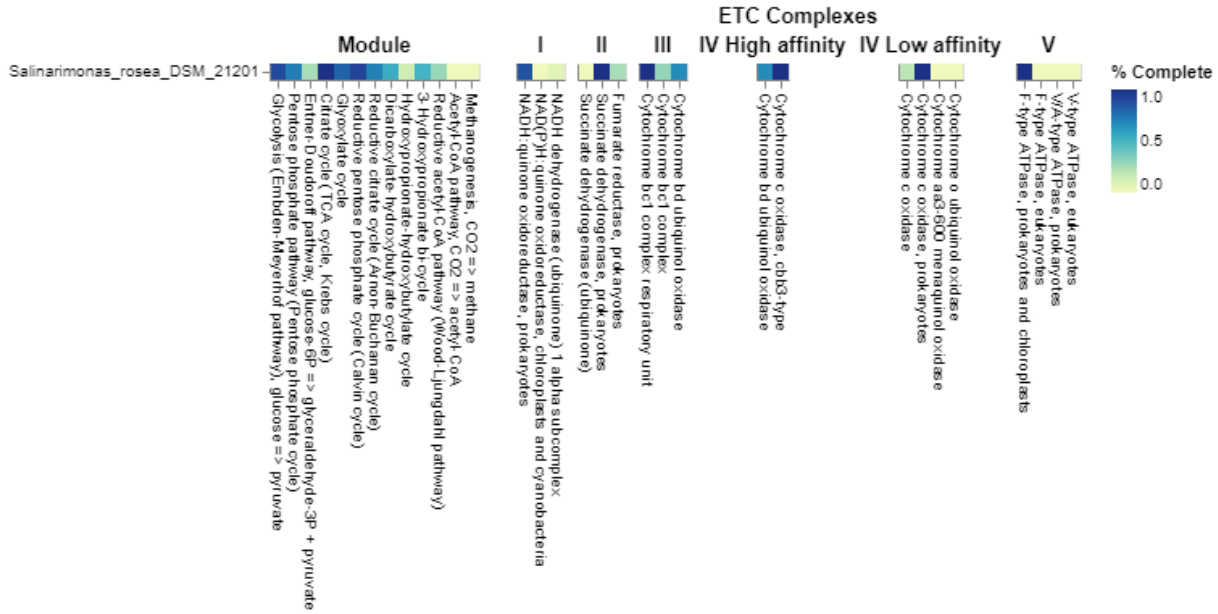

Figure 4.8. Carbohydrate, nitrogen, and sulfur metabolism information on *S. rosea* from DRAM app in KBase. Reactions marked in green are predicted to be present. *S. rosea* is predicted to be capable of degrading starch, polyphenols, chitin, and various polyglucans, all of which can be produced by algae (Stengel et al., 2011; Weber et al., 2022). The polyphenol degradation genes encode enzymes for the degradation of lignin and lignin breakdown products like vanillin. Dissimilatory nitrogen and sulfur metabolism are poorly represented. CAZY refers to carbohydrate-active enzymes (Shaffer et al., 2020).

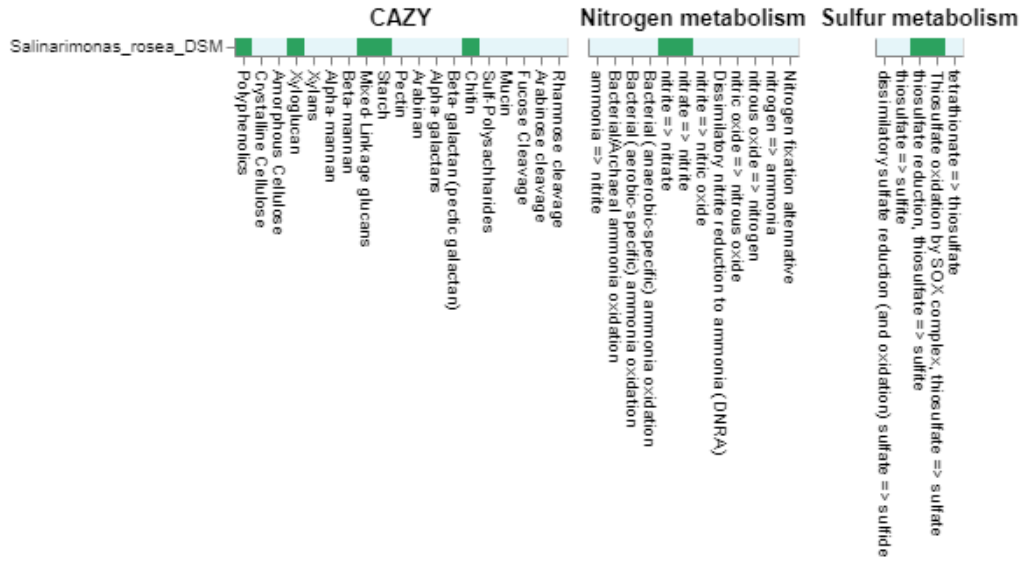

The RAST annotation was used to build four metabolic models. Three of these models were genome-scale metabolic models (GEMs), while one model was a core model. The KBase gram-negative template was used for the biomass composition of all models. Each GEM was gapfilled using a different media formulation. “Gapfilling” refers to the process by which missing reactions in a model are identified and, if appropriate, reactions are added to the model to fill the gap. In any model, there will be missing reactions in metabolic pathways, sometimes making it impossible for the model to function even under conditions where the organism has been shown experimentally to grow. These gaps must be resolved for the model to be an accurate

representation of the organism. Gapfilling in KBase is automated and helps streamline what is typically one of the most onerous steps in the model building process (Faria et al., 2018).

There are several possible causes for these missing reactions:

1. Sequencing or assembly issue. The enzyme that catalyzes the reaction is present, but the sequence encoding this enzyme was missed during the sequencing process or lost during the assembly process. The likelihood of this occurring will depend on the level of completeness and the quality of the genome used to build the model. Consult the results of the CheckM analysis of the genome used to construct the model to determine the likelihood of this possibility. See Seif et al., 2020 for a detailed analysis of assembly and sequencing issues that can cause mistakes in growth predictions (Seif et al., 2020).
2. Annotation issue. The enzyme that catalyzes the reaction is present, but was missed during the annotation process, perhaps as a result of the database or the settings used during annotation. Annotating using multiple methods in KBase may help with this problem. For example, apply and compare RAST and Prokka annotations. BLAST searches can be run on enzymes of interest if there are any specific concerns. BLASTn may be helpful in resolving some annotation issues (Seif et al., 2020).
3. Unclassified/unknown enzyme. There is an enzyme present in the genome that can catalyze the reaction, but the gene sequence is divergent enough from known enzymes that it was not properly annotated. Promiscuous enzymes and as-yet unclassified enzymes would be causes of this type of gap. This issue is best

resolved by comparing experimental data to model predictions and confirming that the model predicts growth for each experimental condition that supports growth. Several tools exist to facilitate this process, most notably Biolog plates, but it is still a laborious process (D. L. Sutherland et al., 2021). KBase does have a specific app for incorporating experimental growth data: the Simulate Growth on Phenotype Data app. If experiments are prohibitively difficult, then sequences from literature can be searched against the genome and the missing reactions can be added if these enzymes are detected.

4. Enzyme is not present. It is possible that there is a true lesion in the pathway. An incomplete pathway is a potential sign of auxotrophy and could represent an opportunity for community interactions. Note that in this case, unlike the above cases, gapfilling is not warranted and would result in an erroneous metabolic model. Auxotrophy is discussed in more detail in the "Interactions Due to Vitamin Auxotrophies" section.

In KBase, different media formulations can be used to represent the availability of different nutrients to the organism. The level of gapfilling that is implemented depends on media that is used, as gapfilling forces the model to represent growth on the supplied media. For example, Argonne LB media contains heme, while the Reference Glucose Minimal media does not. If heme biosynthesis was not originally annotated in the genome, the model that is gapfilled on the minimal media must include heme biosynthesis pathways to function, while a model that is gapfilled on Argonne LB does not require those reactions as heme can simply be taken up from the environment.

Three media types, each requiring a different level of gapfilling, were used to build the three *S. rosea* GEMs: KBase Complete media, Argonne LB media, and Reference Glucose Minimal media. (Note that if a suitable media type is not already present in KBase, a new media can be designed.) Simulations run using KBase complete media require the least gapfilling, as this medium supplies the most biomass precursors. KBase complete media does not have an exact formulation. Instead, its composition is dependent on the transporters that are present in the genome annotation. For every transporter that is annotated, that compound is added to the media and can be taken up by the model. Generally, this works well, but it can cause problems when a transporter is present for a compound that the organism cannot grow on. Type II methanotrophs, for example, have a phosphotransferase system (PTS) but cannot grow on external sugars like glucose (Olga N. Rozova et al., 2021). Gapfilling a methanotroph model on KBase complete media will incorrectly result in the model simulating uptake of and growth on glucose.

Argonne LB media was used to simulate a moderate level of gapfilling. It contains 65 compounds, with some amino acids and cofactors included in the media, meaning that biosynthetic pathways for compounds like heme or vitamin B_{12} are not necessary. Finally, the Reference Glucose Minimal media was used to represent the highest level of gapfilling. This media contains only glucose as a carbon source. Nitrogen is supplied as ammonium, phosphorous as phosphate, and sulfur as sulfate. This type of media requires the most complete biosynthetic pathways to simulate growth.

The three GEMs were compared manually to check for any major differences between the gapfilling methods (e.g., presence of entirely different pathways or growth modes in one model and not in another), which could be indicative of errors within the gapfilling process. The

Compare Models app was also used to determine the reactions and compounds that the three models share. The core metabolic model was excluded from this analysis, as its small number of reactions skews the statistical analysis, but it was still qualitatively checked against the core metabolism of the three GEMs.

Additional characterization was performed on the model that was gapfilled with Reference Glucose Minimal media (the model with the most gapfilled reactions). The Run Model Characterization app was used to summarize pathway completion values, auxotrophy predictions, and key model parameters like the number of reactions and compounds included. This app also provides information about the number of reactions that are essential for biomass production and the number of reactions that are blocked. Finally, TranSyT was used to further refine the transporter reactions in the *S. rosea* model run using Argonne LB (Lagoa et al., 2021).

Suggested apps for running modeling predictions or incorporating experimental data are included at the end of the narrative. An example flux balance analysis prediction was run on the GEM gapfilled with Argonne LB with biomass as the objective function to verify model function. The Simulate Growth on Phenotype Data app can be used to include growth information on different nutrient sources, like the information obtained from Biolog assays. This app could help with errors introduced during the gapfilling process due to the presence of transporters for compounds that the organism cannot grow on, like in the methanotroph/PTS example. The Compare Flux with Expression app can be used to compare gene expression data to flux predictions.

General Overview of *S. rosea* Metabolism

EMP (Embden-Meyerhof-Parnas) glycolysis, the pentose phosphate pathway, and the citric acid cycle are either complete or mostly complete, suggesting that *S. rosea* can grow on many sugars and simple carbohydrates in addition to the more complex starch, polyglucans, polyphenols, and chitin predicted by DRAM. Transporters are present for many polysaccharides and for smaller sugars. The presence of multiple cytochrome oxidases in the electron transport chain indicates that *S. rosea* is likely capable of aerobic respiration. Dissimilatory nitrogen and sulfur metabolism are limited and not expected to be a major source of energy for growth. Lactate dehydrogenase, formate dehydrogenase, and alcohol dehydrogenase are present, indicating that anaerobic fermentation is possible. These predictions match well with the known growth abilities of *S. rosea* YIM YD3 (Liu et al., 2010).

Several genes related to pH homeostasis were identified. The DRAM annotation includes multiple Na^+:H^+ antiporters, which can be used to import protons to the cytosol, making them crucial in maintaining cytosolic pH during alkaliphilic growth. These antiporters can also help cells cope with saline conditions by exporting Na^+ (Krulwich et al., 2011). Additional enzymes for osmotic pressure regulation were also found. “Osmoprotectant” transporters were identified with DRAM, and ATP-dependent ectoine and glycine betaine transporters were found in the RAST annotation, as were many transporters for compatible solutes like sucrose (Fenizia et al., 2020; Oren, 2001). *S. rosea* does not have annotated genes for the synthesis of ectoine or sucrose, but it does encode the enzymes for synthesis of glycine betaine and trehalose (Shivanand & Mugeraya, 2011).

Gapfilling Analysis

The purpose of the gapfilling analysis is to highlight the assumptions that go into automated GEM building and to demonstrate methods to validate those assumptions. KBase Complete media, Argonne LB media, and Reference Glucose Minimal media were used as the criteria for gapfilling on each of the three GEMs. There was good agreement between each of the models, and, as expected, the models that were gapfilled on the most complete media types required fewer reactions to be added to simulate biomass production. The models that were gapfilled on KBase Complete media and Argonne LB media both required about 50 additional reactions, mostly for specific cell membrane components that are included in the KBase gram-negative biomass reaction, which requires 89 compounds. The model that was gapfilled on Reference Glucose Minimal media needed 72 additional reactions to satisfy the biomass reaction. Most of these were, again, cell membrane components, but some were related to vitamin biosynthesis, especially biotin and pantothenate, for which *S. rosea* is likely auxotrophic. *S. rosea* YIM YD3, which has been isolated and characterized, did not have any auxotrophies (Liu et al., 2010); however, a different *S. rosea* genome (*Salinarimonas rosea* DSM 21201), which has not been characterized, was used for this analysis.

Interactions via Biomass Turnover

In the raceway pond system, SLA-04 is acting as a primary producer. Heterotrophic bacteria must acquire nutrients from primary producers, either by predation, by degrading previously lysed cells, or by metabolite transfer (Hunt et al., 2016). Enzymes associated with macromolecule degradation, especially polysaccharide degradation for lysing or catabolizing

algal cell walls, can be associated with algal parasitism (Ramanan et al., 2016). However, these genes would also be useful for a scavenging phenotype and do not necessarily mean that the bacterium is a predator.

S. rosea encodes many peptide transporters. The DRAM annotation includes branched-chain amino acid transporters as well as the peptide/nickel transport system, which is used in the transport of small peptides (Jameh et al., 2016). Peptidases were also identified in the annotations. In addition to protein degradation genes, *S. rosea* encodes acyl-CoA dehydrogenase (EC 1.3.8.7), a key enzyme for the beta-oxidation pathway of fatty acids. Other enzymes associated with fatty acid degradation are also present, including a glyoxylate cycle. Finally, *S. rosea* has a complete glycolytic pathway and many transporters for small sugars and for larger polysaccharides, including cellobiose. DRAM predicts that *S. rosea* can degrade polyglucans, starch, and lignin, which are components of the cell wall and are also important parts of cellular biomass. *S. rosea* also has enzymes for degrading chitin. Chitin-like polysaccharides have been identified in the cell wall of *Chlorella vulgaris* and are hypothesized to contribute to the recalcitrance of the cell walls of *Chlorella* sp. (Weber et al., 2022).

Biomass turnover can be beneficial to algal growth. When bacteria consume dissolved organic carbon (DOC), they produce CO_2 and low molecular weight organic compounds, which can then be re-consumed by the algae (Cho et al., 2015). *S. rosea* encodes a complete citric acid cycle, so it is likely to produce CO_2 during aerobic growth. It also contains many fermentative pathways that could produce compounds like acetate, which has been shown to promote growth in a *Chlorella sorokiniana* strain. Small organic acids can be inhibitory to growth under some conditions, but in high pH cultivation, they are deprotonated and therefore charged, making it

harder for them to leak across the cell membrane and cause damage inside the cell (Lacroux et al., 2021). It is possible that fermentation products secreted by *S. rosea* are beneficial under high alkalinity cultivation but deleterious under lower pH cultivation.

Interactions due to Photosynthetic Byproducts

While carrying out photosynthesis, green algae produce O_2. The concentration of O_2 can reach high levels during daylight growth, especially under high light conditions or in closed photobioreactors (Kazbar et al., 2019). O_2 competes with CO_2 at the active site of ribulose-1,5-bisphosphate carboxylase/oxygenase (RuBisCO), and at high O_2 concentrations, O_2 reacts with ribulose-1,5-bisphosphate to form the toxic metabolic intermediate 2-phosphoglycolate. 2-phosphoglycolate (and the related molecules glycolate and glyoxylate) inhibit several enzymes within the Calvin cycle and glycolysis, effectively shutting down biomass production pathways. The photorespiratory cycle is used by photosynthetic organisms to quickly detoxify these compounds, but it has high metabolic costs, including the loss of CO_2, the production of NH_3 and H_2O_2, and the consumption of ATP (Dellero et al., 2016). The costs of the photorespiratory cycle and the stress from reactive oxygen species (ROS) can impact algal biomass production under industrial growth conditions (Kazbar et al., 2019; Taubert et al., 2019).

The *S. rosea* genome contains the genes for phosphoglycolate phosphatase, glycolate oxidase, glyoxylate/hydroxypyruvate reductase, and a glycolate permease. It is possible that *S. rosea* could consume excreted glycolate from the media during the daytime, helping to alleviate the negative growth effects of glycolate toxicity on SLA-04. *S. rosea* is also predicted to be aerobic, meaning that it could also decrease O_2 levels during the day, reducing the creation of

ROS and the competition between O_2 and CO_2 at the RuBisCO active site (A. E. Beck et al., 2017). At night, however, *S. rosea* may compete with SLA-04 for available O_2.

Interactions due to Vitamin Auxotrophies

Vitamin auxotrophies in both prokaryotes and eukaryotes are widespread (Seif et al., 2020), and crossfeeding of vitamins is thought to be integral to the formation and stability of many microbial communities (Romine et al., 2017; Zengler & Zaramela, 2018). In a 2006 survey of 306 algal species, roughly 50% of the algae were auxotrophic for vitamin B_{12}, about a quarter required vitamin B_1 (thiamine), and about 5% required biotin (vitamin B_7) (Croft et al., 2006). Studies of vitamin exchange in algal communities are generally focused towards consortia design for industrial use, meaning that the auxotrophies in the algae are subjected to the most analysis (Kouzuma & Watanabe, 2015; Sun et al., 2018), but for community modeling it is important to also consider the auxotrophies of any potential symbionts and what resources they may be acquiring from the algae. This is especially true for SLA-04, which can be grown on Bold's Basal Medium without vitamin additions but may still benefit from vitamins produced by associated microbes.

Microbial community members can acquire vitamins via cross-feeding or through scavenging of lysed cells (Romine et al., 2017). It is generally thought that vitamin transfer in algal/bacterial systems is due to mutualistic relationships (Ramanan et al., 2016). For example, researchers have shown that heterotrophic bacteria and algae that are grown in media lacking carbon and vitamin B_{12} maintain their population ratios until either external carbon or vitamins are added, indicating a mutualistic relationship between the two (Grant et al., 2014; Kazamia et al., 2012). Estimates of the bacterial population size vs. the algal population size can also provide

insight as to whether there are enough bacteria to supply all the vitamins that the algal population needs through natural bacterial senescence and lysing alone (Grant et al., 2014).

In KBase, organisms are considered auxotrophic for vitamins if they are missing multiple enzymes in the synthetic pathway. This matches well with standards in the field for determining auxotrophy, which rely either on the absence of enzymes in a pathway or the lack of an entire pathway. In the first case, the phenotype can potentially be rescued by the addition of precursors to the vitamin. It should be noted, however, that the loss of a single enzyme in a pathway can also cause auxotrophy. It is possible that the early stages of niche differentiation are more likely to result in auxotrophy from a single missing enzyme or a loss of function mutation (Seif et al., 2020), while evolution that is further along may result in the entire pathway being lost, as there is no benefit to keeping extra genes that are not being used (Croft et al., 2006).

Loss of function mutations have several causes, but single nucleotide polymorphisms (SNPs) are the most difficult to pinpoint and must be either determined experimentally or found in literature and then searched for manually in the genome with BLAST or a similar program (Seif et al., 2020). As mentioned above, it is also possible for a single missing enzyme in a pathway to be a cause of auxotrophy, despite KBase's apparent requirement for multiple missing enzymes. Therefore, any predictions of auxotrophy from the Run Model Characterization app should be double-checked either using BLAST or confirmed using experimental growth data.

Another way to verify auxotrophy predictions in KBase is by looking for vitamin transporters or for transporters of vitamin precursors. Romine et al. note that microbes that have transporters for vitamins or precursors that they can produce themselves often use energy-independent transporters, which could be bidirectional, allowing for either production or

consumption of the compound depending on the transient needs of the cell (Romine et al., 2017). An energy-requiring transporter may be a sign that the organism is truly auxotrophic for the compound being transported.

Vitamin B_{12} (cobalamin) cross-feeding is one of the best studied vitamin exchanges in algal-bacterial communities, as no eukaryotes are known to synthesize vitamin B_{12}. Algae with a methionine synthase that require vitamin B_{12} must obtain either it or related compounds like pseudocobalamin from bacterial community members to produce methionine (Helliwell et al., 2016; Kazamia et al., 2012). Algae that are not auxotrophic for vitamin B_{12} use an alternative, non-cobalamin dependent enzyme for methionine synthesis. The SLA-04 genome encodes both the cobalamin-dependent and the cobalamin-independent methionine synthases. In other algae that encode both versions of the methionine synthase, however, expression of the cobalamin-independent version is repressed when cobalamin is available in the media, leaving this open as a possible interaction between SLA-04 and *S. rosea* (Helliwell et al., 2011; Kazamia et al., 2012). Cobalamin auxotrophy is not considered in the Run Model Characterization app's Auxotrophy Statistics. Manual analysis shows that there are some lesions present in the *S. rosea* pathways for cobalamin biosynthesis, and while more detailed investigations are needed, it is possible that both SLA-04 and *S. rosea* rely on added cobalamin or on other community members for their supply of this vitamin.

Biotin (vitamin B_7) is an essential cofactor for acetyl-CoA carboxylase, which is a key enzyme in fatty acid biosynthesis. All microbes require biotin, and about 5% of algae are auxotrophic for the vitamin (Croft et al., 2006). The SLA-04 genome contains the enzymes required for the synthesis of biotin and pimeloyl-CoA, a biotin precursor. *S. rosea*, however, is

predicted to be auxotrophic for biotin. It would rely either on SLA-04 or on other community members for its biotin supply.

Thiamine (vitamin B_1; active form is thiamine pyrophosphate or TPP) is, like biotin, universally required. It is needed for many enzymes in central carbon metabolism (Croft et al., 2006). SLA-04 has the required enzymes for thiamine biosynthesis from glycine. In the *S. rosea* model, the thiamine diphosphate synthesis pathway was heavily gapfilled (15/88 reactions), and the presence of an energy-dependent transporter for this compound lends support to *S. rosea* being auxotrophic for TPP despite the predictions made by the Run Model Characterization app. A thiamine ATP transporter was also identified in the RAST annotation.

S. rosea was also identified as being auxotrophic for pantothenate (vitamin B_5). The RAST annotation includes an energy-dependent transporter for pantetheine, a pantothenate precursor.

S. rosea additionally encodes an energy-dependent transporter for protoporphyrin (a heme precursor) and heme (prosthetic group used in cytochromes). Both EC 1.3.3.4 and EC 1.3.5.3, which catalyze the final step in heme synthesis, are missing from the RAST annotation. It is possible that *S. rosea* is auxotrophic for heme, as well, despite its predicted aerobic metabolism. A recent survey revealed that heme auxotrophy is likely widespread in bacteria, even in obligate aerobes, although the authors do note that it is possible that unknown heme biosynthetic pathways exist (S. Kim et al., 2021). Alternatively, heme uptake may be a way to acquire iron, which is likely to be scarce in high pH systems. ATP-dependent heme exporters are also used to regulate heme biosynthesis, which involves multiple steps that can induce reactive oxidative species as byproducts and can therefore be toxic to organisms (S. Kim et al., 2021), but

the absence of several necessary biosynthetic enzymes coupled with the presence of a transporter suggest potential auxotrophy in *S. rosea*.

Additional Interactions

There are likely many interactions between algae and bacteria beyond the ones examined here. Some bacteria can produce algal-growth promoting factors like indole acetate and other auxins (Borowitzka, 2016; Goecke et al., 2010). *S. rosea* does encode the genes for production of indole acetate. Bacteria are also proposed to be a major source of siderophores and other metal chelators, which can help algae access metal ions necessary for metabolism (Fuentes et al., 2016). Hundreds of bacterial siderophores have been described in the literature (Hider & Kong, 2010). A search of the *S. rosea* genome for common siderophores revealed only citrate. Due to the large diversity of siderophore compounds, however, it is possible that enzymes related to siderophore production are unknown and are therefore unlikely to be annotated. Experimental techniques for the identification of siderophores, such as the chrome azurol S assay (Louden et al., 2011; Pérez-Miranda et al., 2007), may be preferable to genomic analysis.

Conclusion

This tutorial demonstrates the use of KBase for analysis of potential microbial community interactions using the example of *Salinarimonas rosea*. *S. rosea* is expected to catabolize components of SLA-04 biomass for both reduced carbon species and for specific vitamins. While breaking down macromolecules, *S. rosea* likely produces CO_2 and fermentation byproducts like acetate, which SLA-04 could use as carbon sources. It may also supply cobalamin to SLA-04, although additional analysis would be needed to confirm this. Finally, *S.*

rosea can also synthesize glycine betaine, a compatible solute that could be used by SLA-04 under high osmotic pressure conditions.

Chapter Acknowledgements

Thanks to Nazanin Nowzaridalini, Dr. Sridhar Viamajala, and Isaac Miller for their insights into the growth of SLA-04. Thanks also to Dr. Huyen Bui for assisting with data collection.

CHAPTER FIVE

EPILOGUE

Overview

This work uses metabolic modeling to compare the metabolisms of green microalgae and aerobic methanotrophs, two microorganisms that grow on single carbon compounds. Chapter One provides an overview of the two organisms, their capacity to accumulate carbon and energy storage compounds, and their roles as primary producers in the environment. Chapter Two uses elementary flux mode analysis to investigate aerobic methanotroph metabolism under O_2 limited conditions. Denitrification and carbon storage compound degradation are compared as survival strategies for these obligate aerobes. Chapter Three examines compatible solute production in green microalgae using flux balance analysis. Chapter Four provides an example of how sequencing data can be used to explore community interactions in KBase.

Future Directions

Chapter Two provides a detailed workflow for construction of core metabolic models for organisms with uncommon metabolisms. These metabolic types are difficult to capture using automated modeling techniques, and there are few works that describe the process of troubleshooting metabolic models of these organisms. This chapter is prepared as a manuscript draft that will instruct beginning modelers on the development of accurate metabolic models with unusual energy metabolisms. The manuscript will also provide instruction on how metabolic modeling can be used to guide cultivation techniques. For example, global warming

potential calculations have been incorporated into the model, which both demonstrates real world applications of metabolic modeling and showcases a method for model analysis. A similar technique could be used to evaluate inhibitory properties of different metabolic byproducts like methanol or to compare the copper costs of different phenotypes.

Further analysis of the effects copper and iron limitation on methanotroph metabolism will be added into this manuscript. Membrane real estate predictions are also to be included. Membrane real estate analysis is a modeling technique that considers the space available on the cell membrane as a limiting resource. Only a certain percent of the membrane is available for occupancy by transporters and the electron transport chain—how a cell optimizes its use of that space depends on the stresses imposed by the cultivation environment. Methanotrophs provide an interesting case study in this area, as their membrane availability greatly increases under high levels of copper availability, providing additional room for the many membrane enzymes that are employed in methane oxidation.

Chapter Three investigates the role of compatible solutes in adaptation of *Chlorella sorokiniana* SLA-04 to high salt stress. Experiments are currently underway to characterize SLA-04's salt tolerance and to determine which compatible solutes it produces. The results of these experiments will be incorporated into future modeling predictions. Biolog plate assays are being used to characterize the carbon and nitrogen sources that SLA-04 can use, which will also be included in the model. Finally, the SLA-04 model is being transferred to KBase format for easier sharing between research groups.

Chapter Four details a workflow for the use of metagenome sequencing data to model interactions within an algal community. This workflow will be used to analyze sequencing

results from an ongoing project. Three isolates are to be sequenced; core metabolic models will be built for each and calibrated using Biolog data on carbon source utilization.

REFERENCES CITED

Abby, S., Touchon, M., de Jode, A., Grimsley, N., & Piganeau, G. (2014). Bacteria in Ostreococcus tauri cultures - friends, foes or hitchhikers? *Frontiers in Microbiology*, *5*(SEP), 1–10. https://doi.org/10.3389/fmicb.2014.00505

Abdellaoui, N., Kim, M. J., & Choi, T. J. (2019). Transcriptome analysis of gene expression in Chlorella vulgaris under salt stress. *World Journal of Microbiology and Biotechnology*, *35*(9), 1–11. https://doi.org/10.1007/s11274-019-2718-6

Adeosun, E. K., Smith, T. J., Hoberg, A. M., Velarde, G., Ford, R., & Dalton, H. (2004). Formaldehyde dehydrogenase preparations from Methylococcus capsulatus (Bath) comprise methanol dehydrogenase and methylene tetrahydromethanopterin dehydrogenase. *Microbiology*, *150*(3), 707–713. https://doi.org/10.1099/mic.0.26707-0

Akberdin, I. R., Thompson, M., Hamilton, R., Desai, N., Alexander, D., Henard, C. A., Guarnieri, M. T., & Kalyuzhnaya, M. G. (2018). Methane utilization in Methylomicrobium alcaliphilum 20ZR: A systems approach. *Scientific Reports*, *8*(1), 1–13. https://doi.org/10.1038/s41598-018-20574-z

Anthony, C. (1982). The biochemistry of methylotrophs. In *Trends in Biochemical Sciences*. https://doi.org/10.1016/0968-0004(83)90116-0

Anthony, C., Ghosh, M., & Blake, C. C. F. (1994). The structure and function of methanol dehydrogenase and related quinoproteins containing pyrrolo-quinoline quinone. *Biochemical Journal*, *304*(3), 665–674. https://doi.org/10.1042/bj3040665

Anthony, Christopher. (1992). The c-type cytochromes of methylotrophic bacteria. *BBA - Bioenergetics*, *1099*(1), 1–15. https://doi.org/10.1016/0005-2728(92)90181-Z

Anthony, Christopher. (2011). How Half a Century of Research was Required to Understand Bacterial Growth on C 1 and C 2 Compounds; the Story of the Serine Cycle and the Ethylmalonyl-CoA Pathway. *Science Progress*, *94*(2), 109–137. https://doi.org/10.3184/003685011X13044430633960

Anthony, Christopher, & Williams, P. (2003). The structure and mechanism of methanol dehydrogenase. *Biochimica et Biophysica Acta - Proteins and Proteomics*, *1647*(1–2), 18–23. https://doi.org/10.1016/S1570-9639(03)00042-6

Armenteros, J. J. A., Salvatore, M., Emanuelsson, O., Winther, O., Von Heijne, G., Elofsson, A., & Nielsen, H. (2019). Detecting sequence signals in targeting peptides using deep learning. *Life Science Alliance*, *2*(5), 1–14. https://doi.org/10.26508/lsa.201900429

Auman, A. J., Lidstrom, M. E., & Speake, C. C. (2001). nifH Sequences and Nitrogen Fixation in Type I and Type II Methanotrophs. *Applied and Environmental Microbiology*, *67*(9),

4009–4016. https://doi.org/10.1128/AEM.67.9.4009

Balasubramanian, R., Kenney, G. E., & Rosenzweig, A. C. (2011). Dual pathways for copper uptake by methanotrophic bacteria. *Journal of Biological Chemistry*, *286*(43), 37313–37319. https://doi.org/10.1074/jbc.M111.284984

Balasubramanian, R., & Rosenzweig, A. C. (2008). Copper methanobactin: a molecule whose time has come. *Current Opinion in Chemical Biology*, *12*(2), 245–249. https://doi.org/10.1016/j.cbpa.2008.01.043

Beck, A. E. (2020). Metabolic efficiency of sugar co-metabolism and phenol degradation in Alicyclobacillus acidocaldarius for improved lignocellulose processing. *Processes*, *8*(5). https://doi.org/10.3390/PR8050502

Beck, A. E., Bernstein, H. C., & Carlson, R. P. (2017). Stoichiometric network analysis of cyanobacterial acclimation to photosynthesis-associated stresses identifies heterotrophic niches. *Processes*, *5*(2). https://doi.org/10.3390/pr5020032

Beck, A. E., Schepens, D., McGill, S. L., Heys, J. J., Gedeon, T., & Carlson, R. P. (2022). *Emergent Properties of Co-Metabolism in Escherichia coli: Membrane Real Estate as a Growth-Limiting Criterion. Manuscript in Progress.*

Beck, A., Hunt, K., & Carlson, R. (2018). Measuring Cellular Biomass Composition for Computational Biology Applications. *Processes*, *6*(5), 38. https://doi.org/10.3390/pr6050038

Becker, S. A., Feist, A. M., Mo, M. L., Hannum, G., Palsson, B., & Herrgard, M. J. (2007). Quantitative prediction of cellular metabolism with constraint-based models: The COBRA Toolbox. *Nature Protocols*, *2*(3), 727–738. https://doi.org/10.1038/nprot.2007.99

Benedetti, M., Vecchi, V., Barera, S., & Dall'Osto, L. (2018). Biomass from microalgae: The potential of domestication towards sustainable biofactories. *Microbial Cell Factories*, *17*(1), 1–18. https://doi.org/10.1186/s12934-018-1019-3

Borowitzka, M. A. (2016). *Chemically-Mediated Interactions in Microalgae* (Issue Borowitzka). https://doi.org/10.1007/978-3-319-24945-2_15

Borowitzka, M. A., Beardall, J., & Raven, J. A. (2016). The Physiology of Microalgae. In M. A. Borowitzka (Ed.), *Developments in Applied Phycology*. Springer. https://doi.org/10.1016/j.plantsci.2010.11.010

Bowen, B., Faria, J. P., Yu, D., Chandonia, J.-M., DeJongh, M., Land, M. L., Parrello, B., Chan, S. Y., Gerlach, W., Yoo, S., Kamimura, R. T., Harris, N. L., Baumohl, J., Henry, C. S., Fang, G., Dehal, P., Best, A. A., Bun, C. C., Kumari, S., … Haun, H. L. (2018). KBase: The United States Department of Energy Systems Biology Knowledgebase. *Nature Biotechnology*, *36*(7), 566–569. https://doi.org/10.1038/nbt.4163

Brust, H., Orzechowski, S., & Fettke, J. (2020). Starch and glycogen analyses: Methods and techniques. *Biomolecules*, *10*(7), 1–26. https://doi.org/10.3390/biom10071020

But, S. Y., Egorova, S. V., Khmelenina, V. N., & Trotsenko, Y. A. (2017). Biochemical properties and phylogeny of hydroxypyruvate reductases from methanotrophic bacteria with different c1-assimilation pathways. *Biochemistry (Moscow)*, *82*(11), 1295–1303. https://doi.org/10.1134/S0006297917110074

But, S. Y., Egorova, S. V., Khmelenina, V. N., & Trotsenko, Y. A. (2019). Serine-glyoxylate aminotranferases from methanotrophs using different C1-assimilation pathways. *Antonie van Leeuwenhoek, International Journal of General and Molecular Microbiology*, *112*(5), 741–751. https://doi.org/10.1007/s10482-018-1208-4

But, S. Yu, Dedysh, S. N., Popov, V. O., Pimenov, N. V., & Khmelenina, V. N. (2020). Construction of a Type-I Metanotroph with Reduced Capacity for Glycogen and Sucrose Accumulation. *Applied Biochemistry and Microbiology*, *56*(5), 538–543. https://doi.org/10.1134/S0003683820050063

But, S Y, Egorova, S. V, Khmelenina, V. N., & Mustakhimov, I. I. (2020). Malyl-CoA lyase provides glycine/glyoxylate synthesis in type I methanotrophs. *FEMS Microbiology Letters*, *367*(24), 1–8. https://doi.org/10.1093/femsle/fnaa207

Canadell, J. G., Monteiro, P. M. S., Costa, M. H., Cunha, L. C. da, Cox, P. M., Eliseev, A. V., Henson, S., Ishii, M., Jaccard, S., Koven, C., Lohila, A., Patra, P. K., Piao, S., Rogelj, J., Syampungani, S., Zaehle, S., & Zickfeld, K. (2021). Global Carbon and other Biogeochemical Cycles and Feedbacks. In V. Masson-Delmotte, P. Zhai, A. Pirani, S. L. Connors, C. Péan, S. Berger, N. Caud, Y. Chen, L. Goldfarb, M. I. Gomis, M. Huang, K. Leitzell, E. Lonnoy, J. B. R. Matthews, T. K. Maycock, T. Waterfield, O. Yelekçi, R. Yu, & B. Zhou (Eds.), *Climate Change 2021: The Physical Science Basis. Contribution of Working Group I to the Sixth Assessment Report of the Intergovernmental Panel on Climate Change* (pp. 673–816). Cambridge University Press. https://doi.org/10.1017/9781009157896.007

Carlson, R. P. (2007). Metabolic systems cost-benefit analysis for interpreting network structure and regulation. *Bioinformatics*, *23*(10), 1258–1264. https://doi.org/10.1093/bioinformatics/btm082

Carlson, R. P. (2009). Decomposition of complex microbial behaviors into resource-based stress responses. *Bioinformatics*, *25*(1), 90–97. https://doi.org/10.1093/bioinformatics/btn589

Carlson, R. P., Oshota, O., Shipman, M., Caserta, J. A., Hu, P., Saunders, C. W., Xu, J., Jay, Z. J., Reeder, N., Richards, A., Pettigrew, C., & Peyton, B. M. (2016). Integrated molecular, physiological and in silico characterization of two Halomonas isolates from industrial brine. *Extremophiles*, *20*(3), 261–274. https://doi.org/10.1007/s00792-015-0806-6

Carlson, R., & Srienc, F. (2004). Fundamental Escherichia coli Biochemical Pathways for

Biomass and Energy Production: Creation of Overall Flux States. *Biotechnology and Bioengineering*, *86*(2), 149–162. https://doi.org/10.1002/bit.20044

Cecchin, M., Marcolungo, L., Rossato, M., Girolomoni, L., Cosentino, E., Cuine, S., Li-Beisson, Y., Delledonne, M., & Ballottari, M. (2019). Chlorella vulgaris genome assembly and annotation reveals the molecular basis for metabolic acclimation to high light conditions. *Plant Journal*, *100*(6), 1289–1305. https://doi.org/10.1111/tpj.14508

Chang, J., Gu, W., Park, D., Semrau, J. D., Dispirito, A. A., & Yoon, S. (2018). Methanobactin from Methylosinus trichosporium OB3b inhibits N2O reduction in denitrifiers. *ISME Journal*, *12*(8), 2086–2089. https://doi.org/10.1038/s41396-017-0022-8

Chistoserdova, L., Gomelsky, L., Vorholt, J. A., Gomelsky, M., Tsygankov, Y. D., & Lidstrom, M. E. (2000). Analysis of two formaldehyde oxidation pathways in Methylobacillus flagellatus KT, a ribulose monophosphate cycle methylotroph. *Microbiology*, *146*(1), 233–238. https://doi.org/10.1099/00221287-146-1-233

Chistoserdova, L., Vorholt, J. A., Thauer, R. K., & Lidstrom, M. E. (1998). C1 transfer enzymes and coenzymes linking methylotrophic bacteria and methanogenic archaea. *Science*, *281*(5373), 99–102. https://doi.org/10.1126/science.281.5373.99

Cho, D. H., Ramanan, R., Heo, J., Lee, J., Kim, B. H., Oh, H. M., & Kim, H. S. (2015). Enhancing microalgal biomass productivity by engineering a microalgal-bacterial community. *Bioresource Technology*, *175*, 578–585. https://doi.org/10.1016/j.biortech.2014.10.159

Choi, D.-W., Kuntz, R. C., Boyd, E. S., Semrau, J. D., Antholine, W. E., Han, J.-I., Zahn, J. A., Boyd, J. M., Mora, A. M. de la, & DiSpirito, A. A. (2003). The Membrane-Associated Methane Monooxygenase (pMMO) and pMMO-NADH:Quinone Oxidoreductase Complex from Methylococcus capsulatus Bath. *Journal of Bacteriology*, *185*(19), 5755–5764. https://doi.org/10.1128/JB.185.19.5755

Choi, D. W., Semrau, J. D., Antholine, W. E., Hartsel, S. C., Anderson, R. C., Carey, J. N., Dreis, A. M., Kenseth, E. M., Renstrom, J. M., Scardino, L. L., Van Gorden, G. S., Volkert, A. A., Wingad, A. D., Yanzer, P. J., McEllistrem, M. T., de la Mora, A. M., & DiSpirito, A. A. (2008). Oxidase, superoxide dismutase, and hydrogen peroxide reductase activities of methanobactin from types I and II methanotrophs. *Journal of Inorganic Biochemistry*, *102*(8), 1571–1580. https://doi.org/10.1016/j.jinorgbio.2008.02.003

Costa, C., Dijkema, C., Friedrich, M., García-Encina, P., Fernández-Polanco, F., & Stams, A. J. M. (2000). Denitrification with methane as electron donor in oxygen-limited bioreactors. *Applied Microbiology and Biotechnology*, *53*(6), 754–762. https://doi.org/10.1007/s002530000337

Cotruvo, J. A. (2019). The Chemistry of Lanthanides in Biology: Recent Discoveries, Emerging Principles, and Technological Applications. *ACS Central Science*, *5*(9), 1496–1506.

https://doi.org/10.1021/acscentsci.9b00642

Croft, M. T., Warren, M. J., & Smith, A. G. (2006). Algae need their vitamins. *Eukaryotic Cell*, *5*(8), 1175–1183. https://doi.org/10.1128/EC.00097-06

Crowther, G. J., Kosály, G., & Lidstrom, M. E. (2008). Formate as the main branch point for methylotrophic metabolism in Methylobacterium extorquens AM1. *Journal of Bacteriology*, *190*(14), 5057–5062. https://doi.org/10.1128/JB.00228-08

Dam, B., Dam, S., Blom, J., & Liesack, W. (2013). Genome Analysis Coupled with Physiological Studies Reveals a Diverse Nitrogen Metabolism in Methylocystis sp. Strain SC2. *PLoS ONE*, *8*(10). https://doi.org/10.1371/journal.pone.0074767

Dellero, Y., Jossier, M., Schmitz, J., Maurino, V. G., & Hodges, M. (2016). Photorespiratory glycolate-glyoxylate metabolism. *Journal of Experimental Botany*, *67*(10), 3041–3052. https://doi.org/10.1093/jxb/erw090

DiSpirito, A. A., Kuntz, R. C., Choi, D.-W., & Zahn, J. A. (2004). Chapter 7: Respiration in Methanotrophs. In D. Zannoni (Ed.), *Respiration in Archaea and Bacteria* (pp. 150–164).

Doran, P. M. (1997). Material Balances. In *Bioprocess Engineering Principles* (1st ed., pp. 75–76). Academic Press Limited.

Edirisinghe, J. N., Weisenhorn, P., Conrad, N., Xia, F., Overbeek, R., Stevens, R. L., & Henry, C. S. (2016). Modeling central metabolism and energy biosynthesis across microbial life. *BMC Genomics*, *17*(1), 1–11. https://doi.org/10.1186/s12864-016-2887-8

Farhan Ul Haque, M., Gu, W., DiSpirito, A. A., & Semrau, J. D. (2016). Marker exchange mutagenesis of mxaF, encoding the large subunit of the Mxa methanol dehydrogenase, in Methylosinus trichosporium OB3b. *Applied and Environmental Microbiology*, *82*(5), 1549–1555. https://doi.org/10.1128/AEM.03615-15

Farhan Ul Haque, M., Kalidass, B., Bandow, N., Turpin, E. A., DiSpirito, A. A., & Semrau, J. D. (2015). Cerium Regulates Expression of Alternative Methanol Dehydrogenases in Methylosinus trichosporium OB3b. *Applied and Environmental Microbiology*, *81*(21), 7546–7552. https://doi.org/10.1128/AEM.02542-15

Faria, J. P., Rocha, M., Rocha, I., & Henry, C. S. (2018). Methods for automated genome-scale metabolic model reconstruction. *Biochemical Society Transactions*, *46*(4), 931–936. https://doi.org/10.1042/BST20170246

Fenizia, S., Thume, K., Wirgenings, M., & Pohnert, G. (2020). Ectoine from bacterial and algal origin is a compatible solute in microalgae. *Marine Drugs*, *18*(1), 1–13. https://doi.org/10.3390/md18010042

Forster, P., Storelvmo, T., Armour, K., Collins, W., Dufresne, J.-L., Frame, D., Lunt, D. J.,

Mauritsen, T., Palmer, M. D., Watanabe, M., Wild, M., & Zhang, H. (2021). The Earth's Energy Budget, Climate Feedbacks, and Climate Sensitivity. In V. Masson-Delmotte, P. Zhai, A. Pirani, S. L. Connors, C. Péan, S. Berger, N. Caud, Y. Chen, L. Goldfarb, M. I. Gomis, M. Huang, K. Leitzell, E. Lonnoy, J. B. R. Matthews, T. K. Maycock, T. Waterfield, O. Yelekçi, R. Yu, & B. Zhou (Eds.), *Climate Change 2021: The Physical Science Basis. Contribution of Working Group I to the Sixth Assessment Report of the Intergovernmental Panel on Climate Change* (pp. 923–1054). https://doi.org/10.1017/9781009157896.009

Fu, Y., Li, Y., & Lidstrom, M. (2017). The oxidative TCA cycle operates during methanotrophic growth of the Type I methanotroph Methylomicrobium buryatense 5GB1. *Metabolic Engineering*, *42*(December 2016), 43–51. https://doi.org/10.1016/j.ymben.2017.05.003

Fuentes, J., Garbayo, I., Cuaresma, M., Montero, Z., González-del-Valle, M., & Vílchez, C. (2016). Impact of Microalgae-Bacteria Interactions on the Production of Algal Biomass and Associated Compounds. *Marine Drugs*, *14*(5), 100. https://doi.org/10.3390/md14050100

Goecke, F., Labes, A., Wiese, J., & Imhoff, J. (2010). Chemical interactions between marine macroalgae and bacteria. *Marine Ecology Progress Series*, *409*, 267–299. https://doi.org/10.3354/meps08607

Gong, M., & Bassi, A. (2016). Carotenoids from microalgae: A review of recent developments. *Biotechnology Advances*, *34*(8), 1396–1412. https://doi.org/10.1016/j.biotechadv.2016.10.005

Good, N. M., Moore, R. S., Suriano, C. J., & Martinez-Gomez, N. C. (2019). Contrasting in vitro and in vivo methanol oxidation activities of lanthanide-dependent alcohol dehydrogenases XoxF1 and ExaF from Methylobacterium extorquens AM1. *Scientific Reports*, *9*(1), 1–12. https://doi.org/10.1038/s41598-019-41043-1

Goyal, A. (2007). Osmoregulation in Dunaliella, Part II: Photosynthesis and starch contribute carbon for glycerol synthesis during a salt stress in Dunaliella tertiolecta. *Plant Physiology and Biochemistry*, *45*(9), 705–710. https://doi.org/10.1016/j.plaphy.2007.05.009

Grant, M. A. A., Kazamia, E., Cicuta, P., & Smith, A. G. (2014). Direct exchange of vitamin B 12 is demonstrated by modelling the growth dynamics of algal-bacterial cocultures. *ISME Journal*, *8*(7), 1418–1427. https://doi.org/10.1038/ismej.2014.9

Gu, W., & Semrau, J. D. (2017). Copper and cerium-regulated gene expression in Methylosinus trichosporium OB3b. *Applied Microbiology and Biotechnology*, *101*(23–24), 8499–8516. https://doi.org/10.1007/s00253-017-8572-2

Guerrero-Cruz, S., Vaksmaa, A., Horn, M. A., Niemann, H., Pijuan, M., & Ho, A. (2021). Methanotrophs: Discoveries, Environmental Relevance, and a Perspective on Current and Future Applications. *Frontiers in Microbiology*, *12*(May), 1–28. https://doi.org/10.3389/fmicb.2021.678057

Guschina, I. A., & Harwood, J. L. (2006). Lipids and lipid metabolism in eukaryotic algae. *Progress in Lipid Research*, *45*(2), 160–186. https://doi.org/10.1016/j.plipres.2006.01.001

Hagemann, M. (2016). Coping with High and Variable Salinity: Molecular Aspects of Compatible Solute Accumulation. In *The Physiology of Microalgae* (pp. 359–372). https://doi.org/10.1007/978-3-319-24945-2

Hakemian, A. S., Kondapalli, K. C., Telser, J., Hoffman, B. M., Stemmler, Ti. L., & Rosenzweig, A. C. (2008). The Metal Centers of Particulate Methane Monooxygenase from Methylosinus trichosporium OB3b. *Biochemistry*, *47*(26), 6793–6801. https://doi.org/10.1021/bi800598h.The

Hakemian, A. S., & Rosenzweig, A. C. (2007). The biochemistry of methane oxidation. *Annual Review of Biochemistry*, *76*, 223–241. https://doi.org/10.1146/annurev.biochem.76.061505.175355

Hanifzadeh, M. M., Garcia, E. C., & Viamajala, S. (2018). Production of lipid and carbohydrate from microalgae without compromising biomass productivities: Role of Ca and Mg. *Renewable Energy*, *127*, 989–997. https://doi.org/10.1016/j.renene.2018.05.012

Hanson, R., & Hanson, T. (1996). Methanotrophic Bacteria. *Microbiology Reviews*, *60*(2), 439–471. https://doi.org/10.1002/0471263397.env316

He, L., Groom, J. D., & Lidstrom, M. E. (2020). The Entner-Doudoroff Pathway is an Essential Metabolic Route for Methylotuvimicrobium buryatense 5GB1C . *Applied and Environmental Microbiology*, *November*. https://doi.org/10.1128/aem.02481-20

Hejazi, M. A., & Wijffels, R. H. (2004). Milking of microalgae. *Trends in Biotechnology*, *22*(4), 189–194. https://doi.org/10.1016/j.tibtech.2004.02.009

Helliwell, Katherine E., Wheeler, G. L., Leptos, K. C., Goldstein, R. E., & Smith, A. G. (2011). Insights into the Evolution of Vitamin B12 Auxotrophy from Sequenced Algal Genomes. *Molecular Biology and Evolution*, *28*(10), 2921–2933. https://doi.org/10.1093/molbev/msr124

Helliwell, Katherine Emma, Lawrence, A. D., Holzer, A., Kudahl, U. J., Sasso, S., Kräutler, B., Scanlan, D. J., Warren, M. J., & Smith, A. G. (2016). Cyanobacteria and Eukaryotic Algae Use Different Chemical Variants of Vitamin B12. *Current Biology*, *26*(8), 999–1008. https://doi.org/10.1016/j.cub.2016.02.041

Hibi, Y., Asai, K., Arafuka, H., Hamajima, M., Iwama, T., & Kawai, K. (2011). Molecular structure of La3+-induced methanol dehydrogenase-like protein in Methylobacterium radiotolerans. *Journal of Bioscience and Bioengineering*, *111*(5), 547–549. https://doi.org/10.1016/j.jbiosc.2010.12.017

Hider, R. C., & Kong, X. (2010). Chemistry and biology of siderophores. *Natural Product*

Reports, *27*(5), 637–657. https://doi.org/10.1039/b906679a

Hunt, K. A., Folsom, J. P., Taffs, R. L., & Carlson, R. P. (2014). Complete enumeration of elementary flux modes through scalable demand-based subnetwork definition. *Bioinformatics*, *30*(11), 1569–1578. https://doi.org/10.1093/bioinformatics/btu021

Hunt, K. A., Jennings, R. de M., Inskeep, W. P., & Carlson, R. P. (2016). Stoichiometric modelling of assimilatory and dissimilatory biomass utilisation in a microbial community. *Environmental Microbiology*, *18*(12), 4946–4960. https://doi.org/10.1111/1462-2920.13444

Jameh, N., Galia, W., Awussi, A. A., Roux, E., Genay, M., Perrin, C., & Dary-Mourot, A. (2016). Characterization of a new peptide transport system in Streptococcus thermophilus. *Food Research International*, *86*, 34–45. https://doi.org/10.1016/j.foodres.2016.04.039

Johnson, X., & Alric, J. (2013). Central carbon metabolism and electron transport in chlamydomonas reinhardtii: Metabolic constraints for carbon partitioning between oil and starch. *Eukaryotic Cell*, *12*(6), 776–793. https://doi.org/10.1128/EC.00318-12

Jollie, D. R., & Lipscomb, J. D. (1991). Formate dehydrogenase from Methylosinus trichosporium OB3b: Purification and spectroscopic characterization of the cofactors. *Journal of Biological Chemistry*, *266*(32), 21853–21863. https://doi.org/10.1016/s0021-9258(18)54716-5

Kalidass, B., Ul-Haque, M. F., Baral, B. S., DiSpirito, A. A., & Semrau, J. D. (2014). Competition between Metals for Binding to Methanobactin Enables Expression of Soluble Methane Monooxygenase in the Presence of Copper. *Applied and Environmental Microbiology*, *81*(3), 1024–1031. https://doi.org/10.1128/aem.03151-14

Kalyuzhnaya, M. G., Yang, S., Rozova, O. N., Smalley, N. E., Clubb, J., Lamb, A., Gowda, G. A. N., Raftery, D., Fu, Y., Bringel, F., Vuilleumier, S., Beck, D. A. C., Trotsenko, Y. A., Khmelenina, V. N., & Lidstrom, M. E. (2013). Highly efficient methane biocatalysis revealed in a methanotrophic bacterium. *Nature Communications*, *4*(May), 1–7. https://doi.org/10.1038/ncomms3785

Kanehisa, M., Sato, Y., & Morishima, K. (2016). BlastKOALA and GhostKOALA: KEGG Tools for Functional Characterization of Genome and Metagenome Sequences. *Journal of Molecular Biology*, *428*(4), 726–731. https://doi.org/10.1016/j.jmb.2015.11.006

Kazamia, E., Czesnick, H., Nguyen, T. T. Van, Croft, M. T., Sherwood, E., Sasso, S., Hodson, S. J., Warren, M. J., & Smith, A. G. (2012). Mutualistic interactions between vitamin B12-dependent algae and heterotrophic bacteria exhibit regulation. *Environmental Microbiology*, *14*(6), 1466–1476. https://doi.org/10.1111/j.1462-2920.2012.02733.x

Kazbar, A., Cogne, G., Urbain, B., Marec, H., Le-Gouic, B., Tallec, J., Takache, H., Ismail, A., & Pruvost, J. (2019). Effect of dissolved oxygen concentration on microalgal culture in photobioreactors. *Algal Research*, *39*(June 2018), 101432.

https://doi.org/10.1016/j.algal.2019.101432

Khmelenina, V. N., But, S. Y., Rozova, O. N., & Trotsenko, Y. A. (2019). Metabolic features of aerobic methanotrophs: News and views. *Current Issues in Molecular Biology*, *33*, 85–99. https://doi.org/10.21775/CIMB.033.085

Khmelenina, V. N., Kalyuzhnaya, M. G., Sakharovsky, V. G., Snzina, N. E., Trotsenko, Y. A., & Gottschalk, G. (1999). Osmoadaptation in halophilic and alkaliphilic methanotrophs. *Archives of Microbiology*, *172*(5), 321–329. https://doi.org/10.1007/s002030050786

Khmelenina, V. N., Rozova, O. N., Akberdin, I. R., Kalyuzhnaya, M. G., & Trotsenko, Y. A. (2018). Pyrophosphate-dependent enzymes in methanotrophs: New findings and views. In *Methane Biocatalysis: Paving the Way to Sustainability* (pp. 83–98). https://doi.org/10.1007/978-3-319-74866-5_6

Kim, H. J., Galeva, N., Larive, C. K., Alterman, M., & Graham, D. W. (2005). Purification and physical-chemical properties of methanobactin: A chalkophore from Methylosinus trichosporium OB3b. *Biochemistry*, *44*(13), 5140–5148. https://doi.org/10.1021/bi047367r

Kim, S., Kang, I., Lee, J.-W., Jeon, C. O., Giovannoni, S. J., & Cho, J.-C. (2021). Heme auxotrophy in abundant aquatic microbial lineages. *Proceedings of the National Academy of Sciences*, *118*(47), e2102750118. https://doi.org/10.1073/pnas.2102750118

Kits, K. D., Klotz, M. G., & Stein, L. Y. (2015). Methane oxidation coupled to nitrate reduction under hypoxia by the Gammaproteobacterium Methylomonas denitrificans, sp. nov. type strain FJG1. *Environmental Microbiology*, *17*(9), 3219–3232. https://doi.org/10.1111/1462-2920.12772

Klein, V. J., Irla, M., López, M. G., Brautaset, T., & Brito, L. F. (2022). Unravelling Formaldehyde Metabolism in Bacteria: Road towards Synthetic Methylotrophy. *Microorganisms*, *10*(2). https://doi.org/10.3390/microorganisms10020220

Knapp, C. W., Fowle, D. A., Kulczycki, E., Roberts, J. A., & Graham, D. W. (2007). Methane monooxygenase gene expression mediated by methanobactin in the presence of mineral copper sources. *Proceedings of the National Academy of Sciences of the United States of America*, *104*(29), 12040–12045. https://doi.org/10.1073/pnas.0702879104

Knief, C. (2015). Diversity and habitat preferences of cultivated and uncultivated aerobic methanotrophic bacteria evaluated based on pmoA as molecular marker. *Frontiers in Microbiology*, *6*(DEC). https://doi.org/10.3389/fmicb.2015.01346

Kouzuma, A., & Watanabe, K. (2015). Exploring the potential of algae/bacteria interactions. *Current Opinion in Biotechnology*, *33*, 125–129. https://doi.org/10.1016/j.copbio.2015.02.007

Krulwich, T. A., Sachs, G., & Padan, E. (2011). Molecular aspects of bacterial pH sensing and

homeostasis. *Nature Reviews Microbiology*, *9*(5), 330–343. https://doi.org/10.1038/nrmicro2549

Lacroux, J., Seira, J., Trably, E., Bernet, N., Steyer, J. P., & van Lis, R. (2021). Mixotrophic Growth of Chlorella sorokiniana on Acetate and Butyrate: Interplay Between Substrate, C:N Ratio and pH. *Frontiers in Microbiology*, *12*(July), 1–16. https://doi.org/10.3389/fmicb.2021.703614

Lagoa, D., Faria, J. P., Liu, F., Cunha, E., Henry, C. S., & Dias, O. (2021). TranSyT, the Transport Systems Tracker. *BioRxiv*, 2021.04.29.441738. https://www.biorxiv.org/content/10.1101/2021.04.29.441738v1%0Ahttps://www.biorxiv.org/content/10.1101/2021.04.29.441738v1.abstract

Lawrence, A. J., & Quayle, J. R. (1970). Alternative carbon assimilation pathways in methane-utilizing bacteria. *Journal of General Microbiology*, *63*(3), 371–374. https://doi.org/10.1099/00221287-63-3-371

Lee, D.-H., Madhavaraj, L., Han, G. H., Lee, H., Lee, S.-G., & Kim, S. W. (2020). Complete Genome Sequence of Methylomonas koyamae LM6, a Potential Aerobic Methanotroph. *Microbiology Resource Announcements*, *9*(6), 14–15. https://doi.org/10.1128/mra.01544-19

Lee, S. W., Keeney, D. R., Lim, D. H., Dispirito, A. A., & Semrau, J. D. (2006). Mixed pollutant degradation by Methylosinus trichosporium OB3b expressing either soluble or particulate methane monooxygenase: Can the tortoise beat the hare. *Applied and Environmental Microbiology*, *72*(12), 7503–7509. https://doi.org/10.1128/AEM.01604-06

Lieberman, R. L., & Rosenzweig, A. C. (2004). Biological Methane Oxidation: Regulation, Biochemistry, and Active Site Structure of Particulate Methane Monooxygenase. *Critical Reviews in Biochemistry and Molecular Biology*, *39*(3), 147–164. https://doi.org/10.1080/10409230490475507

Liska, A. J., Shevchenko, A., Pick, U., & Katz, A. (2004). Enhanced photosynthesis and redox energy production contribute to salinity tolerance in Dunaliella as revealed by homology-based proteomics. *Plant Physiology*, *136*(1), 2806–2817. https://doi.org/10.1104/pp.104.039438

Liu, J. H., Wang, Y. X., Zhang, X. X., Wang, Z. G., Chen, Y. G., Wen, M. L., Xu, L. H., Peng, Q., & Cui, X. L. (2010). Salinarimonas rosea gen. nov., sp. nov., a new member of the α-2 subgroup of the proteobacteria. *International Journal of Systematic and Evolutionary Microbiology*, *60*(1), 55–60. https://doi.org/10.1099/ijs.0.006981-0

Louden, B. C., Haarmann, D., & Lynne, A. M. (2011). Use of Blue Agar CAS Assay for Siderophore Detection. *Journal of Microbiology & Biology Education*, *12*(1), 51–53. https://doi.org/10.1128/jmbe.v12i1.249

Maden, B. E. H. (2000). Tetrahydrofolate and tetrahydromethanopterin compared: functionally

distinct carriers in C1 metabolism. *Biochemical Journal*, *350*(3), 609. https://doi.org/10.1042/0264-6021:3500609

Matsen, J. B., Yang, S., Stein, L. Y., Beck, D., & Kalyuzhnaya, M. G. (2013). Global molecular analyses of methane metabolism in Methanotrophic alphaproteobacterium, methylosinus trichosporium OB3b. Part I: Transcriptomic study. *Frontiers in Microbiology*, *4*(APR), 1–16. https://doi.org/10.3389/fmicb.2013.00040

McCabe, J. W., Vangala, R., & Angel, L. A. (2017). Binding Selectivity of Methanobactin from Methylosinus trichosporium OB3b for Copper(I), Silver(I), Zinc(II), Nickel(II), Cobalt(II), Manganese(II), Lead(II), and Iron(II). *Journal of the American Society for Mass Spectrometry*, *28*(12), 2588–2601. https://doi.org/10.1007/s13361-017-1778-9

Morales-Sánchez, D., Kim, Y., Terng, E. L., Peterson, L., & Cerutti, H. (2017). A multidomain enzyme, with glycerol-3-phosphate dehydrogenase and phosphatase activities, is involved in a chloroplastic pathway for glycerol synthesis in Chlamydomonas reinhardtii. *Plant Journal*, *90*(6), 1079–1092. https://doi.org/10.1111/tpj.13530

Moriyama, T., Toyoshima, M., Saito, M., Wada, H., & Sato, N. (2018). Revisiting the algal "chloroplast lipid droplet": The absence of an entity that is unlikely to exist. *Plant Physiology*, *176*(2), 1519–1530. https://doi.org/10.1104/pp.17.01512

Naizabekov, S., & Lee, E. Y. (2020). Genome-scale metabolic model reconstruction and in silico investigations of methane metabolism in methylosinus trichosporium ob3b. *Microorganisms*, *8*(3). https://doi.org/10.3390/microorganisms8030437

Nakagawa, T., Mitsui, R., Tani, A., Sasa, K., Tashiro, S., Iwama, T., Hayakawa, T., & Kawai, K. (2012). A Catalytic Role of XoxF1 as La3+-Dependent Methanol Dehydrogenase in Methylobacterium extorquens Strain AM1. *PLoS ONE*, *7*(11), 1–7. https://doi.org/10.1371/journal.pone.0050480

Narala, R. R., Garg, S., Sharma, K. K., Thomas-Hall, S. R., Deme, M., Li, Y., & Schenk, P. M. (2016). Comparison of microalgae cultivation in photobioreactor, open raceway pond, and a two-stage hybrid system. *Frontiers in Energy Research*, *4*(AUG), 1–10. https://doi.org/10.3389/fenrg.2016.00029

Neidhardt, F. C., Ingraham, J. L., & Schaechter, M. (1990a). *Physiology of the Bacterial Cell*.

Neidhardt, F. C., Ingraham, J. L., & Schaechter, M. (1990b). *Physiology of the Bacterial Cell*. Sinauer Associates, Inc.

Nguyen, L. T., & Lee, E. Y. (2019). Biological conversion of methane to putrescine using genome-scale model-guided metabolic engineering of a methanotrophic bacterium Methylomicrobium alcaliphilum 20Z. *Biotechnology for Biofuels*, *12*(1), 1–12. https://doi.org/10.1186/s13068-019-1490-z

Oren, A. (2001). The bioenergetic basis for the decrease in metabolic diversity at increasing salt concentrations: Implications for the functioning of salt lake ecosystems. *Hydrobiologia*, *466*, 61–72. https://doi.org/10.1023/A:1014557116838

Oren, A. (2007). DIVERSITY OF ORGANIC OSMOTIC COMPOUNDS AND OSMOTIC ADAPTATION IN CYANOBACTERIA AND ALGAE. In J. Seckbach (Ed.), *Algae and Cyanobacteria in Extreme Environments* (pp. 639–655). Springer.

Oren, A. (2017). Glycerol metabolism in hypersaline environments. *Environmental Microbiology*, *19*(3), 851–863. https://doi.org/10.1111/1462-2920.13493

Orth, J. D., Thiele, I., & Palsson, B. Ø. (2010). What is flux balance analysis? *Nature Biotechnology*, *28*, 245. https://doi.org/10.1038/nbt.1614https://www.nature.com/articles/nbt.1614#supplementary-information

Park, S., Hanna, L., Taylor, R. T., & Droege, M. W. (1991). Batch cultivation of Methylosinus trichosporium OB3b. I: Production of soluble methane monooxygenase . *Biotechnology and Bioengineering*, *38*(4), 423–433. https://doi.org/10.1002/bit.260380412

Patel, R. N., Hou, C. T., Derelanko, P., & Felix, A. (1980). *Purification and Properties of a Heme-Containing Aldehyde Dehydrogenase from Methylosinus trichosporium Methylotrophic organisms are divisible into two groups on the basis of nutritional and biochemical properties . Obligate me- carbon compounds containin*. *203*(2), 654–662.

Pérez-Miranda, S., Cabirol, N., George-Téllez, R., Zamudio-Rivera, L. S., & Fernández, F. J. (2007). O-CAS, a fast and universal method for siderophore detection. *Journal of Microbiological Methods*, *70*(1), 127–131. https://doi.org/10.1016/j.mimet.2007.03.023

Peyraud, R., Kiefer, P., Christen, P., Massou, S., Portais, J. C., & Vorholt, J. A. (2009). Demonstration of the ethylmalonyl-CoA pathway by using13C metabolomics. *Proceedings of the National Academy of Sciences of the United States of America*, *106*(12), 4846–4851. https://doi.org/10.1073/pnas.0810932106

Pieja, A. J., Rostkowski, K. H., & Criddle, C. S. (2011). Distribution and Selection of Poly-3-Hydroxybutyrate Production Capacity in Methanotrophic Proteobacteria. *Microbial Ecology*, *62*(3), 564–573. https://doi.org/10.1007/s00248-011-9873-0

Pieja, A. J., Sundstrom, E. R., & Criddle, C. S. (2011). Poly-3-hydroxybutyrate metabolism in the type II Methanotroph Methylocystis parvus OBBP. *Applied and Environmental Microbiology*, *77*(17), 6012–6019. https://doi.org/10.1128/AEM.00509-11

Pol, A., Barends, T. R. M., Dietl, A., Khadem, A. F., Eygensteyn, J., Jetten, M. S. M., & Op den Camp, H. J. M. (2014). Rare earth metals are essential for methanotrophic life in volcanic mudpots. *Environmental Microbiology*, *16*(1), 255–264. https://doi.org/10.1111/1462-2920.12249

Pomper, B. K., Vorholt, J. A., Chistoserdova, L., Lidstrom, M. E., & Thauer, R. K. (1999). A methenyl tetrahydromethanopterin cyclohydrolase and a methenyl tetrahydrofolate cyclohydrolase in Methylobacterium extorquens AM1. *European Journal of Biochemistry*, *261*(2), 475–480. https://doi.org/10.1046/j.1432-1327.1999.00291.x

Ramanan, R., Kim, B. H., Cho, D. H., Oh, H. M., & Kim, H. S. (2016). Algae-bacteria interactions: Evolution, ecology and emerging applications. *Biotechnology Advances*, *34*(1), 14–29. https://doi.org/10.1016/j.biotechadv.2015.12.003

Raven, J. A., & Beardall, J. (2016). Dark Respiration and Organic Carbon Loss. In *The Physiology of Microalgae* (pp. 129–140). https://doi.org/10.1007/978-3-319-24945-2

Reijnders, M. J. M. F., van Heck, R. G. A., Lam, C. M. C., Scaife, M. A., dos Santos, V. A. P. M., Smith, A. G., & Schaap, P. J. (2014). Green genes: Bioinformatics and systems-biology innovations drive algal biotechnology. *Trends in Biotechnology*, *32*(12), 617–626. https://doi.org/10.1016/j.tibtech.2014.10.003

Ren, Q., De Roo, G., Ruth, K., Witholt, B., Zinn, M., & Thöny-Meyer, L. (2009). Simultaneous accumulation and degradation of polyhydroxyalkanoates: Futile cycle or clever regulation? *Biomacromolecules*, *10*(4), 916–922. https://doi.org/10.1021/bm801431c

Romine, M. F., Rodionov, D. A., Maezato, Y., Osterman, A. L., & Nelson, W. C. (2017). Underlying mechanisms for syntrophic metabolism of essential enzyme cofactors in microbial communities. *ISME Journal*, *11*(6), 1434–1446. https://doi.org/10.1038/ismej.2017.2

Roslev, P., & King, G. M. (1994). Survival and recovery of methanotrophic bacteria starved under oxic and anoxic conditions. *Applied and Environmental Microbiology*, *60*(7), 2602–2608. https://doi.org/10.1128/aem.60.7.2602-2608.1994

Roslev, P., & King, G. M. (1995). Aerobic and anaerobic starvation metabolism in methanotrophic bacteria. *Applied and Environmental Microbiology*, *61*(4), 1563–1570. https://doi.org/10.1128/aem.61.4.1563-1570.1995

Ross, M. O., & Rosenzweig, A. C. (2017). A tale of two methane monooxygenases. *J Biol Inorg Chem*, *22*(2–3), 307–319. https://doi.org/10.1007/s11065-015-9294-9.Functional

Rostkowski, K. H., Pfluger, A. R., & Criddle, C. S. (2013). Stoichiometry and kinetics of the PHB-producing Type II methanotrophs Methylosinus trichosporium OB3b and Methylocystis parvus OBBP. *Bioresource Technology*, *132*, 71–77. https://doi.org/10.1016/j.biortech.2012.12.129

Rowe, E., Palsson, B. O., & King, Z. A. (2018). Escher-FBA: a web application for interactive flux balance analysis. *BMC Systems Biology*, *12*(1), 84. https://doi.org/10.1186/s12918-018-0607-5

Rozova, O. N., Khmelenina, V. N., & Trotsenko, Y. A. (2012). Characterization of recombinant ppi-dependent 6-phosphofructokinases from methylosinus trichosporium OB3b and methylobacterium nodulans ORS 2060. *Biochemistry (Moscow)*, *77*(3), 288–295. https://doi.org/10.1134/S0006297912030078

Rozova, Olga N., Ekimova, G. A., Molochkov, N. V., Reshetnikov, A. S., Khmelenina, V. N., & Mustakhimov, I. I. (2021). Enzymes of an alternative pathway of glucose metabolism in obligate methanotrophs. *Scientific Reports*, *11*(1), 1–11. https://doi.org/10.1038/s41598-021-88202-x

Rozova, Olga N., Khmelenina, V. N., Gavletdinova, J. Z., Mustakhimov, I. I., & Trotsenko, Y. A. (2015). Acetate kinase-an enzyme of the postulated phosphoketolase pathway in Methylomicrobium alcaliphilum 20Z. *Antonie van Leeuwenhoek, International Journal of General and Molecular Microbiology*, *108*(4), 965–974. https://doi.org/10.1007/s10482-015-0549-5

Sato, N., & Toyoshima, M. (2021). Dynamism of Metabolic Carbon Flow of Starch and Lipids in Chlamydomonas debaryana. *Frontiers in Plant Science*, *12*(March). https://doi.org/10.3389/fpls.2021.646498

Sauer, T., & Galinski, E. A. (1998). Bacterial milking: A novel bioprocess for production of compatible solutes. *Biotechnology and Bioengineering*, *57*(3), 306–313. https://doi.org/10.1002/(SICI)1097-0290(19980205)57:3<306::AID-BIT7>3.0.CO;2-L

Schada von Borzyskowski, L., Sonntag, F., Pöschel, L., Vorholt, J. A., Schrader, J., Erb, T. J., & Buchhaupt, M. (2018). Replacing the Ethylmalonyl-CoA Pathway with the Glyoxylate Shunt Provides Metabolic Flexibility in the Central Carbon Metabolism of Methylobacterium extorquens AM1. *ACS Synthetic Biology*, *7*(1), 86–97. https://doi.org/10.1021/acssynbio.7b00229

Schellenberger, J., Lewis, N. E., & Palsson, B. (2011). Elimination of thermodynamically infeasible loops in steady-state metabolic models. *Biophysical Journal*, *100*(3), 544–553. https://doi.org/10.1016/j.bpj.2010.12.3707

Segrè, D., Vitkup, D., & Church, G. M. (2002). Analysis of optimality in natural and perturbed metabolic networks. *Proceedings of the National Academy of Sciences of the United States of America*, *99*(23), 15112–15117. https://doi.org/10.1073/pnas.232349399

Seif, Y., Choudhary, K. S., Hefner, Y., Anand, A., Yang, L., & Palsson, B. O. (2020). Metabolic and genetic basis for auxotrophies in Gram-negative species. *Proceedings of the National Academy of Sciences of the United States of America*, *117*(11), 6264–6273. https://doi.org/10.1073/pnas.1910499117

Semrau, J. D., DiSpirito, A. A., Gu, W., & Yoon, S. (2018). Metals and Methanotrophy. *Applied and Environmental Microbiology*, *84*(6), 1–14. https://doi.org/10.1128/AEM.02289-17

Semrau, J. D., Dispirito, A. A., & Yoon, S. (2010). Methanotrophs and copper. *FEMS Microbiology Reviews*, *34*(4), 496–531. https://doi.org/10.1111/j.1574-6976.2010.00212.x

Shaffer, M., Borton, M. A., McGivern, B. B., Zayed, A. A., La Rosa, S. L. 0003 3527 8101, Solden, L. M., Liu, P., Narrowe, A. B., Rodríguez-Ramos, J., Bolduc, B., Gazitúa, M. C., Daly, R. A., Smith, G. J., Vik, D. R., Pope, P. B., Sullivan, M. B., Roux, S., & Wrighton, K. C. (2020). DRAM for distilling microbial metabolism to automate the curation of microbiome function. *Nucleic Acids Research*, *48*(16), 8883–8900. https://doi.org/10.1093/nar/gkaa621

Shelley, F., Grey, J., & Trimmer, M. (2014). Widespread methanotrophic primary production in lowland chalk rivers. *Proceedings of the Royal Society B: Biological Sciences*, *281*(1783), 20132854. https://doi.org/10.1098/rspb.2013.2854

Shivanand, P., & Mugeraya, G. (2011). Halophilic bacteria and their compatible solutes - osmoregulation and potential applications. *Current Science*, *100*(10), 1516–1521.

Stanley, S. H., Prior, S. D., Leak, D. J., & Dalton, H. (1983). Copper stress underlies the fundamental change in intracellular location of methane mono-oxygenase in methane-oxidizing organisms: Studies in batch and continuous cultures. *Biotechnology Letters*, *5*(7), 487–492. https://doi.org/10.1007/BF00132233

Stein, L. Y. (2011). Surveying N2O-producing pathways in bacteria. *Methods in Enzymology*, *486*(C), 131–152. https://doi.org/10.1016/B978-0-12-381294-0.00006-7

Stein, L. Y. (2020). The Long-Term Relationship between Microbial Metabolism and Greenhouse Gases. *Trends in Microbiology*, *28*(6), 500–511. https://doi.org/10.1016/j.tim.2020.01.006

Stein, L. Y., & Klotz, M. G. (2011). Nitrifying and denitrifying pathways of methanotrophic bacteria. *Biochemical Society Transactions*, *39*(6), 1826–1831. https://doi.org/10.1042/BST20110712

Stein, L. Y., Yoon, S., Semrau, J. D., DiSpirito, A. A., Crombie, A., Murrell, J. C., Vuilleumier, S., Kalyuzhnaya, M. G., Op Den Camp, H. J. M., Bringel, F., Bruce, D., Cheng, J. F., Copeland, A., Goodwin, L., Han, S., Hauser, L., Jetten, M. S. M., Lajus, A., Land, M. L., … Klotz, M. G. (2010). Genome sequence of the obligate methanotroph Methylosinus trichosporium strain OB3b. *Journal of Bacteriology*, *192*(24), 6497–6498. https://doi.org/10.1128/JB.01144-10

Stengel, D. B., Connan, S., & Popper, Z. A. (2011). Algal chemodiversity and bioactivity: Sources of natural variability and implications for commercial application. *Biotechnology Advances*, *29*(5), 483–501. https://doi.org/10.1016/j.biotechadv.2011.05.016

Strong, P. J., Xie, S., & Clarke, W. P. (2015). Methane as a resource: Can the methanotrophs add value? *Environmental Science and Technology*, *49*(7), 4001–4018.

https://doi.org/10.1021/es504242n

Subramanian, S., Barry, A. N., Pieris, S., & Sayre, R. T. (2013). Comparative energetics and kinetics of autotrophic lipid and starch metabolism in chlorophytic microalgae: Implications for biomass and biofuel production. *Biotechnology for Biofuels*, *6*(1), 1–12. https://doi.org/10.1186/1754-6834-6-150

Sun, X. M., Ren, L. J., Zhao, Q. Y., Ji, X. J., & Huang, H. (2018). Microalgae for the production of lipid and carotenoids: A review with focus on stress regulation and adaptation. *Biotechnology for Biofuels*, *11*(1), 1–16. https://doi.org/10.1186/s13068-018-1275-9

Sutherland, D. L., Burke, J., & Ralph, P. J. (2021). High-throughput screening for heterotrophic growth in microalgae using the Biolog Plate assay. *New Biotechnology*, *65*(August), 61–68. https://doi.org/10.1016/j.nbt.2021.08.001

Sutherland, M. A. (2000). *The Molecular Composition of Cells*. The Cell: A Molecular Approach. 2nd Edition. https://www.ncbi.nlm.nih.gov/books/NBK9879/

Tardif, M., Atteia, A., Specht, M., Cogne, G., Rolland, N., Brugière, S., Hippler, M., Ferro, M., Bruley, C., Peltier, G., Vallon, O., & Cournac, L. (2012). Predalgo: A new subcellular localization prediction tool dedicated to green algae. *Molecular Biology and Evolution*, *29*(12), 3625–3639. https://doi.org/10.1093/molbev/mss178

Taubert, A., Jakob, T., & Wilhelm, C. (2019). Glycolate from microalgae: an efficient carbon source for biotechnological applications. *Plant Biotechnology Journal*, *17*(8), 1538–1546. https://doi.org/10.1111/pbi.13078

Taymaz-Nikerel, H., Borujeni, A. E., Verheijen, P. J. T., Heijnen, J. J., & van Gulik, W. M. (2010). Genome-derived minimal metabolic models for Escherichia coli MG1655 with estimated in vivo respiratory ATP stoichiometry. *Biotechnology and Bioengineering*, *107*(2), 369–381. https://doi.org/10.1002/bit.22802

Tays, C., Guarnieri, M. T., Sauvageau, D., & Stein, L. Y. (2018). Combined effects of carbon and nitrogen source to optimize growth of proteobacterial methanotrophs. *Frontiers in Microbiology*, *9*(SEP), 1–14. https://doi.org/10.3389/fmicb.2018.02239

Thiele, I., & Palsson, B. Ø. (2010). A protocol for generating a high-quality genome-scale metabolic reconstruction. *Nature Protocols*, *5*(1), 93–121. https://doi.org/10.1038/nprot.2009.203

Thomson, A. W., O'Neill, J. G., & Wilkinson, J. F. (1976). Acetone production by methylobacteria. *Archives of Microbiology*, *109*(3), 243–246. https://doi.org/10.1007/BF00446635

Tonge, G. M., Drozd, J. W., & Higgins, I. J. (1977). Energy Coupling in Methylosinus trichosporium. *Journal of General Microbiology*, *99*, 229–232.

Trinh, C. T., Wlaschin, A., & Srienc, F. (2009). Elementary Mode Analysis: A Useful Metabolic Pathway Analysis Tool for Characterizing Cellular Metabolism. *Applied Microbiology*, *81*(5), 813–826. https://doi.org/10.1007/s00253-008-1770-1.Elementary

Tymoczko, J. L., Berg, J. M., & Stryer, L. (2015). *Biochemistry: A Short Course* (Third Edit). W. H Freeman & Company.

Vadlamani, A., Pendyala, B., Viamajala, S., & Varanasi, S. (2019). High Productivity Cultivation of Microalgae without Concentrated CO 2 Input (supplemental). *ACS Sustainable Chemistry and Engineering*, *7*(2), 1933–1943. https://doi.org/10.1021/acssuschemeng.8b04094

Vadlamani, A., Viamajala, S., Pendyala, B., & Varanasi, S. (2017a). Cultivation of Microalgae at Extreme Alkaline pH Conditions: A Novel Approach for Biofuel Production. *ACS Sustainable Chemistry and Engineering*, *5*(8), 7284–7294. https://doi.org/10.1021/acssuschemeng.7b01534

Vadlamani, A., Viamajala, S., Pendyala, B., & Varanasi, S. (2017b). Cultivation of Microalgae at Extreme Alkaline pH Conditions: A Novel Approach for Biofuel Production. *ACS Sustainable Chemistry and Engineering*, *5*(8), 7284–7294. https://doi.org/10.1021/acssuschemeng.7b01534

Van Dien, S. J., & Lidstrom, M. E. (2002). Stoichiometric model for evaluating the metabolic capabilities of the facultative methylotroph Methylobacterium extorquens AM1, with application to reconstruction of C3 and C4 metabolism. *Biotechnology and Bioengineering*, *78*(3), 296–312. https://doi.org/10.1002/bit.10200

Varma, A., & Palsson, B. O. (1994). Stoichiometric flux balance models quantitatively predict growth and metabolic by-product secretion in wild-type Escherichia coli W3110. *Applied and Environmental Microbiology*, *60*(10), 3724–3731. http://www.ncbi.nlm.nih.gov/pubmed/7986045%0Ahttp://www.pubmedcentral.nih.gov/articlerender.fcgi?artid=PMC201879

Vecherskaya, M., Dijkema, C., & Stams, A. J. M. (2001). Intracellular PHB conversion in a Type II methanotroph studied by 13C NMR. *Journal of Industrial Microbiology and Biotechnology*, *26*(1–2), 15–21. https://doi.org/10.1038/sj.jim.7000086

Vecherskaya, Margarita, Dijkema, C., Saad, H. R., & Stams, A. J. M. (2009). Microaerobic and anaerobic metabolism of a Methylocystis parvus strain isolated from a denitrifying bioreactor. *Environmental Microbiology Reports*, *1*(5), 442–449. https://doi.org/10.1111/j.1758-2229.2009.00069.x

Vekeman, B., Kerckhof, F. M., Cremers, G., de Vos, P., Vandamme, P., Boon, N., Op den Camp, H. J. M., & Heylen, K. (2016). New Methyloceanibacter diversity from North Sea sediments includes methanotroph containing solely the soluble methane monooxygenase. *Environmental Microbiology*, *18*(12), 4523–4536. https://doi.org/10.1111/1462-2920.13485

Vitova, M., Bisova, K., Kawano, S., & Zachleder, V. (2014). Accumulation of energy reserves in algae: From cell cycles to biotechnological applications. *Biotechnology Advances*, *33*(6), 1204–1218. https://doi.org/10.1016/j.biotechadv.2015.04.012

von Kamp, A., Thiele, S., Hädicke, O., & Klamt, S. (2017). Use of CellNetAnalyzer in biotechnology and metabolic engineering. *Journal of Biotechnology*, *261*(May), 221–228. https://doi.org/10.1016/j.jbiotec.2017.05.001

Vorholt, J. A. (2002). Cofactor-dependent pathways of formaldehyde oxidation in methylotrophic bacteria. *Archives of Microbiology*, *178*(4), 239–249. https://doi.org/10.1007/s00203-002-0450-2

Weber, S., Grande, P. M., Blank, L. M., & Klose, H. (2022). Insights into cell wall disintegration of Chlorella vulgaris. *PLoS ONE*, *17*(1 January 2022), 1–14. https://doi.org/10.1371/journal.pone.0262500

Whittenbury, R., Phillips, K. C., & Wilkinson, J. F. (1970). Enrichment, Isolation and Some Properties of Methane-utilizing Bacteria. *Journal of General Microbiology*, *61*(2), 205–218. https://doi.org/10.1099/00221287-61-2-205

Wilkinson, J. F. (1959). The problem of energy-storage compounds in bacteria. *Experimental Cell Research*, *7*(SUPPL.), 111–130. https://doi.org/10.1016/0014-4827(59)90237-X

Wilkinson, J. F. (1963). Carbon and Energy Storage in Bacteria. *Journal of General Microbiology*, *32*, 171–176. https://doi.org/10.1099/00221287-32-2-171

Wood, A. P., Aurikko, J. P., & Kelly, D. P. (2004). A challenge for 21st century molecular biology and biochemistry: What are the causes of obligate autotrophy and methanotrophy? *FEMS Microbiology Reviews*, *28*(3), 335–352. https://doi.org/10.1016/j.femsre.2003.12.001

Yang, S., Matsen, J. B., Konopka, M., Green-Saxena, A., Clubb, J., Sadilek, M., Orphan, V. J., Beck, D., & Kalyuzhnaya, M. G. (2013). Global molecular analyses of methane metabolism in methanotrophic alphaproteobacterium, methylosinus trichosporium OB3b. Part II. metabolomics and 13C-labeling study. *Frontiers in Microbiology*, *4*(APR), 1–13. https://doi.org/10.3389/fmicb.2013.00070

Yap, B. H. J., Crawford, S. A., Dagastine, R. R., Scales, P. J., & Martin, G. J. O. (2016). Nitrogen deprivation of microalgae: effect on cell size, cell wall thickness, cell strength, and resistance to mechanical disruption. *Journal of Industrial Microbiology and Biotechnology*, *43*(12), 1671–1680. https://doi.org/10.1007/s10295-016-1848-1

Yoch, D. C., Chen, Y. P., & Hardin, M. G. (1990). Formate dehydrogenase from the methane oxidizer Methylosinus trichosporium OB3b. *Journal of Bacteriology*, *172*(8), 4456–4463. https://doi.org/10.1128/jb.172.8.4456-4463.1990

Zahn, J. A., Bergmann, D. J., Boyd, J. M., Kunz, R. C., & DiSpirito, A. A. (2001). Membrane-

associated quinoprotein formaldehyde dehydrogenase from Methylococcus capsulatus Bath. *Journal of Bacteriology*, *183*(23), 6832–6840. https://doi.org/10.1128/JB.183.23.6832-6840.2001

Zengler, K., & Zaramela, L. S. (2018). The social network of microorganisms--how auxotrophies shape complex communities. *Nature Reviews Microbiology*, *16*(6), 383–390. https://doi.org/10.1038/s41579-018-0004-5

Zhang, T., Zhou, J., Wang, X., & Zhang, Y. (2019). Poly-β-hydroxybutyrate production by Methylosinus trichosporium ob3b at different gas-phase conditions. *Iranian Journal of Biotechnology*, *17*(1), 10–16. https://doi.org/10.21859/ijb.1866

Zorz, J. K., Sharp, C., Kleiner, M., Gordon, P. M. K., Pon, R. T., Dong, X., & Strous, M. (2019). A shared core microbiome in soda lakes separated by large distances. *Nature Communications*, *10*(1), 1–10. https://doi.org/10.1038/s41467-019-12195-5